AD NUMBER
ADB006949
LIMITATION CHANGES
TO: **Approved for public release; distribution is unlimited.**
FROM: **Distribution authorized to U.S. Gov't. agencies only; Test and Evaluation; JAN 1975. Other requests shall be referred to Air Force Materials Laboratory, Attn: MBC, Wright-Patterson AFB OH 45433.**
AUTHORITY
WL/DOA via ltr, 25 Feb 1994

AFML-TR-74-65, PART III

(12)

AD B006949

SOME MECHANICAL PROPERTIES OF KEVLAR AND OTHER HEAT RESISTANT, NONFLAMMABLE FIBERS, YARNS AND FABRICS

Fabric Research Laboratories

MARCH 1975

TECHNICAL REPORT AFML-TR-74-65, PART III
REPORT FOR PERIOD JANUARY 1973 – DECEMBER 1974

Distribution limited to U.S. Government agencies only; test and evaluation; January 1975. Other requests for this document must be referred to the Air Force Materials Laboratory, Nonmetallic Materials Division, Composite and Fibrous Materials Branch, AFML/MBC, Wright-Patterson Air Force Base, Ohio 45433.

Prepared for
AIR FORCE MATERIALS LABORATORY
AIR FORCE SYSTEMS COMMAND
WRIGHT-PATTERSON AIR FORCE BASE, OHIO

NOTICE

When Government drawings, specifications, or other data are used for any purpose other than in connection with a definitely related Government procurement operation, the United States Government thereby incurs no responsibility nor any obligation whatsoever; and the fact that the Government may have formulated, furnished, or in any way supplied the said drawings, specifications, or other data, is not to be regarded by implication or otherwise as in any manner licensing the holder or any other person or corporation, or conveying any rights or permission to manufacture, use, or sell any patented invention that may in any way be related thereto.

Copies of this report should not be returned unless return is required by security considerations, contractual obligations, or notice on a specific document.

This report was prepared by Fabric Research Laboratories, Dedham, Mass., under U.S. Government Contract No. F33615-73-C-5034. The work was initiated under Project 7320, "Fibrous Structural Materials," and was conducted from January 2, 1973 through December 31, 1974. It was administered under the direction of the Air Force Materials Laboratory, Air Force Systems Command, with Mr. Stanley Schulman acting as project engineer.

Mr. Norman J. Abbott was the FRL director responsible for the overall program. The laboratory studies were carried out by Miss Pamela Aist, Mr. David Brookstein, Mr. James G. Donovan, Miss Gertrud Gotz, Mr. Joseph S. Panto, Dr. S. Leigh Phoenix, Mrs. Meredith M. Schoppee and Mr. John Skelton. The photomicrographs were taken by Mr. Leo Barish. The authors wish to express their appreciation to Dr. Milton M. Platt, Vice-President of FRL, for handling contractual matters and for many helpful discussions throughout the course of the work.

This report was submitted by the authors in March 1975.

This technical report has been reviewed and is approved for publication.

S Schulman

S. Schulman, Project Monitor

For the Director

T J Reinhart

T. J. Reinhart, Chief
Composites and Fibrous Materials Branch
Nonmetallic Materials Division

UNCLASSIFIED

SECURITY CLASSIFICATION OF THIS PAGE (When Data Entered)

(19) **REPORT DOCUMENTATION PAGE**

READ INSTRUCTIONS BEFORE COMPLETING FORM

1. REPORT NUMBER (18) AFML-TR-74-65-P[redacted]t [redacted]-3 — 2. GOVT ACCESSION NO.	3. RECIPIENT'S CATALOG NUMBER
4. TITLE (and Subtitle) (6) Some Mechanical Properties of Kevlar and Other Heat Resistant, Nonflammable Fibers, Yarns and Fabrics.	5. TYPE OF REPORT & PERIOD COVERED Final, 1/2/73 - 12/31/74 6. PERFORMING ORG. REPORT NUMBER
7. AUTHOR(s) (10) Norman J. Abbott, James G. Donovan, Meredith M. Schoppee John Skelton	8. CONTRACT OR GRANT NUMBER(s) (15) F33615-73-C-5034
9. PERFORMING ORGANIZATION NAME AND ADDRESS Fabric Research Laboratories 1000 Providence Highway, Dedham, Mass. 02026	10. PROGRAM ELEMENT, PROJECT, TASK AREA & WORK UNIT NUMBERS Project 7320 (16) Task 732002 (17) AF-7320
11. CONTROLLING OFFICE NAME AND ADDRESS (12) 128 p. (11)	12. REPORT DATE March 1975 13. NUMBER OF PAGES 115
14. MONITORING AGENCY NAME & ADDRESS (if different from Controlling Office)	15. SECURITY CLASS. (of this report) Unclassified 15a. DECLASSIFICATION/DOWNGRADING SCHEDULE

16. DISTRIBUTION STATEMENT (of this Report)

Distribution limited to U. S. Government agencies only; test and evaluation; January 1975. Other requests for this document must be referred to the Air Force Materials Laboratory, Nonmetallic Materials Division, Composite and Fibrous Materials Branch, AFML/MBC, Wright-Patterson Air Force Base, Ohio 45433.

17. DISTRIBUTION STATEMENT (of the abstract entered in Block 20, if different from Report)

Same

18. SUPPLEMENTARY NOTES

None

(9) Final rept. 2 Jan 73-31 Dec 74

19. KEY WORDS (Continue on reverse side if necessary and identify by block number)

Kevlar yarns, polybenzimidazole yarns, tensile tests, torsion tests, bending recovery, effect of strain rate, effect of temperature, wet tensile tests, cycling fatigue, tensile strain recovery, torsional hysteresis, effect of radiant heat, fiber morphology

20. ABSTRACT (Continue on reverse side if necessary and identify by block number)

The results of the first year's work under this contract are reported in full in AFML-TR-74-65, Parts I and II, and are only summarized herein.

Results of the second year's work are described in full. The tensile properties of wet Kevlar yarns were measured at 70° and 190°F, as well as the response of Kevlar 29 yarn to low speed tensile strain cycling at 70° and 400°F. Torsional stress-strain behavior of Kevlar fibers and yarns was studied exten-

DD FORM 1 JAN 73 1473 EDITION OF 1 NOV 65 IS OBSOLETE

133 275

AIR FORCE - 8-9-75 - 175

SECURITY CLASSIFICATION OF THIS PAGE (When Data Entered)

20. Abstract (Cont.)

sively, including the effect of elevated temperature exposure on this behavior. The bending recovery of Kevlar filaments was measured for different imposed curvatures and different times under strain. The effect of exposure to elevated temperature or bending recovery was investigated, and some deductions made concerning the behavior of these fibers in compression, particularly in respect to the existence of compressive yield. Preliminary measurements of the tensile properties of Durette and HT-4 fabrics under radiant heat flux were made, and the value of such measurements discussed. Finally, the morphology of Kevlar 49 fibers subjected to various types of mechanical working was examined using a scanning electron microscope.

TABLE OF CONTENTS

Section		Page
I	INTRODUCTION AND SUMMARY	1
II	SUMMARY OF FIRST YEAR'S WORK	3
	1. Thermal Stabilization of PBI Fabric	3
	2. Tensile Properties	3
	3. Critical Impact Velocity	16
	4. Kevlar Fiber Properties	17
	5. Twisted Kevlar Yarns	17
	6. Loop and Knot Strength	20
	7. Other Miscellaneous Activities	20
III	TENSILE PROPERTIES	25
	1. Wet Kevlar Yarns	25
	2. Low Speed Tensile Strain Cycling of Kevlar 29 Yarn at 70°F and 400°F	25
	a. Introduction	25
	b. Experimental Procedure	29
	c. Experimental Results and Discussion	29
	d. Conclusions	34
IV	TORSIONAL STRESS-STRAIN BEHAVIOR OF KEVLAR FIBERS AND YARNS	35
	1. Introduction	35
	2. Calibration and Testing Techniques	35
	3. Torsional Stress-Strain Properties of Kevlar Fiber Compared to those of Nylon, Nomex, and Polyester	40
	4. Effect of Previous Exposure to an Extreme Twist Level upon the Tensile Properties of Kevlar 49 Fiber	56
	5. Effect of Elevated Temperature Exposure on the Torsional Recovery of Kevlar 29 Yarn	56
	6. Changes in Torsional Stress-Strain Characteristics Induced by Heat Setting Kevlar 29 Yarn	65
V	BENDING RECOVERY OF KEVLAR FILAMENTS	73
	1. Introduction	73
	2. Experimental Procedure	73
	3. Experimental Results and Discussion	77
	4. Theoretical Analysis of Bending Recovery	84
	5. Compressive Yield Strain	84
	6. Conclusions	93

TABLE OF CONTENTS (Cont.)

Section		Page
VI	MECHANICAL PROPERTIES OF FABRICS IN A RADIANT HEAT ENVIRONMENT	95
	1. Introduction	95
	2. Experimental Procedure	95
	3. Experimental Results and Discussion	97
	4. Future Plans	105
VII	KEVLAR 49 FIBER MORPHOLOGY	107
VIII	CONCLUSIONS	113
	REFERENCES	115

LIST OF ILLUSTRATIONS

Figure		Page
1	Stress-Strain Diagrams for Kevlar 29 Yarn Tensile Tested at a Strain Rate of 0.167%/sec (10%/min) at Various Temperatures (based upon at-temperature yarn dimensions)	4
2	Stress-Strain Diagrams for Kevlar 49 Yarn Tensile Tested at a Strain Rate of 0.167%/see (10%/min) at Various Temperatures (based upon at-temperature yarn dimensions)	5
3	Stress-Strain Diagrams for PRD-49 IV Yarn Tensile Tested at a Strain Rate of 0.167%/see (10%/min) at Various Temperatures (based upon at-temperature yarn dimensions)	6
4	Stress-Strain Diagrams for PBI Yarn Tensile Tested at a Strain Rate of 0.167%/sec (10%/min) at Various Temperatures (based upon at-temperature yarn dimensions)	7
5	Stress-Strain Diagrams for Kevlar 29 Yarn Tensile Tested at a Strain Rate of 8000%/sec at Various Temperatures (based upon at-temperature yarn dimensions)	8
6	Stress-Strain Diagrams for Kevlar 49 Yarn Tensile Tested at a Strain Rate of 8000%/sec at Various Temperatures (based upon at-temperature yarn dimensions)	9
7	Stress-Strain Diagrams for PRD-49 IV Yarn Tensile Tested at a Strain Rate of 8000%/see at Various Temperatures (based upon at-temperature yarn dimensions	10
8	Stress-Strain Diagrams for PBI Yarn Tensile Tested at a Strain Rate of 8000%/sec at Various Temperatures (based upon at-temperature yarn dimensions)	11
9	Rupture Tenacity as a Funetion of Tensile Test Temperature at (a) Low Strain rate and (b) High Strain Rate (based upon denier measured at 70°F)	12
10	Rupture Elongation as a Funetion of Tensile Test Temperature at (a) Low Strain Rate and (b) High Strain Rate (based upon at-temperature yarn dimensions)	13
11	Initial Modulus as a Function of Tensile Test Temperature at (a) Low Strain Rate and (b) High Strain Rate (based upon at-temperature yarn dimensions)	14

LIST OF ILLUSTRATIONS (Cont.)

Figure		Page
12	Energy to Rupture as a Function of Tensile Test Temperature at (a) Low Strain Rate and (b) High Strain Rate (based upon at-temperature yarn dimensions)	15
13	Typical Stress-Strain Diagrams of Kevlar 29 Twisted Yarn	18
14	Typical Stress-Strain Diagrams of Kevlar 49 Twisted Yarn	19
15	Loop and Knot Strength of Twisted Kevlar 29 Yarn	21
16	Loop and Knot Strength of Twisted Kevlar 49 Yarn	22
17	Loop Efficiency of Twisted Kevlar Yarns	23
18	Knot Efficiency of Twisted Kevlar Yarns	24
19	Tensile Test Configuration using Capstan Jaws	26
20	Typical Load-Elongation Diagrams for 400 Denier Kevlar 29 Yarn, 5 tpi, Obtained on Teflon Taped Capstan Jaws - 70°F and 400°F	31
21	Cycle Lifetime of 400 Denier Kevlar 29 Yarn, 5 tpi, at 70°F and 400°F	32
22	The FRL Torsion Measurement Device	36
23	Torsion Device Calibration Curve Obtained Using 25 Micron Diameter Chromel R Wire and a Torsional Pendulum	37
24	Length Retraction of 1.5 Denier Fibers as a Function of Torsional Strain	41
25	Typical Torsional Stress-Strain Diagram for 1.5 Denier Kevlar 29 Fiber	44
26	Typical Torsional Stress-Strain Diagram for 1.5 Denier Kevlar 49 Fiber	45
27	Typical Torsional Stress-Strain Diagram for 2 Denier Nylon Fiber	46
28	Typical Torsional Stress-Strain Diagram for 2 Denier Nomex Fiber	47
29	Typical Torsional Stress-Strain Diagram for 2 Denier Dacron Polyester Fiber	48

LIST OF ILLUSTRATIONS (Cont.)

Figure		Page
30	Torsional Stress-Strain Diagram for a Single Specimen of 1.5 Denier Kevlar 29 Fiber Cycled to Several Strain Levels	49
31	Torsional Stress-Strain Diagram for a Single Specimen of 1.5 Denier Kevlar 49 Fiber Cycled to Several Strain Levels	50
32	Torsional Stress-Strain Diagram for a Single Specimen of 2 Denier Nylon Fiber Cycled to Several Strain Levels	51
33	Torsional Stress-Strain Diagram for a Single Specimen of 2 Denier Nomex Fiber Cycled to Several Strain Levels	52
34	Torsional Stress-Strain Diagram for a Single Specimen of 2 Denier Dacron Polyester Fiber Cycled to Several Strain Levels	53
35	Torsional Strain Recovery of Several Fibers Measured at the Zero Torque Level	55
36	Typical Torsional Stress-Strain Diagram for 1.5 Denier Kevlar 29 Fiber Removed from 100 Denier Yarn	59
37	Torsional Stress-Strain Diagram for a Single Specimen of 1.5 Denier Kevlar 29 Fiber Taken from 100 Denier Yarn and Cycled to Several Strain Levels	60
38	The Effect of Elevated Temperature Exposure on the Torsional Recovery Characteristics of 100 Denier Kevlar 29 Yarn	61
39	Effect of Twist, Both Heat-Set and Not Set, on the Tensile Strength of 100 Denier Kevlar 29 Yarn	64
40	Torsional Recovery and Tenacity Loss as a Function of Setting Temperature for 100 Denier Kevlar 29 Yarn	67
41	Torsional Stress-Strain Diagram for 100 Denier Kevlar 29 Yarn Strained in Both the S (+) and Z (-) Directions	68
42	Torsional Stress-Strain Diagram for 100 Denier Kevlar 29 Yarn Strained in Both the S (+) and Z (-) Directions After Being Heat-Set at 300°F for One Minute	69
43	Microphotographs (~65X) of 100 Denier Kevlar 29 Yarn Taken at Several Intervals During a Torsion Test	71

LIST OF ILLUSTRATIONS (Cont.)

Figure		Page
44	Anticipated Shape of Kevlar Stress-Strain Diagram	74
45	Filament Bending Recovery Test Fixture	75
46	Recovered Curvature as a Function of Imposed Curvature for Kevlar 29 Filaments at 70°F after Various Times Before Release	80
47	Recovered Curvature as a Function of Imposed Curvature for Kevlar 49 Filaments at 70°F	81
48	Bending Recovery of Kevlar 29 Filaments as a Function of Imposed Curvature at 70°F after Various Times Before Release	82
49	Bending Recovery of Kevlar 49 Filaments as a Function of Imposed Curvature at 70°F	83
50	Recovered Curvature as a Function of Imposed Curvature for Kevlar 29 Filaments after One Minute Exposure at Various Temperatures - Released After Five Minutes	87
51	Bending Recovery of Kevlar 29 Filaments after One Minute Exposure at 400°F as a Function of Imposed Curvature - Released After Five Minutes	88
52	Recovered Curvature as a Function if Imposed Curvature for Kevlar 49 Filaments after One Minute Exposure at Various Temperatures - Released After Five Minutes	89
53	Bending Recovery of Kevlar 49 Filaments after One Minute Exposure at 400°F as a Function of Imposed Curvature - Released After Five Minutes	90
54	Recovered Curvature as a Function of Imposed Curvature for Kevlar 29 and Kevlar 49 Filaments at 70°F and 400°F - Released After Five Minutes	91
55	Onset of Compressive Buckling in a Bent Kevlar Fiber	92
56	Radiant Heaters and Test Chamber; (a) Specimen in Place Between Facing Heaters, (b) Track System for Inserting Test Specimen	96
57	The Effect of Bilateral Radiant Heat Flux and Duration of Exposure on the Strength Retention of Durette Fabric (4.7 oz/sq yd)	99

LIST OF ILLUSTRATIONS (Cont.)

Figure		Page
58	The Effect of Bilateral Radiant Heat Flux and Duration of Exposure on the Rupture Elongation of Durette Fabric (4.7 oz/sq yd)	100
59	The Effect of Bilateral Radiant Heat Flux and Duration of Exposure on the Initial Modulus of Durette Fabric (4.7 oz/sq yd)	101
60	The Effect of Bilateral Radiant Heat Flux and Duration of Exposure on the Strength Retention of HT-4 Fabric (4.7 oz/sq yd)	102
61	The Effect of Bilateral Radiant Heat Flux and Duration of Exposure on the Rupture Elongation of HT-4 Fabric (4.7 oz/sq yd)	103
62	The Effect of Bilateral Radiant Heat Flux and Duration of Exposure on the Initial Modulus of HT-4 Fabric (4.7 oz/sq yd)	104
63	Fiber Cross-Sectioned with a Razor Blade	107
64	Longitudinal View of Virgin Fibers	108
65	Fiber Twisted 70 Turns/cm	109
66	Fiber Twisted 70 Turns/cm and Untwisted	109
67	Fibers Broken in Tension	110
68	Laterally Compressed Fiber	111
69	Overhand Knots in Single Fibers	112

LIST OF TABLES

Table		Page
I	Critical Velocities (ft/sec)	16
II	Kevlar Fiber Properties	17
III	Tensile Properties of 1500 Denier Kevlar 29 Yarn in Water at 70°F and 190°F	27
IV	Tensile Properties of 400 Denier Kevlar 49 Yarns in Water at 70°F and 190°F	28
V	Tensile Properties of 400 Denier Kevlar 29 Yarn, 5 tpi, Obtained on Teflon-Taped Jaws at 70°F and 400°F	30
VI	Recovered Strain in Cycled 400 Denier Kevlar 29 Yarn, 5 tpi, at 70°F and 400°F	34
VII	The Torsional Stiffness of Two Fibers Determined by the Use of a Torsional Pendulum	39
VIII	Torsional Moduli of Five Fibers Determined with the FRL Torsional Measurement Instrument	43
IX	Residual Torsional Strain in Single Fibers Measured after Deformation to Several Levels of Imposed Strain	54
X	Tensile Properties of Kevlar 49 Fiber - Twisted 70 Turns/cm, Then Untwisted (1.0 inch specimen length)	57
XI	Relative Effectiveness of Four Temperatures to Set Twist in 100 Denier Kevlar 29 Yarn	62
XII	Tenacity (gpd) of 100 Denier Kevlar 29 Yarn Twisted to 2.4 Turns/cm (6 turns/inch), Heat Set for One Minute at Each of Several Temperature Levels, and Allowed to Recover Before Tensile Testing	63
XIII	Tenacity (gpd) of 100 Denier Kevlar 29 Yarn at Several Levels of Twist: Not Heat Set	66
XIV	Bending Recovery of Kevlar 29 Filaments at 70°F	78
XV	Bending Recovery of Kevlar 49 Filaments at 70°F	79
XVI	Bending Recovery of Kevlar 29 Filaments after Exposure at Various Temperatures (time before release, 5 minutes)	80

LIST OF TABLES (Cont.)

Table		Page
XVII	Bending Recovery of Kevlar 49 Filaments after Exposure at Various Temperatures (time before release, 5 minutes)	86
XVIII	Bending Strain at Onset of Compressive Buckling in Knotted Kevlar Fibers	93
XIX	Fabric Description and 70°F Tensile Properties of Durette and HT-4 Fabrics	97

SECTION I

INTRODUCTION AND SUMMARY

This report describes the results of two year's work which was concerned largely with the properties of three types of Kevlar fiber, which are new, very high modulus, high tenacity fibers manufactured by E. I. du Pont de Nemours & Co., and suitable for use in conventional textile applications. One of these, called PRD49 Type IV, has been withdrawn by Du Pont and is not, at this time, a commercially available fiber. The other two are items of commerce, and are called Kevlar 29, intended for essentially textile and tire use, and Kevlar 49, thought of primarily as a fiber for use in composites.

In addition to the Kevlar fibers, the properties of PBI have also been studied in some detail. For comparison throughout, nylon and Nomex properties were taken from published reports and papers.

During the first year a treatment which protected thermally stabilized PBI from the effects of repeated laundering was developed. Also tensile properties of yarns were measured over the temperature range -65°F to 800°F, and at strain rates of 0.167%/sec and 8000%/sec. Some fiber properties were also measured, as well as basic characteristics such as dynamic modulus, critical impact velocity, and bending modulus. The effect of twist on yarn properties was studied, and the cause of the strength loss resulting from high twist explored. Loop and knot strengths were measured for yarns at various twist levels.

The results of the first year's work were described fully in Technical Report AFML-TR-74-65, Part II. They are summarized briefly herein.

During the second year a detailed study of the torsional characteristics of Kevlar 29 and Kevlar 49 was carried out. Measurements of bending recovery were also made from various levels of imposed curvature and for several times of residence in the bent state. The response of Kevlar yarns to cyclic straining to various levels at two temperatures was studied, as well as the effect of water on the tensile characteristics of the yarn.

The second year's work is described fully herein.

SECTION II

SUMMARY OF FIRST YEAR'S WORK

1. Thermal Stabilization of PBI Fabric

The thermal stabilization treatment which FRL had developed for PBI fabrics (AFML-TR-72-231, -73-29, -73-130) involved treatment with an acid at fairly high levels of add-on. The effectiveness of the treatment was not altered by leaching in water, but could be reduced by laundering with certain highly alkaline detergents. A study was made to determine the resistance of acid-treated PBI fabric to laundering in various types of detergent, and to develop a treatment which enabled it to resist such laundering without seriously altering its thermal stability. A high temperature heat treatment of the acid-treated PBI was found to stabilize the fabric through 15 washes in even the most severe detergent.

2. Tensile Properties

The tensile properties of four yarns were measured over a range of temperatures from -65°F to as high as the yarns would tolerate, and at strain rates of 0.167%/sec (Instron conditions) and 8000%/sec. In addition to obtaining stress-strain curves at each of these conditions, values were determined for rupture load and elongation, rupture energy and initial modulus. The four yarns which were studied were:

1500 denier Kevlar 29
400 denier Kevlar 49
400 denier PRD49 Type IV
200 denier PBI (polybenzimidazole).

Before testing each yarn, approximately 2 turns per inch of twist were added to consclidate the yarns.

The stress-strain curves obtained are shown in Figures 1 through 8. The change of rupture tenacity, rupture elongation, initial modulus and rupture energy with temperature at each strain rate is shown more clearly in Figures 9 through 12, which include curves for 1050 denier high tenacity nylon and 1200 denier Nomex for comparison.

The outstanding features of these stress-strain characteristics may be summarized as follows:

a. When tested at a strain rate of 0.167%/sec and at 70°F, the tensile properties of the Kevlar yarns differ greatly from those of PBI, nylon, and Nomex. In comparison with this latter group of yarn materials, the Kevlars have very high tenacity, low elongation, high initial modulus, and low energy absorption. Moreover, the stress-strain curves are essentially linear, exhibiting only a small change in slope at a strain level about one-half the rupture strain.

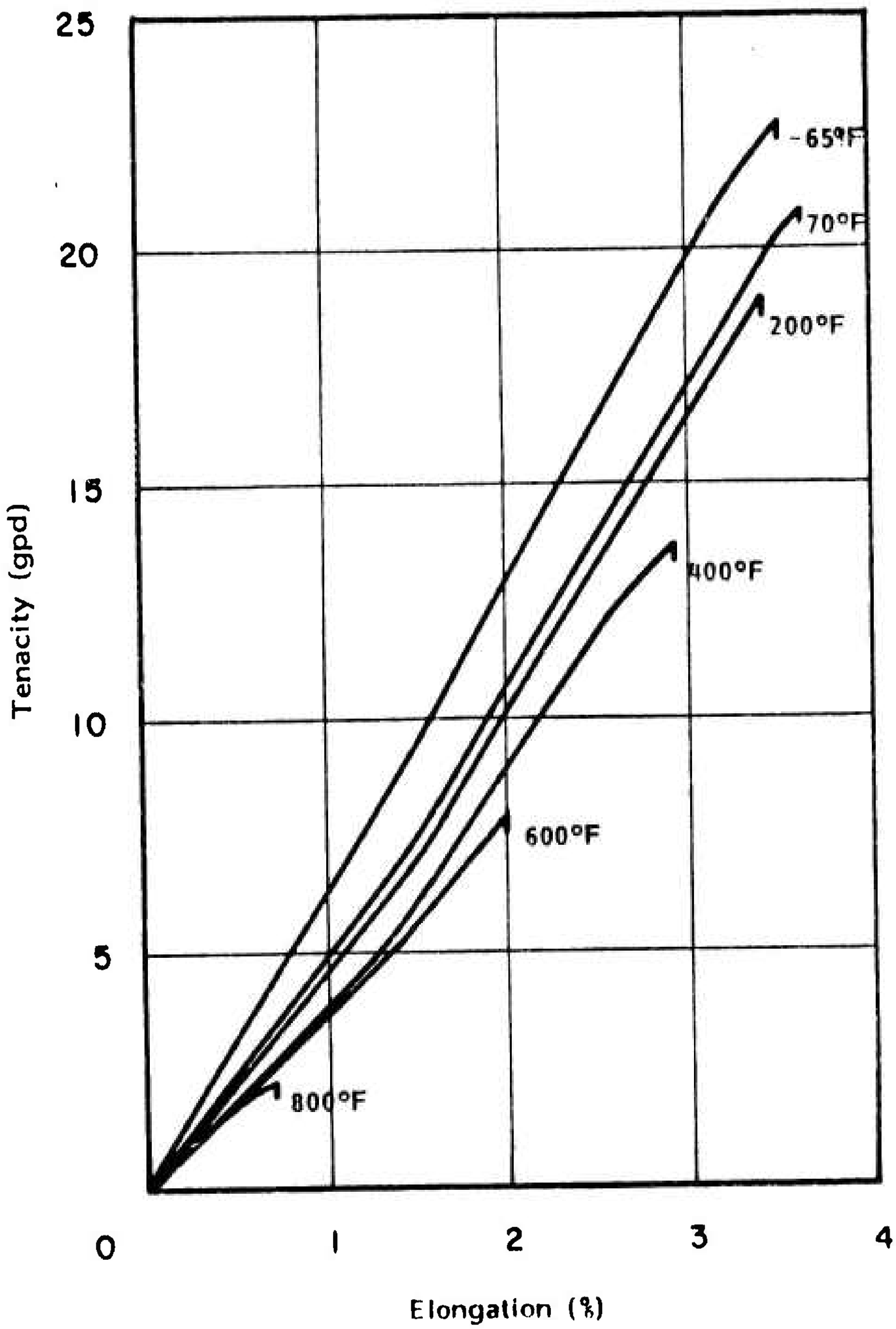

Figure 1. Stress-Strain Diagrams for Kevlar 29 Yarn Tensile Tested at a Strain Rate of 0.167%/sec (10%/min) at Various Temperatures (based upon at-temperature yarn dimensions)

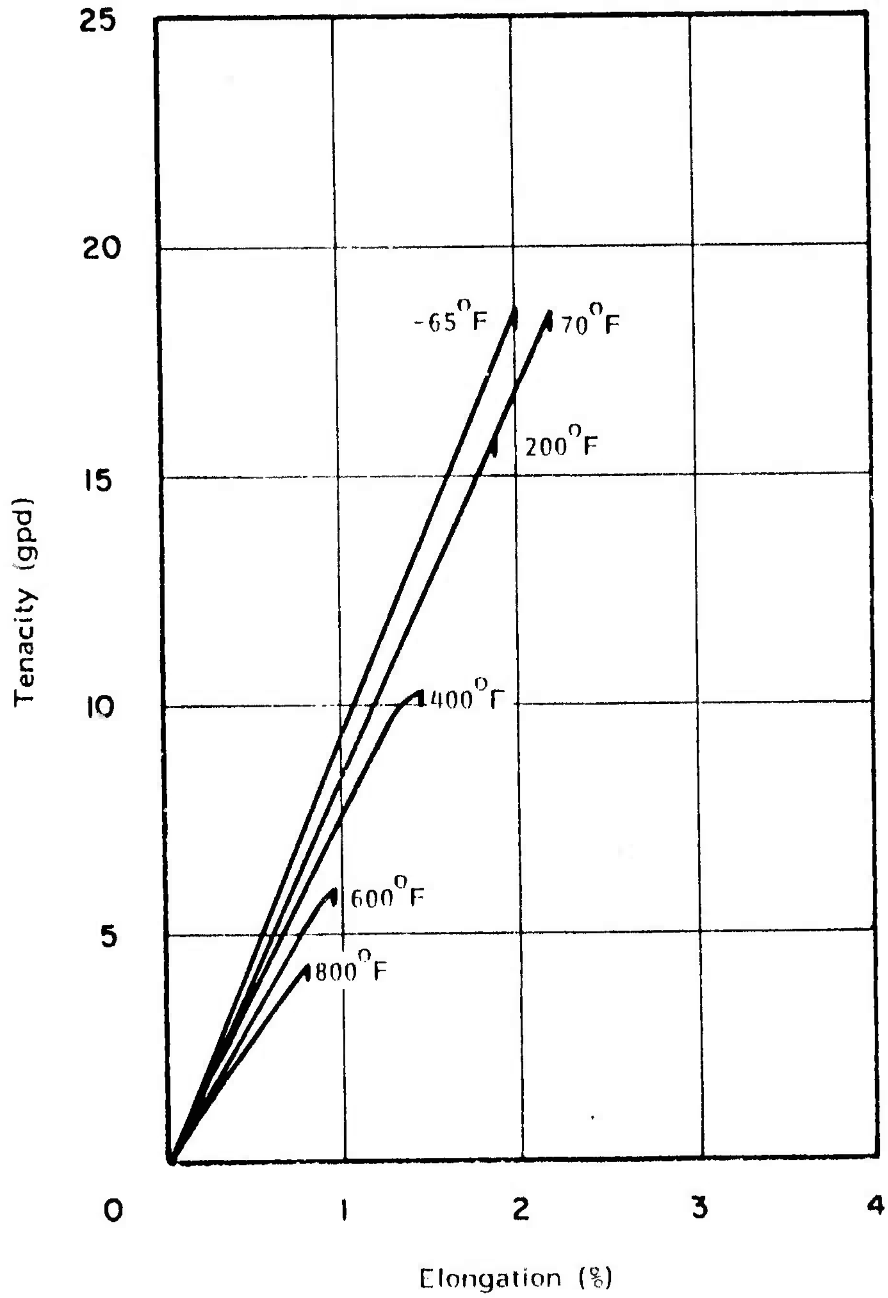

Figure 2. Stress-Strain Diagrams for Kevlar 49 Yarn Tensile Tested at a Strain Rate of 0.167%/sec (10%/min) at Various Temperatures (based upon at-temperature yarn dimensions)

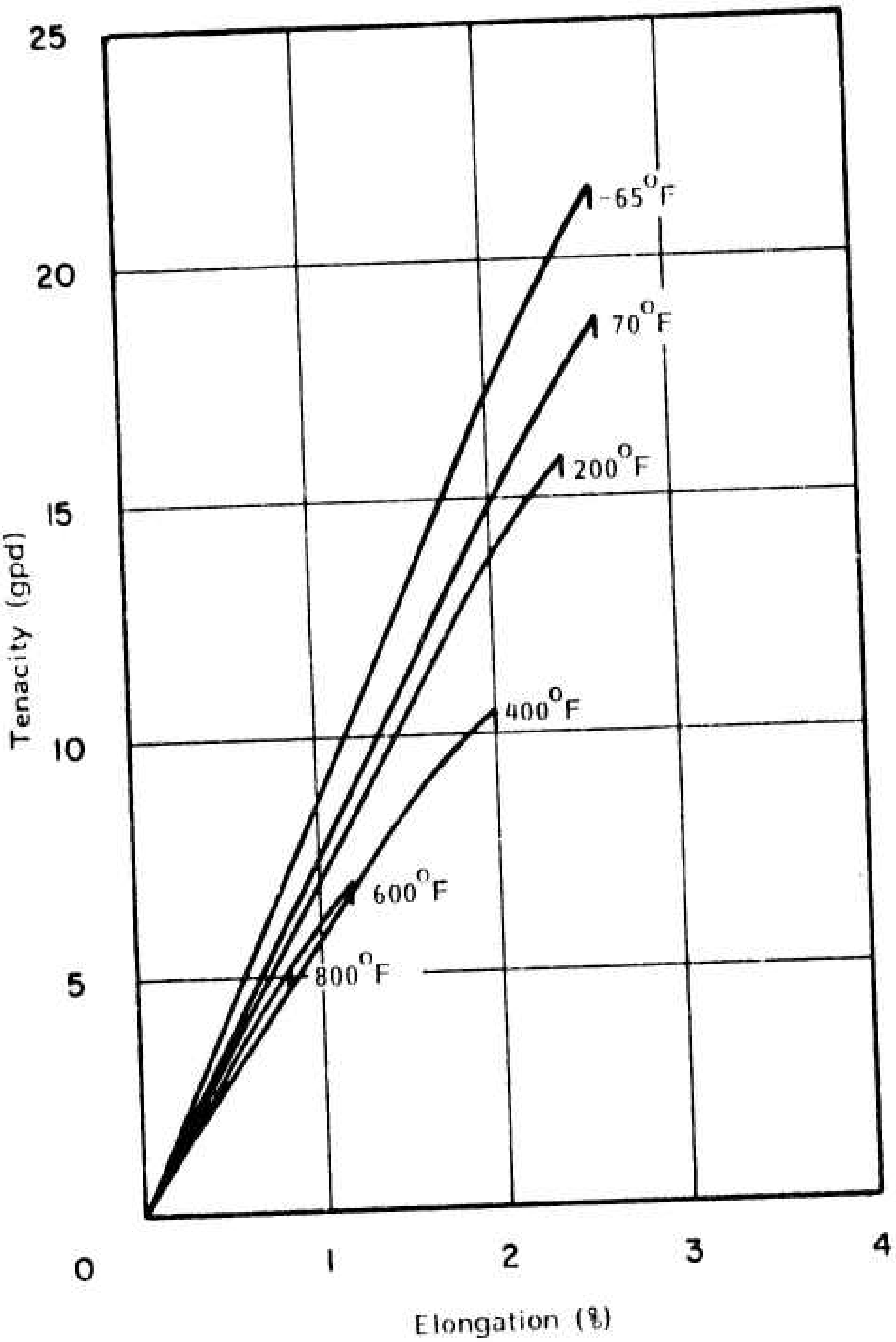

Figure 3. Stress-Strain Diagrams for PRD-49 IV Yarn Tensile Tested at a Strain Rate of 0.167%/sec (10%/min) at Various Temperatures (based upon at-temperature yarn dimensions)

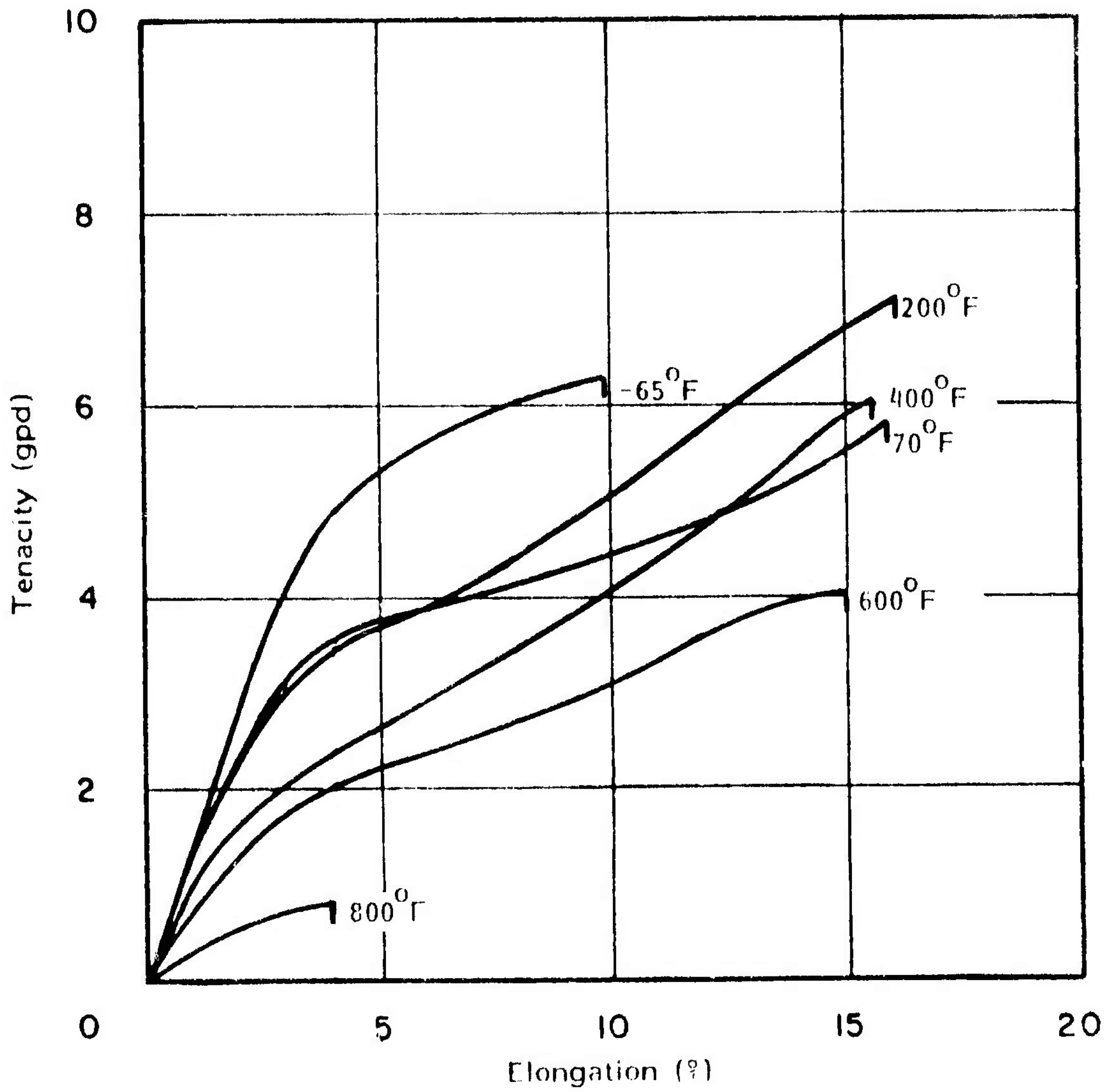

Figure 4. Stress-Strain Diagrams for PBI Yarn Tensile Tested at a Strain Rate of 0.167%/sec (10%/min) at Various Temperatures (based upon at-temperature yarn dimensions)

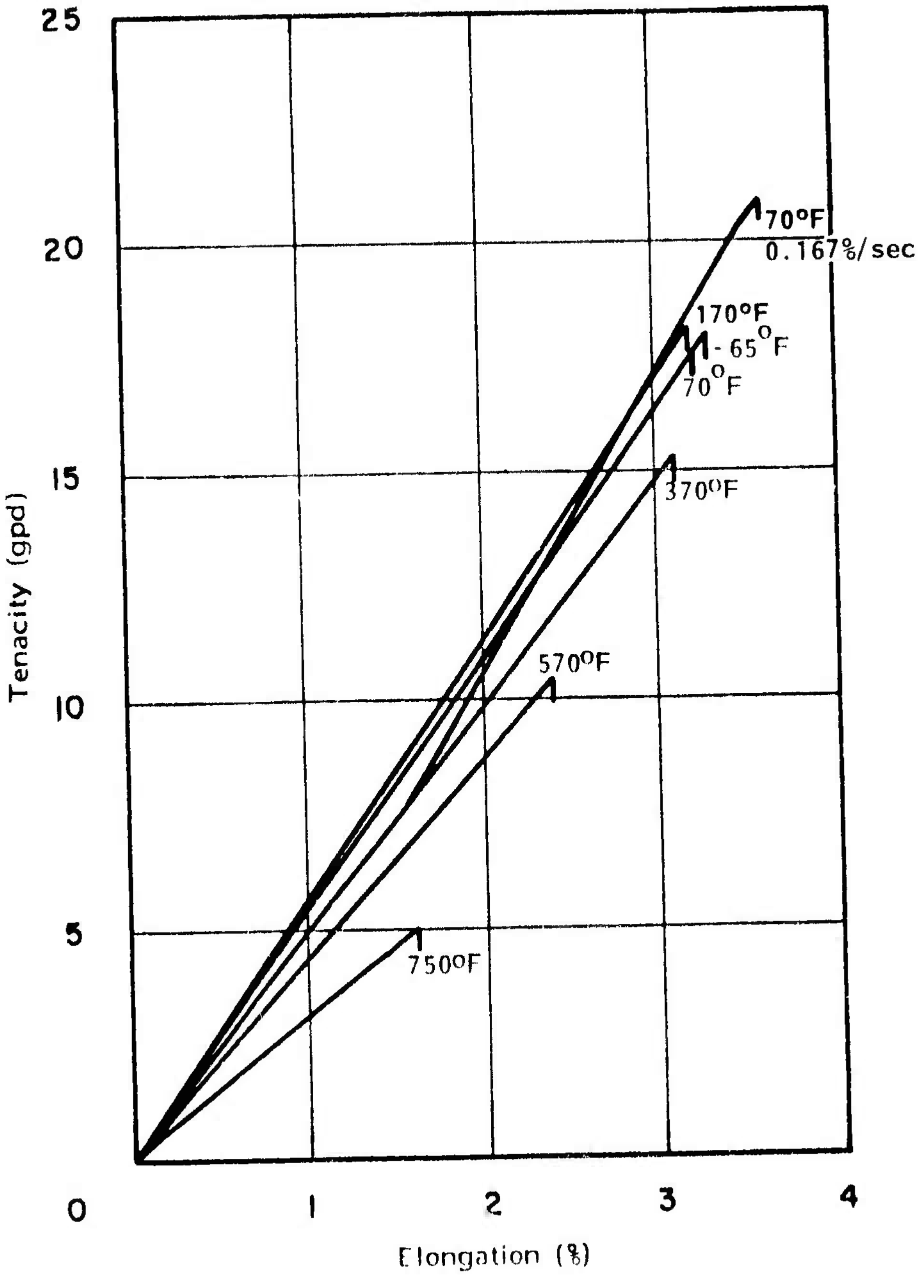

Figure 5. Stress-Strain Daigrams for Kevlar 29 Yarn Tensile Tested at a Strain Rate of 8000%/sec at Various Temperatures (based upon at-temperature yarn dimensions)

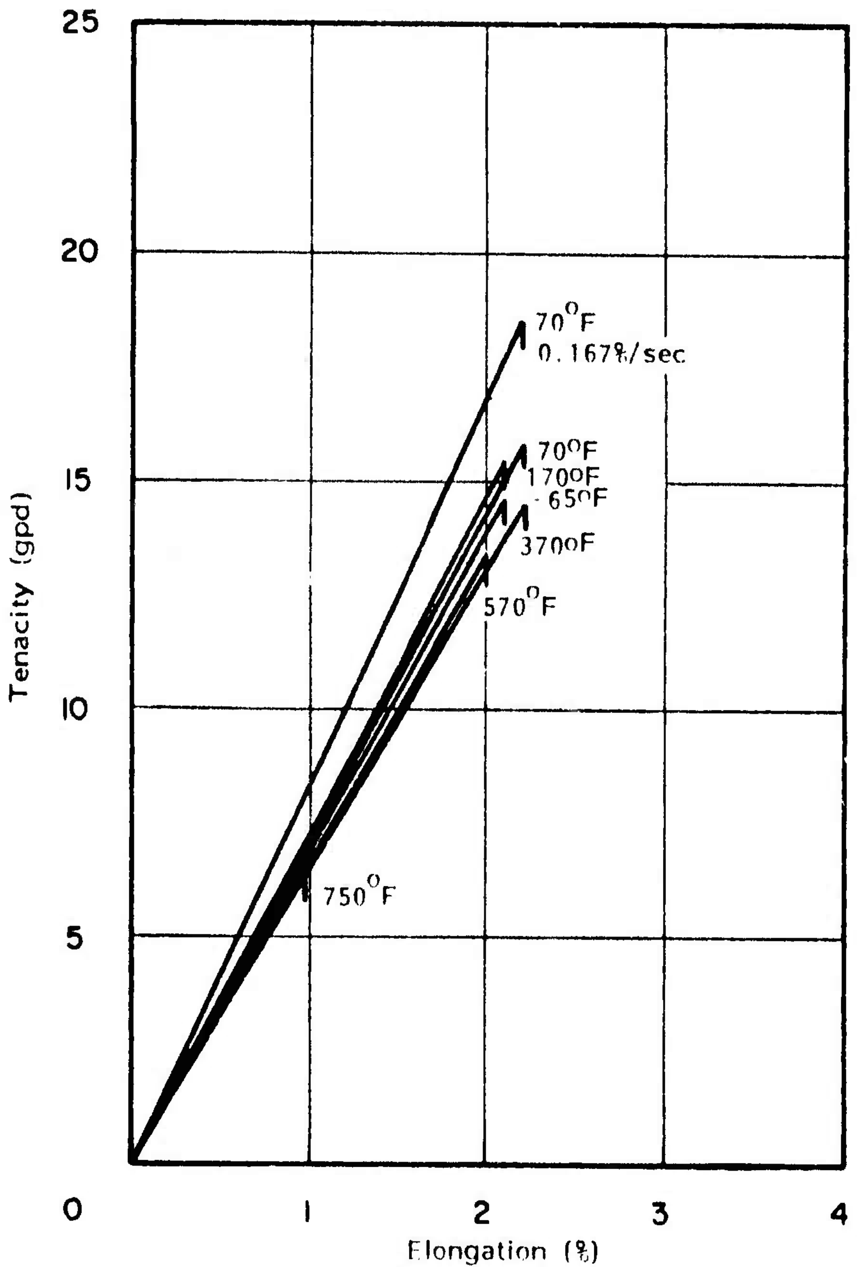

Figure 6. Stress-Strain Diagrams for Kevlar 49 Yarn Tensile Tested at a Strain Rate of 8000%/sec at Various Temperatures (based upon at-temperature yarn dimensions)

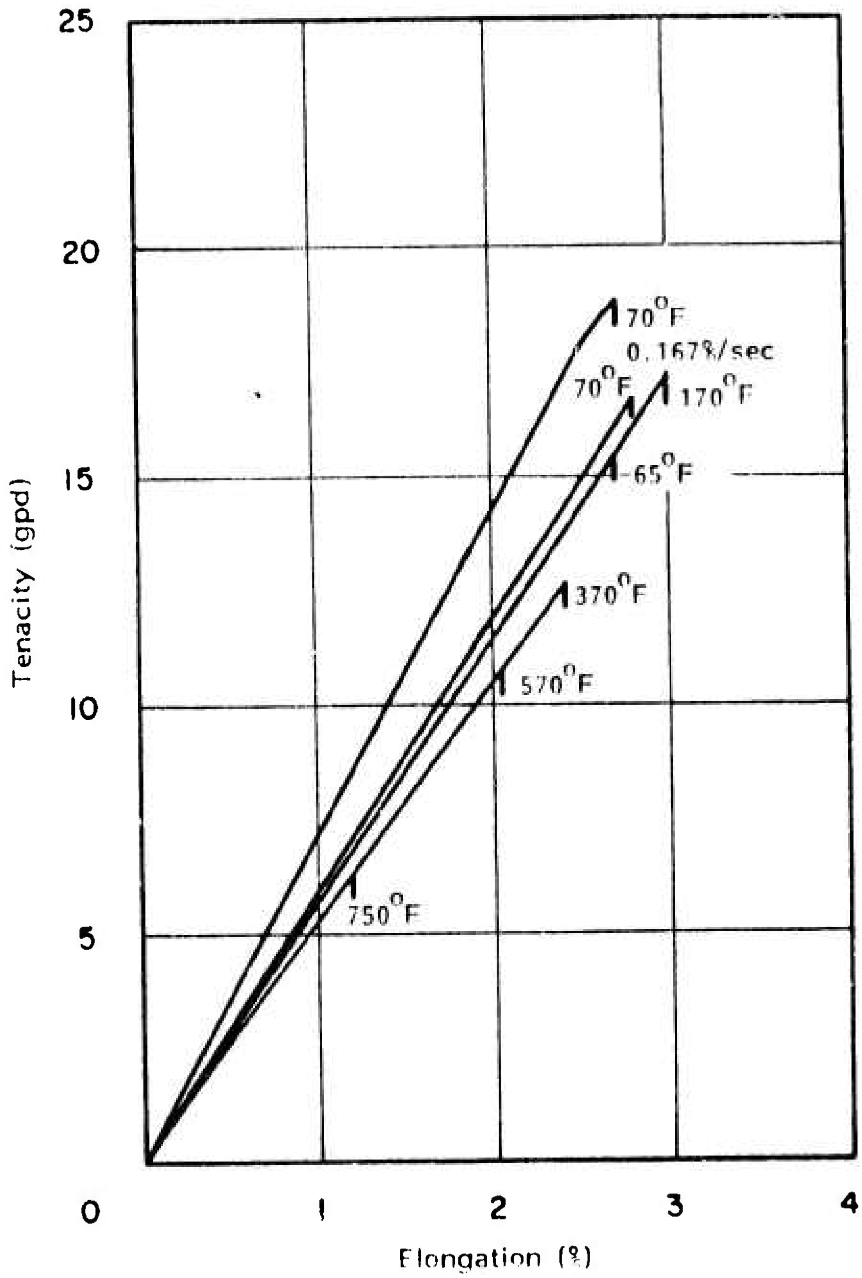

Figure 7. Stress-Strain Diagrams for PRD-49 IV Yarn Tensile Tested at a Strain Rate of 8000%/sec at Various Temperatures (based upon at-temperature yarn dimensions)

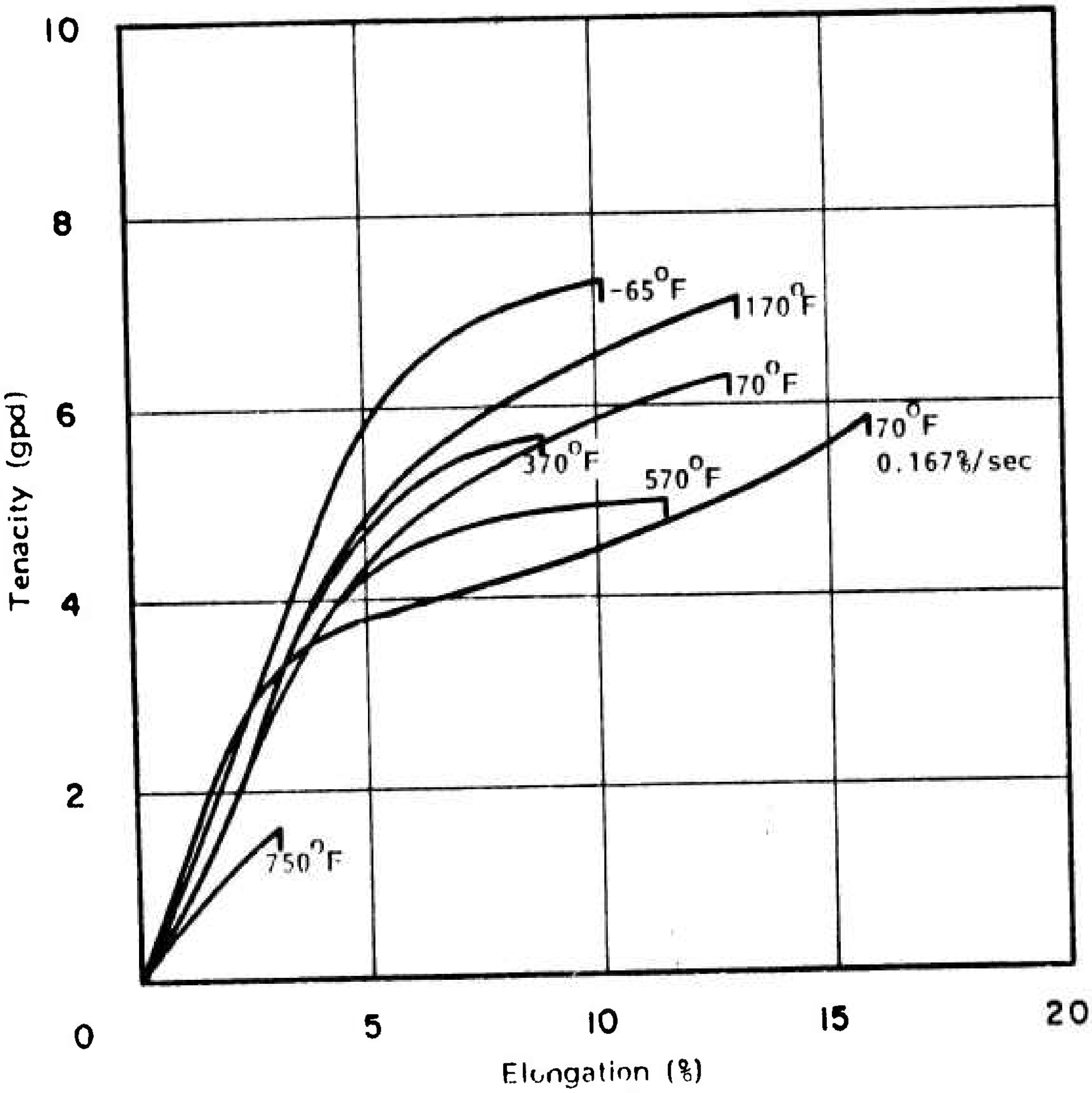

Figure 8. Stress-Strain Diagrams for PBI Yarn Tensile Tested at a Strain Rate of 8000%/sec at Various Temperatures (based upon at-temperature yarn dimensions)

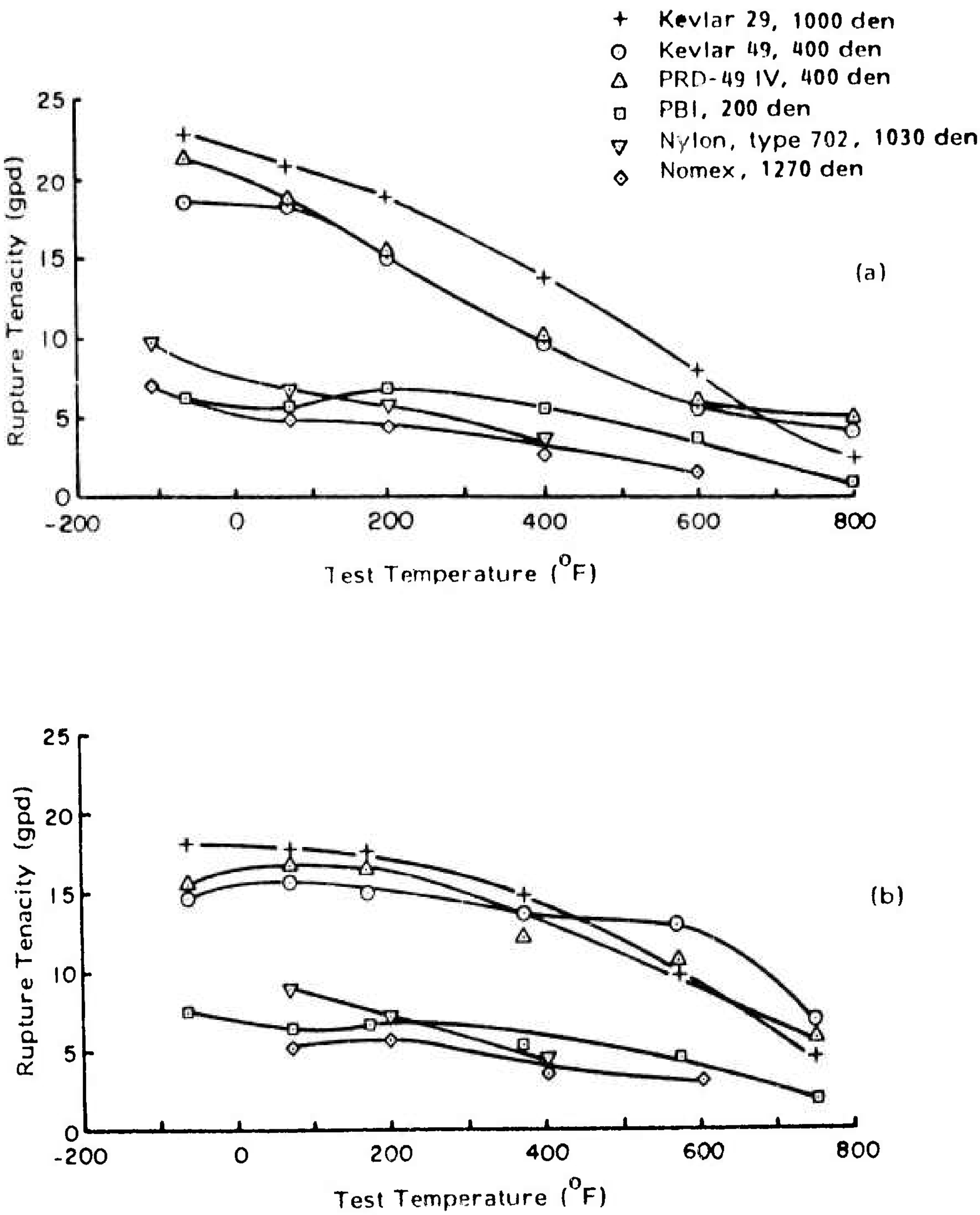

Figure 9. Rupture Tenacity as a Function of Tensile Test Temperature at (a) Low Strain Rate and (b) High Strain Rate (based upon denier measured at 70°F)

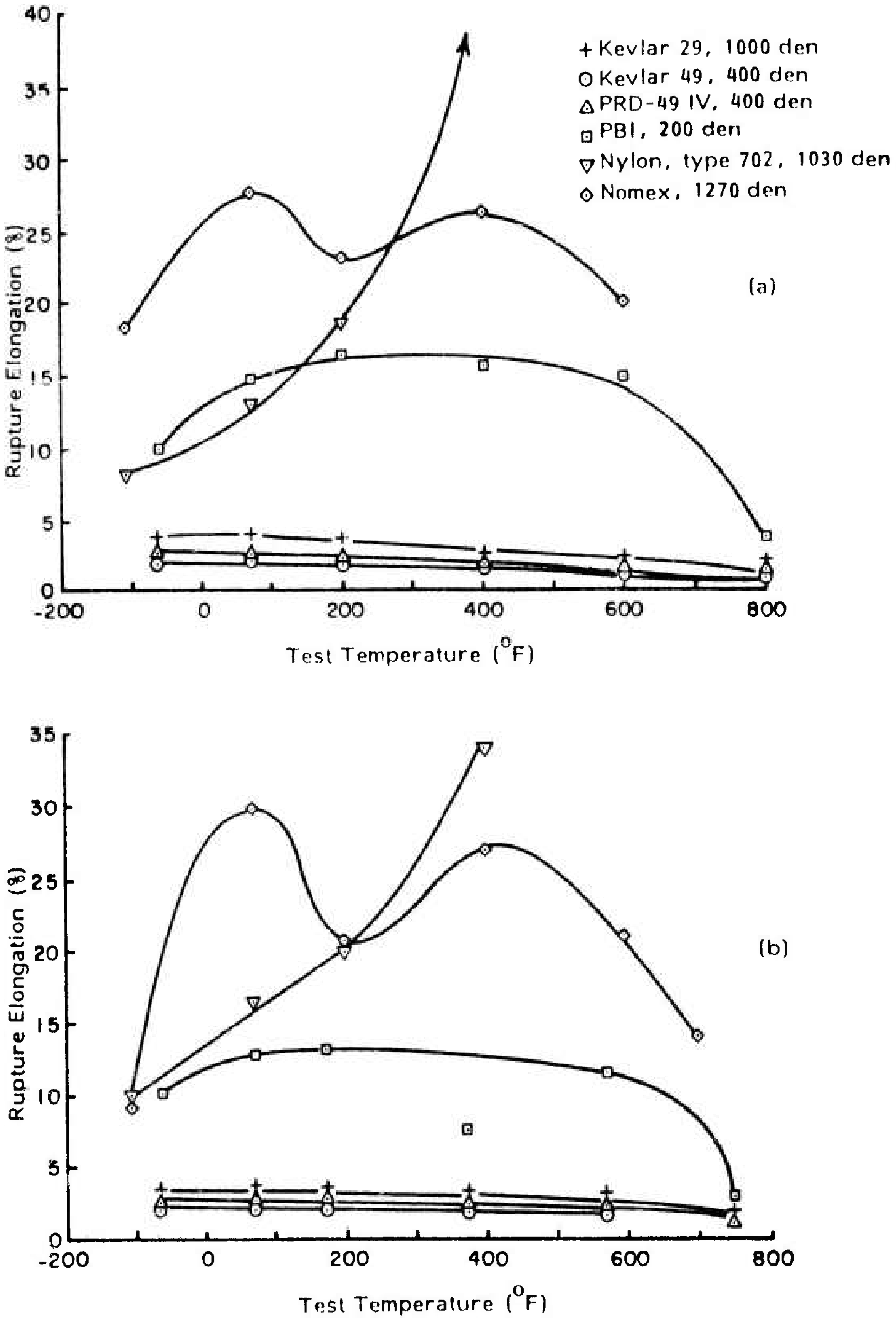

Figure 10. Ruptu. . Elongation as a Function of Tensile Test Temperature at (a) Low Strain Rate and (b) High Strain Rate (based upon at-temperature yarn dimensions)

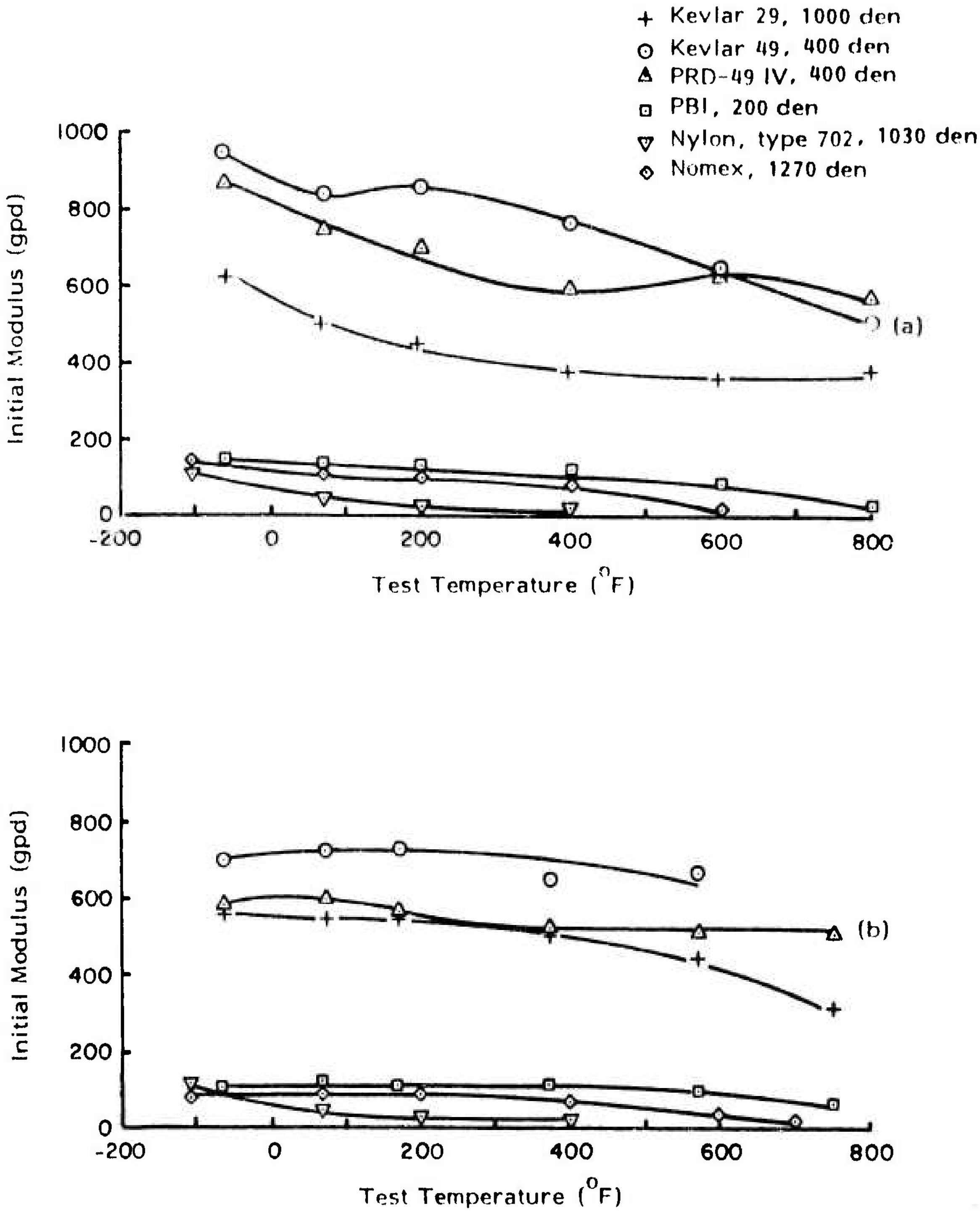

Figure 11. Initial Modulus as a Function of Tensile Test Temperature at (a) Low Strain Rate and (b) High Strain Rate (based upon at-temperature yarn dimensions)

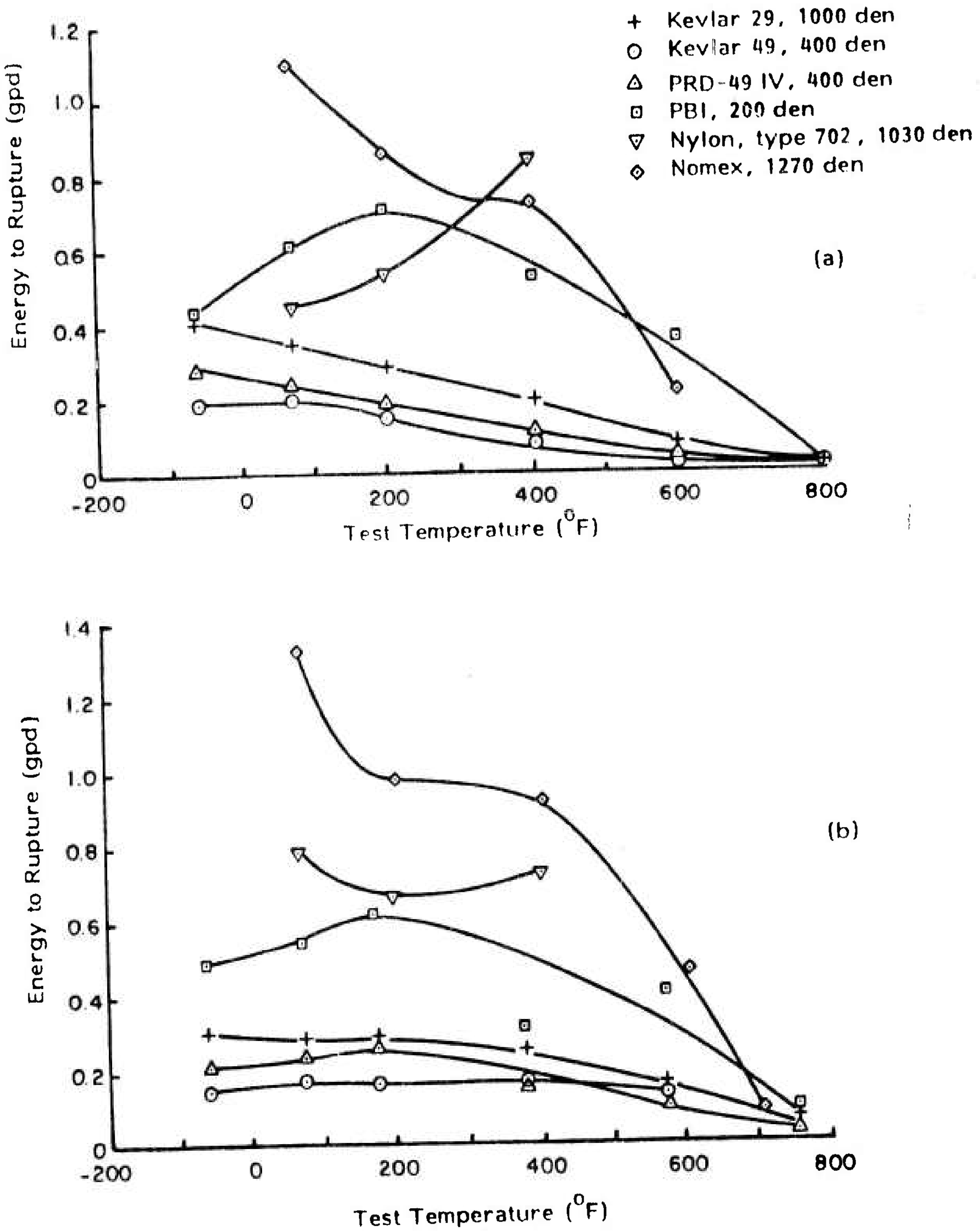

Figure 12. Energy to Rupture as a Function of Tensile Test Temperature at (a) Low Strain Rate and (b) High Strain Rate (based upon at-temperature yarn dimensions)

b. When the rate of strain is increased to 8000%/sec at 70°F, the tensile behavior of the Kevlars remains linear but, unlike most textile fibers, the tenacity drops an average of 14% and rupture elongation is virtually unchanged. The high strain rate behavior of PBI is more typical of that associated with previously known textile materials. At 8000%/sec, the tenacity of PBI increased 8% and the rupture elongation decreased 21%.

c. All four yarn types retained useful tensile properties up to approximately 600°F. Above this temperature rupture elongation and, therefore, rupture energy, fall off drastically, though significant strength was retained even at 800°F.

d. At elevated temperatures, the high strain rate tensile performance of the Kevlars is generally superior to that recorded at Instron testing speeds.

e. At a temperature of -65°F, both high and low strain rate testing of Kevlar yarn revealed only minor changes in tensile properties from those at 70°F. However, PBI, nylon, and Nomex are affected by subambient temperatures when tested at 0.167%/sec, all three showing significant increases in tenacity and decreases in rupture elongation. At the higher strain rate, the effect of subambient temperatures on PBI, nylon, and Nomex becomes a much less important factor.

f. In general, the Kevlar yarns are capable of absorbing only one-half to one-third as much energy in tension as a corresponding high-tenacity nylon. This difference is larger at high strain rates than at low, and at high temperatures than at low.

3. Critical Impact Velocity

Critical velocity is defined as the lowest impact velocity at which the speciment, in this case a yarn, fails immediately at the point of impact. It is the lowest striking velocity at which there is no strain propagation away from the point of impact. The specimen breaks, therefore, without absorbing any of the kinetic energy of the impacting mass. Critical velocity level is generally regarded as an indicator of tensile impact performance. The results obtained for the four yarns, along with nylon and Nomex as comparators, are given in Table I. Values are given for impacts occurring normal and at 45° to the test yarn specimen ($\beta = 90°$ and 45°).

Table I: Critical Velocities (ft/sec)

	$\beta = 90°$	$\beta = 45°$
Kevlar 29	1870	770
Kevlar 49	1620	740
Nylon	2020	1200
Nomex	1450	720

4. Kevlar Fiber Properties

Measurements of the tensile and other properties of Kevlar fibers were made in order to provide a reference with which to compare yarn properties. The results are given in Table II.

Table II: Kevlar Fiber Properties

	Kevlar 29	Kevlar 49
Specific gravity	1.44	1.44
1.5 denier fiber diameter (μm)	12	12
Moisture regain (%) at 70°F, 65%RH	3.9	4.6
Rupture tenacity		
gpd	26	24
$\times 10^3$ psi	475	440
Rupture elongation (%)	3.9	2.3
Initial modulus		
gpd	550	990
$\times 10^6$ psi	10	18
Maximum modulus		
gpd	750	1090
$\times 10^6$ psi	14	20
Bending modulus		
gpd	410	820
$\times 10^6$ psi	7.7	15.3
Calculated axial compression modulus		
gpd	320	600
$\times 10^6$ psi	5.9	11
Dynamic modulus		
gpd	740	1050
$\times 10^6$ psi	14	20

5. Twisted Kevlar Yarns

The effect of increasing levels of twist on the stress-strain characteristics of the Kevlar 29 and Kevlar 49 yarns are shown in Figures 13 and 14. It is common to find a slight increase in tenacity when a small amount of twist is added. The increase in the case of the Kevlars is unusually large. Similarly, the drop-off in

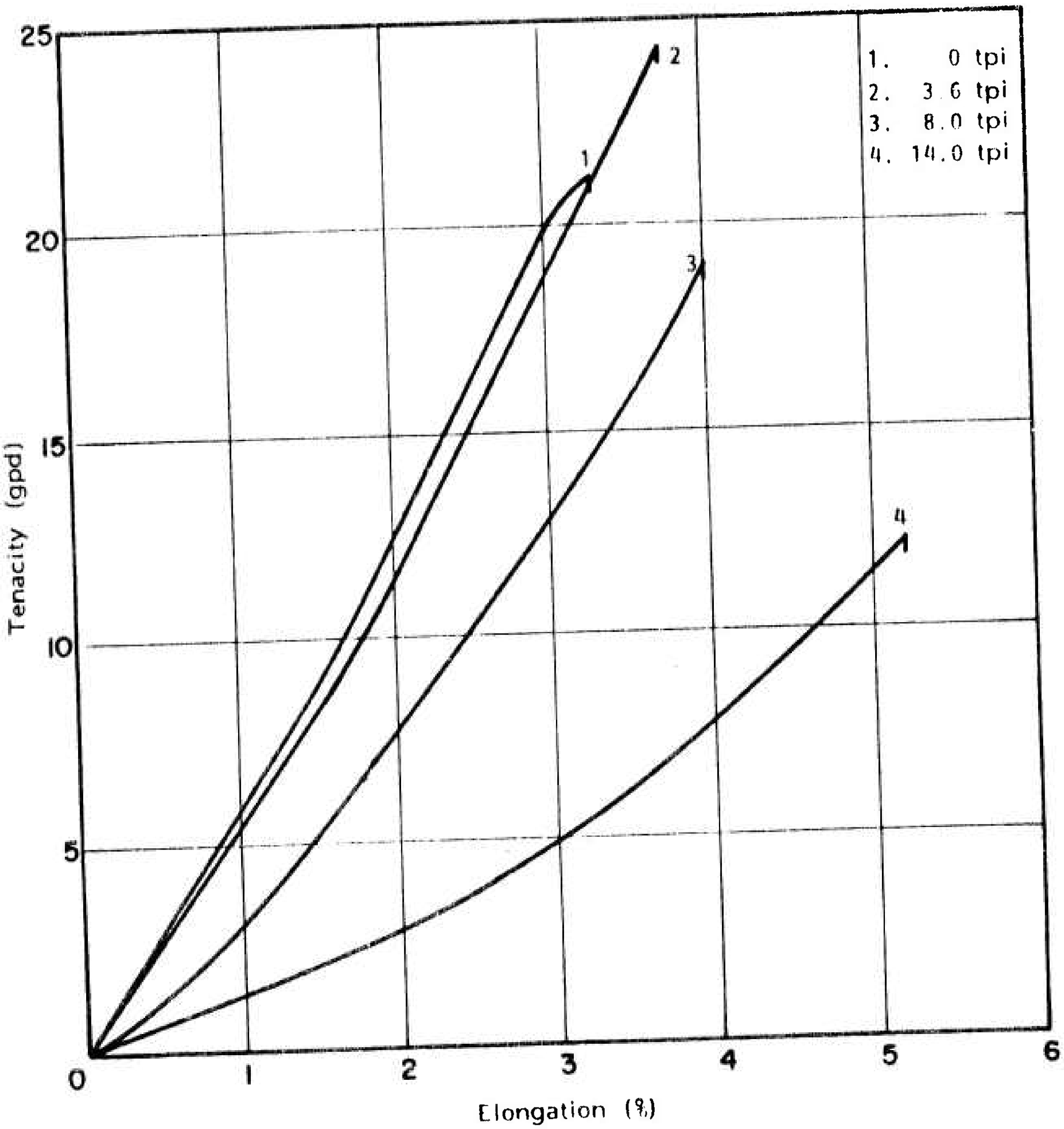

Figure 13. Typical Stress-Strain Diagrams of Kevlar 29 Twisted Yarn

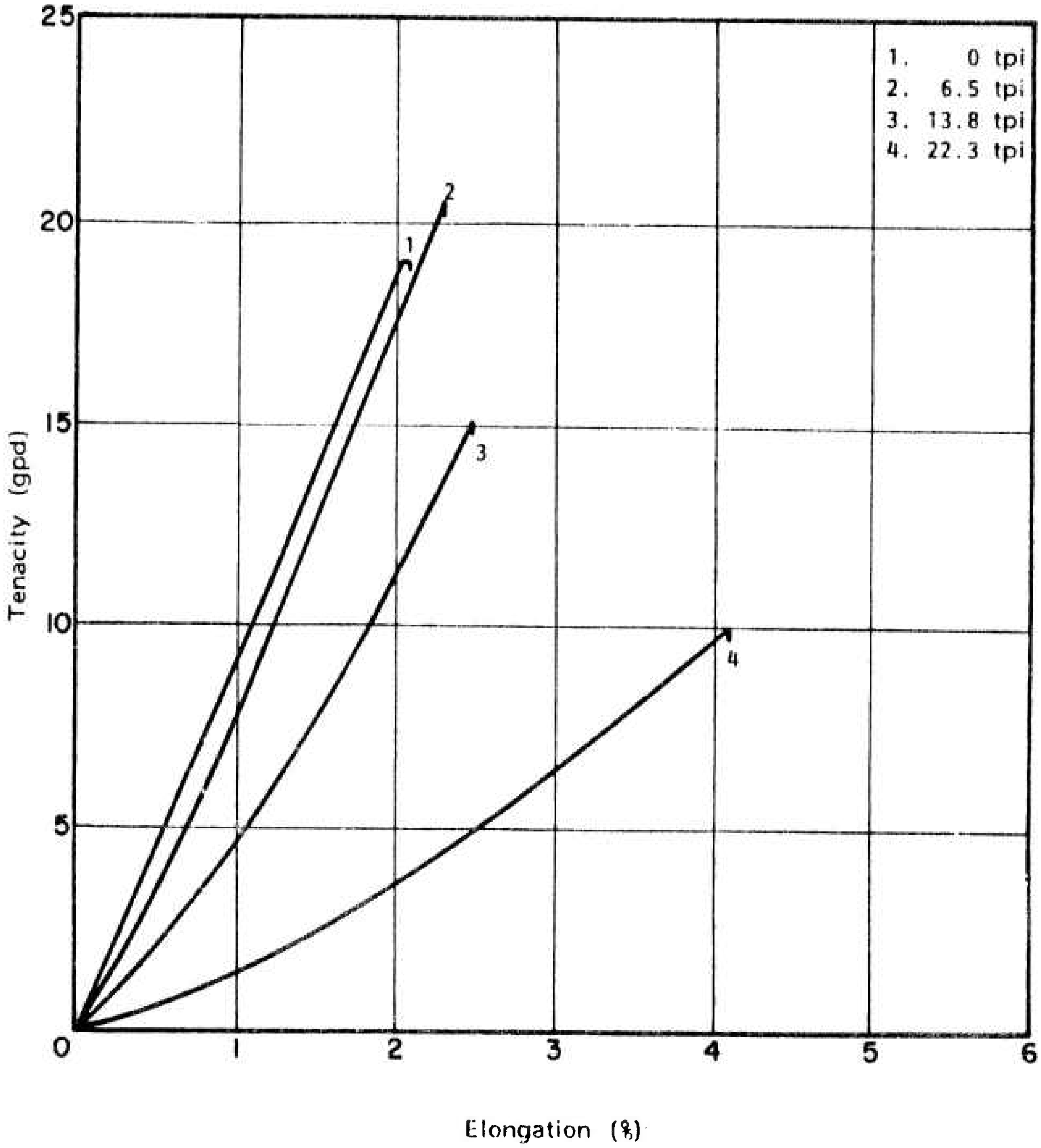

Figure 14. Typical Stress-Strain Diagrams of Kevlar 49 Twisted Yarn

tenacity with increasing twist is larger for the Kevlars than for conventional textile fibers. The decrease in modulus with increasing twist is also more for the Kevlars than can be accounted for by geometric analysis of a model of a conventional twisted yarn structure.

Testing of fibers removed from the twisted yarn showed that fiber damage accounted for more than half of the observed loss in yarn strength due to twisting. A check which was made on the effect of twisting, bending or lateral compression on single fiber strength indicated that the latter caused significant strength loss, pure bending a small amount, and pure twisting none at all. It was concluded that the high strength loss in twisted yarns could be adequately explained by the combined effects of yarn geometry and fiber damage, and that a complete explanation of the type and cause of the fiber damage occurring in twisted yarns would have to await the results of a detailed microscopic examination.

6. Loop and Knot Strength

The loop and knot strengths and efficiencies of Kevlar 29 and Kevlar 49 yarn are illustrated in Figures 15 through 18. At normal twist levels, loop efficiencies are approximately 60% and knot efficiencies approximately 40%.

7. Other Miscellaneous Activities

a. The effect of calendering on heat stabilized and dyed PBI fabric was studied, and a procedure developed which significantly improved both the appearance and the hand of such fabric.

b. During the course of the work, short lengths of several experimental fabrics were woven from stock dyed PBI fiber.

c. The moisture regain of heat stabilized PBI and of HT-4 was determined over a range of humidites. At 65%RH, the values obtained were 15.0% for PBI and 7.4% for HT-4.

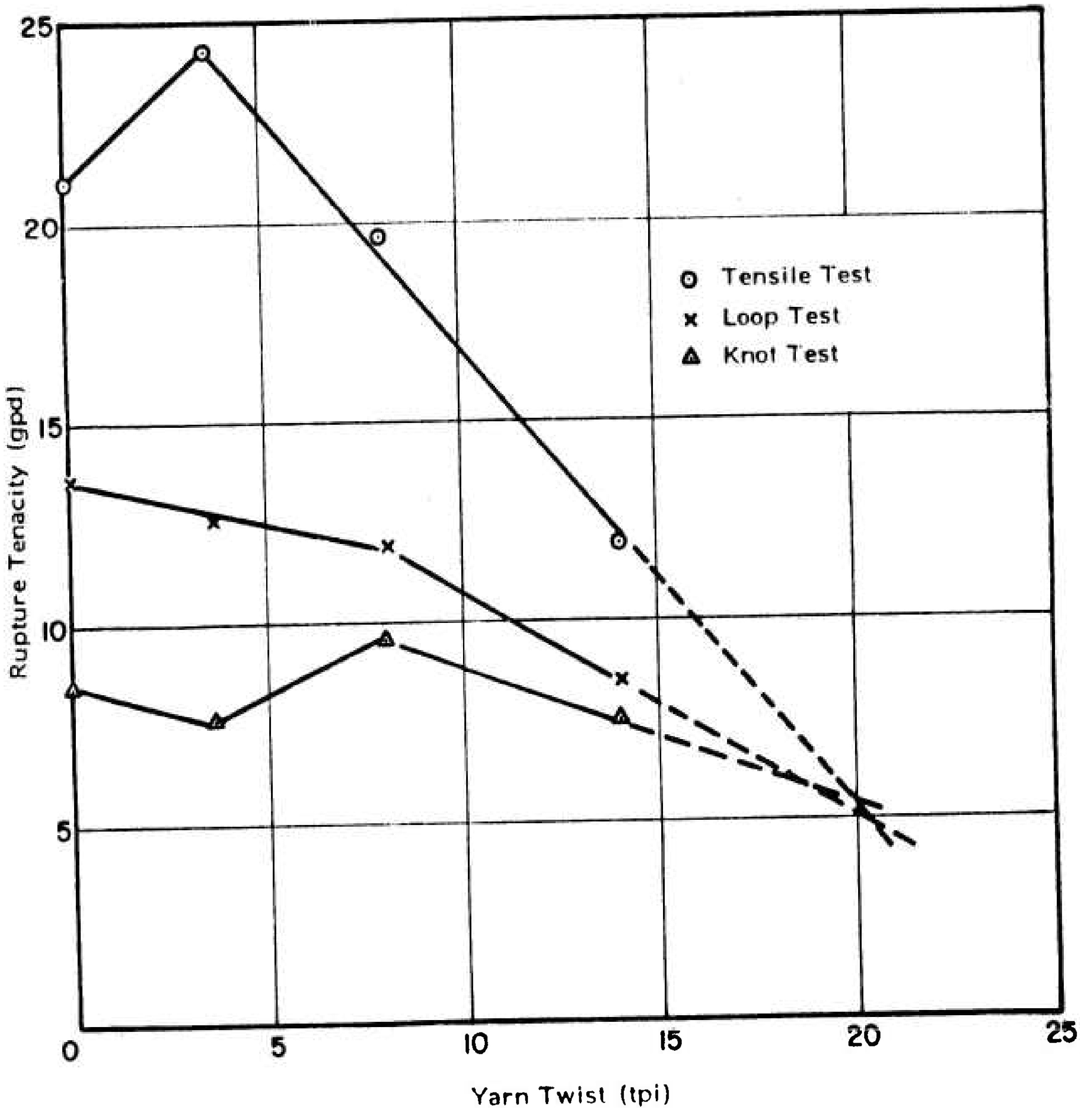

Figure 15. Loop and Knot Strength of Twisted Kevlar 29 Yarn

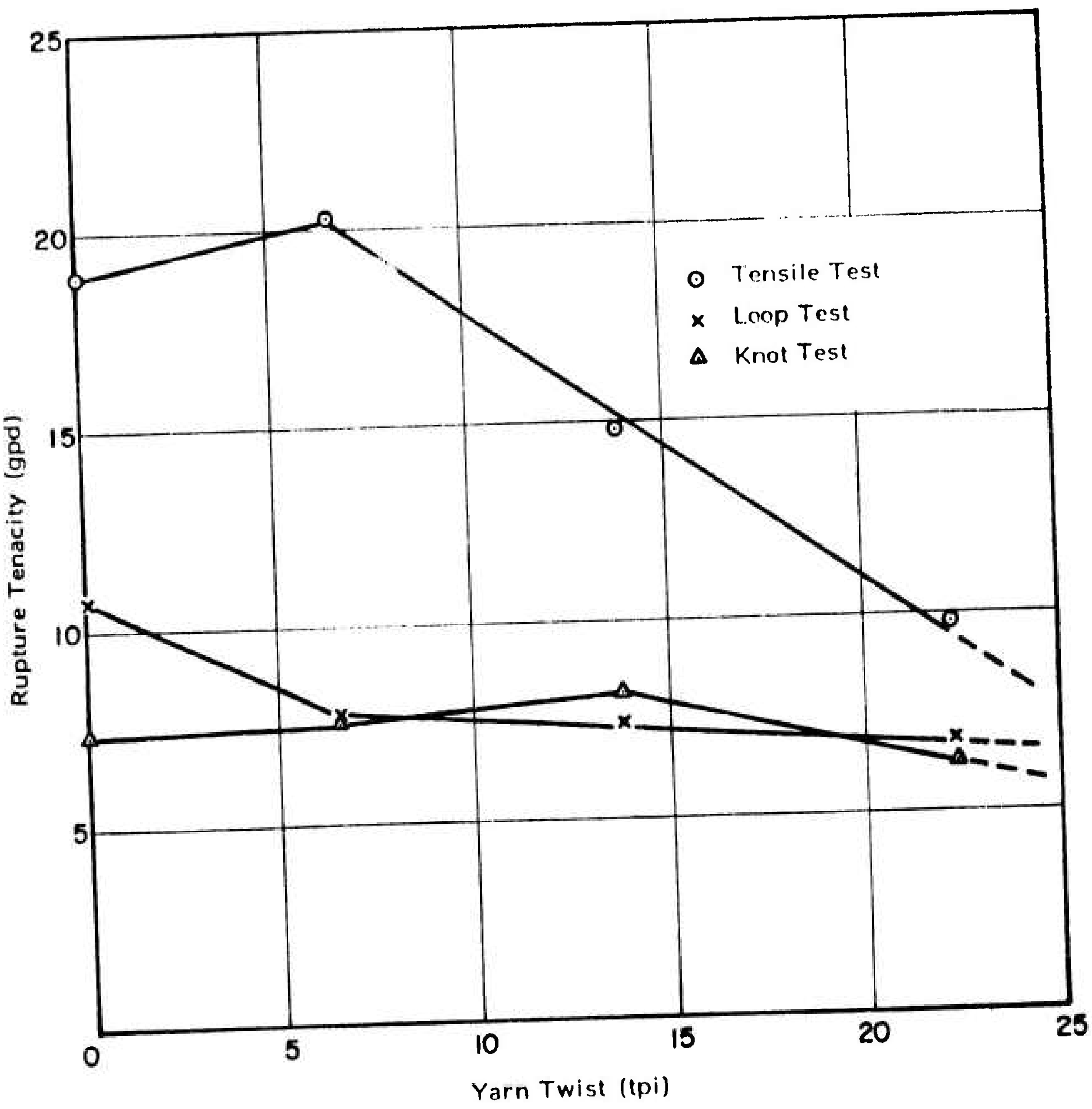

Figure 16. Loop and Knot Strength of Twisted Kevlar 49 Yarn

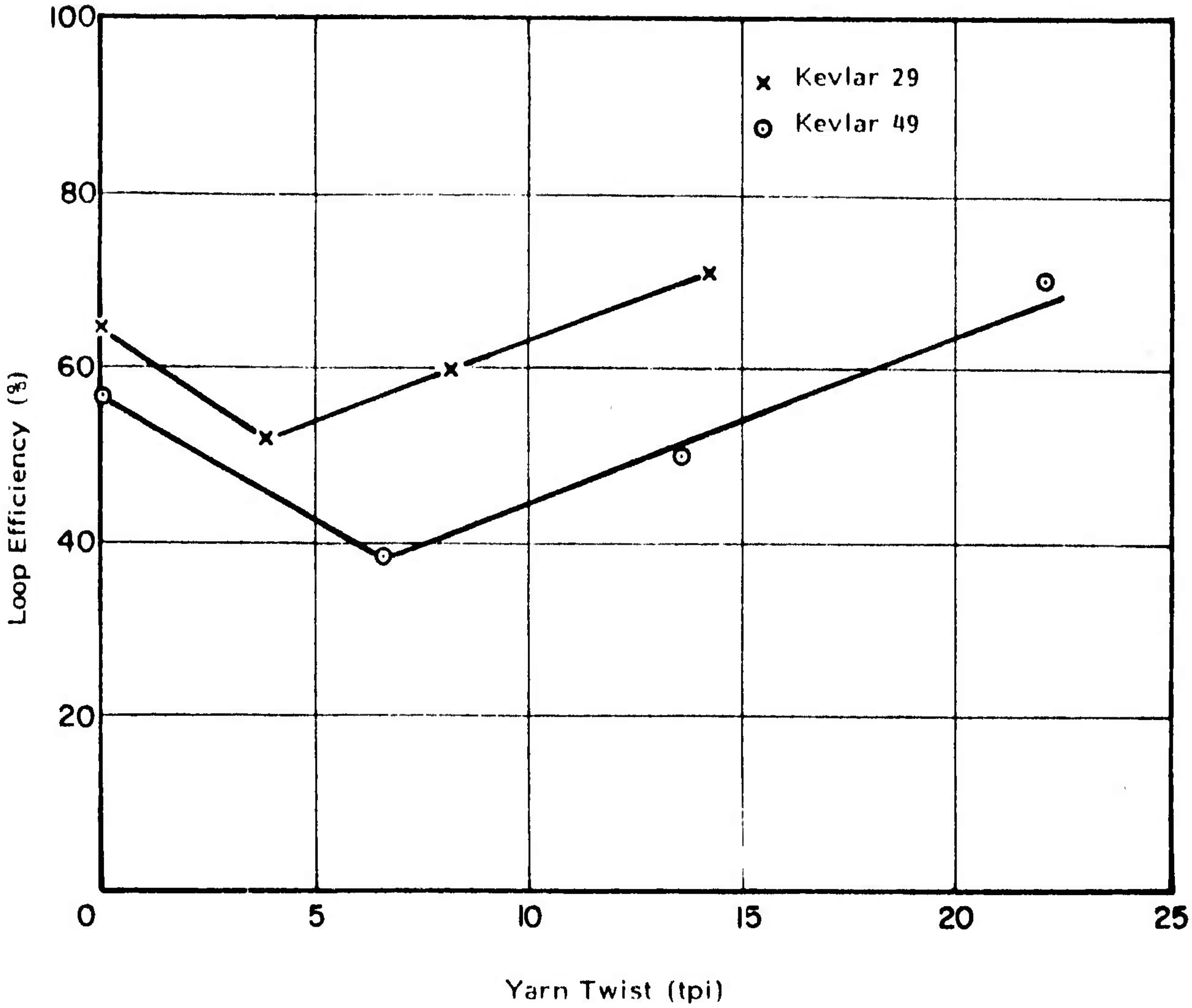

Figure 17. Loop Efficiency of Twisted Kevlar Yarns

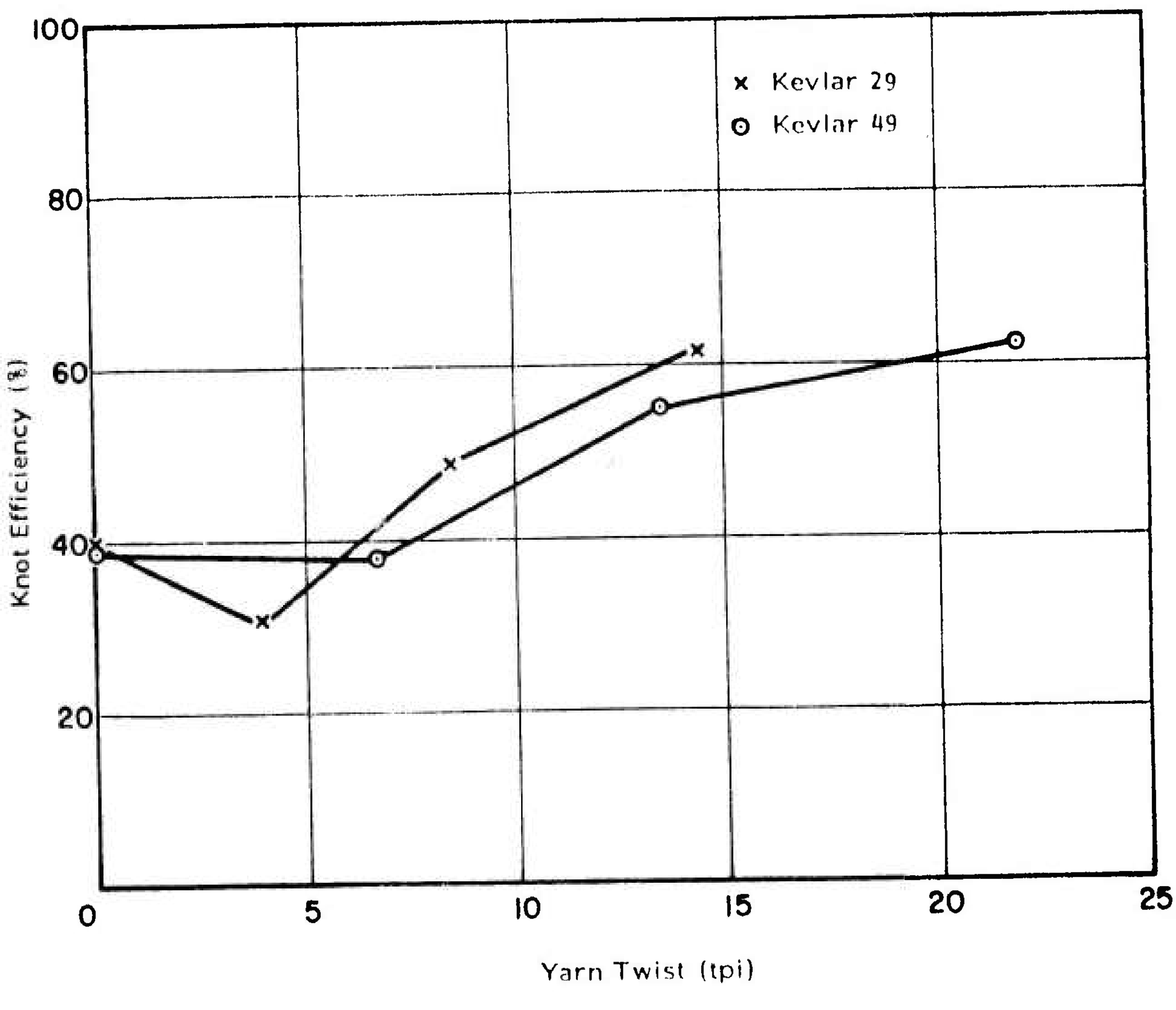

Figure 18. Knot Efficiency of Twisted Kevlar Yarns

SECTION III

TENSILE PROPERTIES

1. Wet Kevlar Yarns

The tensile properties of 1500 denier Kevlar 29 yarn and 400 denier Kevlar 49 yarn were determined in water at both 70°F and 190°F. The yarn specimens were submerged during testing in water contained in a large vessel mounted on the crosshead of an Instron tensile test machine. The 1.0 inch diameter capstan jaws, Figure 19, employed in all previous Kevlar yarn testing were used to grip the specimens. In this case, however, the pulley, attached to the bottom of the vessel by means of a threaded connection, became the bottom jaw. Specimens were mounted in the empty vessel, which was then filled from a reservoir. For the 190°F tests the water in the reservoir was heated to boiling and continuously circulated through the vessel. The specimens were entirely submerged during both the 5 minute soak period and the actual test. A strain rate of 10%/min and a gauge length of 10 inches were used (specimen length, 20 inches).

The tensile data obtained for the Kevlar 29 yarn are given in Table III; that for the Kevlar 49 yarn in Table IV. Data obtained under comparable conditions in air on the same yarns are also given in the tables for comparison. At 70°F the tensile properties of the 1500 denier Kevlar 29 yarn show no change in water; the 400 denier Kevlar 49 yarn retains 95% of its strength while the modulus is essentially unaffected. The wet strength of nylon yarn at 70°F is commonly reported as 80-90% of its conditioned strength. The effect of a test temperature of 200°F is approximately twice as severe in water as in air; the Kevlar 29 yarn retains 92% of its strength in air, 86% in water; the Kevlar 49 yarn retains 87% of its strength in air, 78% in water. The modulus of both materials falls by ~10% in air and ~20% in water at 200°F.

2. Low Speed Tensile Strain Cycling of Kevlar 29 Yarn at 70°F and 400°F

a. Introduction

Most textile structures, including fabrics, webbings, braids and cords, are required to endure repeated straining during use; knowledge of the ability of Kevlar yarns to withstand such cycling, both at ambient and elevated temperatures, will help determine their ultimate usefulness in high performance textile structures. Consequently, the cycle lifetime of 400 denier Kevlar 29 yarn has been measured at 70°F and 400°F at various strain levels. The effect of clamping surface roughness on the cycle lifetime was also investigated. The amount of recovery from various levels of repeated straining is also of importance to the performance of the Kevlar material and was determined as an adjunct to the measurement of cycle lifetime.

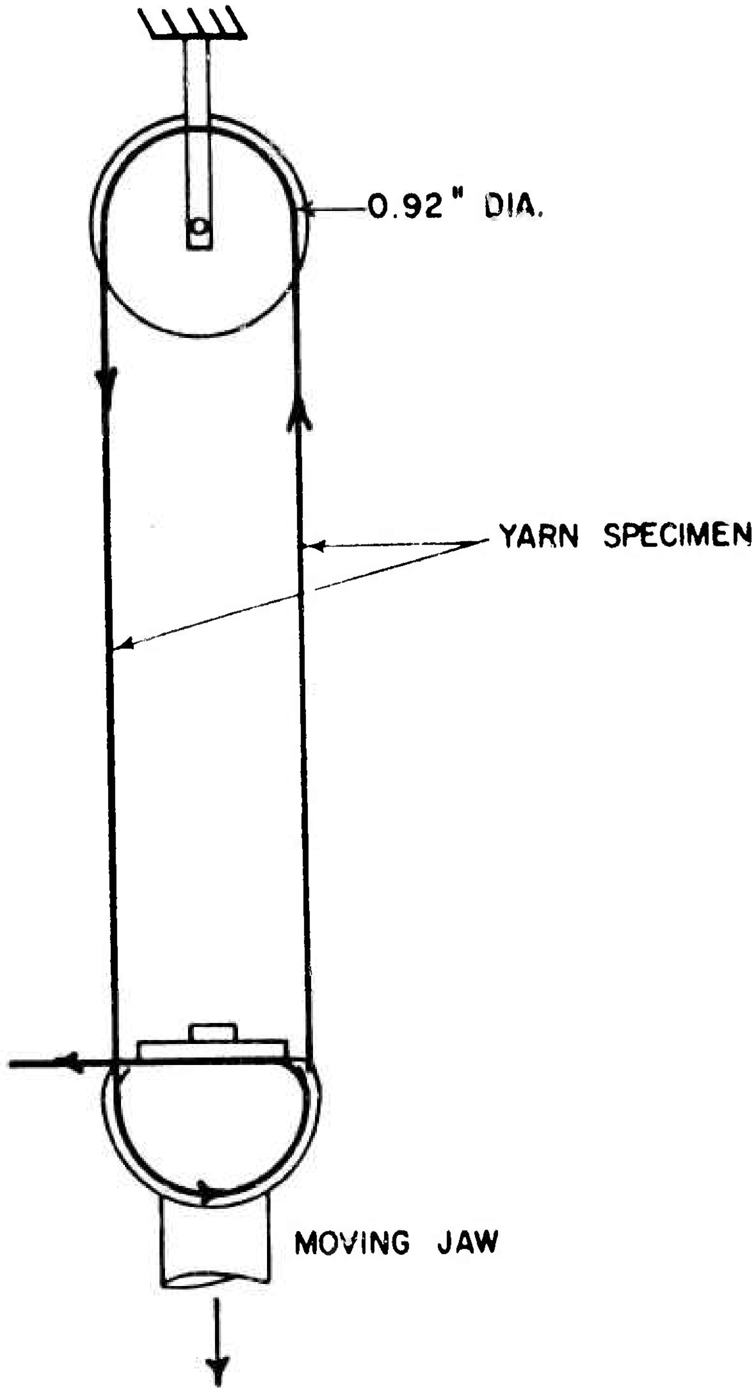

Figure 19. Tensile Test Configuration
Using Capstan Jaws

Table III: Tensile Properties of 1500 Denier Kevlar 29 Yarn in Water at 70°F and 190°F

Test Conditions		Initial Modulus (gpd)	Change in Modulus (%)	Rupture Elongation (%)	Rupture Tenacity (gpd)	Strength Retention (%)
in air, 70°F		480		3.5	19.7	
		481		3.5	18.7	
		480		3.8	20.5	
		490		4.0	20.7	
		494		3.4	19.2	
	Average	485	---	3.6	19.8	---
in water, 70°F		499		3.6	20.3	
		479		3.8	21.0	
		485		3.5	19.3	
		489		3.6	20.3	
		490		3.4	19.4	
	Average	488	0	3.6	20.1	100
in air, 200°F		432		3.5	18.7	
		433		3.3	17.8	
		450		3.4	18.9	
		432		3.4	18.1	
		414		3.5	18.1	
	Average	432	-11	3.4	18.3	92
in water, ~190°F		382		3.5	17.8	
		377		3.4	16.6	
		355		3.6	17.8	
		401		3.5	19.0	
		377		3.0	14.0	
	Average	378	-22	3.4	17.0	86

Table IV: Tensile Properties of 400 Denier Kevlar 49 Yarn in Water at 70°F and 190°F

Test Conditions		Initial Modulus (gpd)	Change in Modulus (%)	Rupture Elongation (%)	Rupture Tenacity (gpd)	Strength Retention (%)
in air, 70°F		911		2.1	19.2	
		910		2.3	21.3	
		899		2.3	20.8	
		901		2.2	20.2	
		901		2.2	20.2	
	Average	904	---	2.2	20.3	---
in water, 70°F		888		2.1	19.2	
		898		2.1	19.9	
		892		2.2	19.9	
		878		2.1	18.7	
		902		2.1	18.7	
	Average	892	- 1	2.1	19.3	95
in air, 200°F		840		2.0	17.5	
		768		2.1	17.6	
		848		1.9	16.8	
		791		2.1	17.8	
		808		2.1	18.5	
	Average	811	-10	2.0	17.6	87
in water, ~190°F		738		1.9	15.2	
		644		1.9	14.9	
		752		2.0	17.1	
		748		1.8	15.1	
		726		2.1	16.8	
	Average	726	-20	1.9	15.8	78

b. Experimental Procedure

Specimens of 400 denier Kevlar 29, twisted 5 tpi, were strained repeatedly in an Instron tensile test machine at a rate of 10%/min both during the loading and unloading portions of the cycle. The one-inch diameter capstan jaws, illustrated in Figure 19, were used to grip the specimens as in all other tensile testing of Kevlar yarn. However, early in the testing program it became apparent that the unpolished, machined steel surface of these jaws was causing significant abrasion damage and premature failure of the yarn. Various other jaw types and contact surface materials were evaluated in an attempt to find a jaw clamping system capable of successfully gripping the specimens at loads near rupture while causing a minimum of abrasion damage. Teflon tape, 5 mils thick, applied to the surface of the capstan jaws was eventually chosen for the remainder of the work since it provides an extremely smooth, friction-free surface in contact with the yarn while retaining the clamping advantage of the capstan jaws.

The effective specimen gauge length, measured at an 8.0 inch distance between capstan centers and determined using the method outlined in Section II,2 of AFML-TR-74-65, Part II, was 10.0 inches on the machined steel surface at 70°F, 10.9 inches on the Teflon surface at 70°F, and 11.2 inches on the Teflon surface at 400°F. The larger effective gauge length on the Teflon surface at 70°F compared with that on the machined steel is an indication of the greater smoothness of Teflon. Elevated temperature further decreases the frictional properties of the Teflon tape.

The 400°F test temperature was achieved in a circulating hot-air oven mounted in an Instron. Specimens were held at temperature for 10 minutes prior to both the initiation of cycling and tensile testing to failure. The Teflon tape survived the 400°F temperature with no apparent damage.

The amount of strain recovery, as a percentage of the applied strain, was measured on the loading portion of the stress-strain diagram at various cycle levels during the lifetime cycling on the Teflon surface. No additional time was allowed for recovery other than that normally occurring at zero load between successive cycles.

c. Experimental Results and Discussion

The tensile properties of the 400 denier Kevlar 29 yarn, 5 tpi, measured at both 70°F and 400°F using Teflon-taped capstans and a strain rate of 10%/min are given in Table V. Typical stress-strain diagrams for the two test temperatures are presented in Figure 20. The yarn retains 69% of its original strength at 400°F and shows a decrease of 13% in the initial modulus. The tensile properties at 400°F vary more about the average value than at 70°F.

The cycle lifetime of the Kevlar 29 yarn is plotted in Figure 21 as a function of the maximum strain to which it was cycled. Data are presented for cycling at 70°F on both the machined steel and the Teflon taped surface of the capstan jaws.

Table V: Tensile Properties of 400 Denier Kevlar 29 Yarn, 5 tpi, Obtained on Teflon-Taped Jaws at 70°F and 400°F

Temp (°F)	Denier	Initial Modulus (gpd)	Rupture Elongation (%)	Rupture Tenacity (gpd)	Strength Retention (%)
70	418	701	3.3	26.1	
	418	691	3.3	25.7	
	418	685	3.3	26.3	
	418	691	3.2	25.0	
	417	654	3.4	26.1	
Average	418	684	3.3	25.8	---
400	396*	575	2.7	20.0	
		581	2.6	19.2	
		660	2.2	16.6	
		601	2.3	16.7	
		572	2.6	17.9	
		586	2.6	18.9	
		616	2.3	16.7	
		624	2.2	16.2	
		583	2.7	19.1	
		563	2.3	16.0	
Average		596	2.5	17.7	69

*70°F denier corrected for 5.2% weight loss at 400°F.

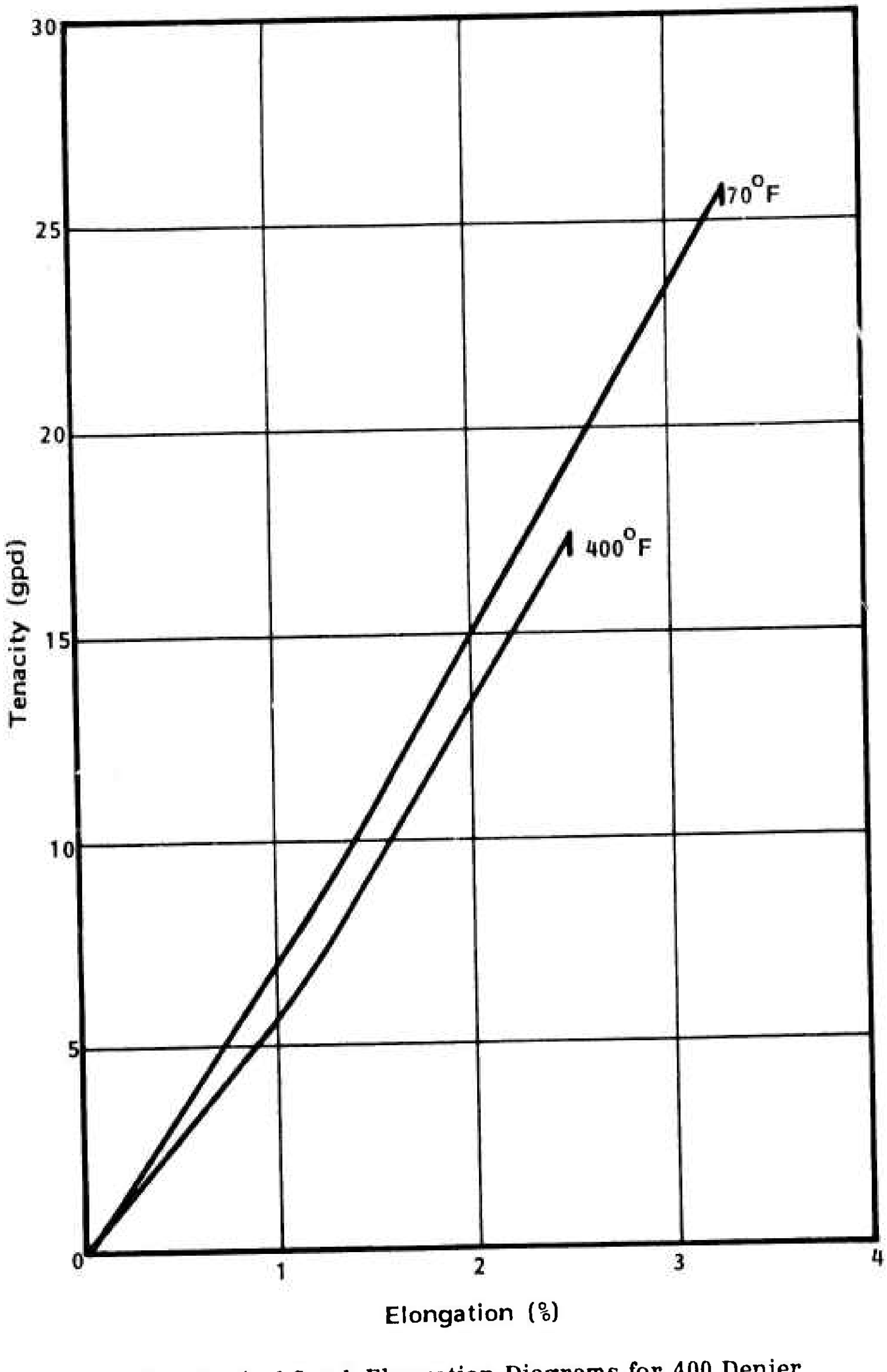

Figure 20. Typical Load-Elongation Diagrams for 400 Denier Kevlar 29 Yarn, 5 tpi, Obtained on Teflon Taped Capstan Jaws - 70°F and 400°F

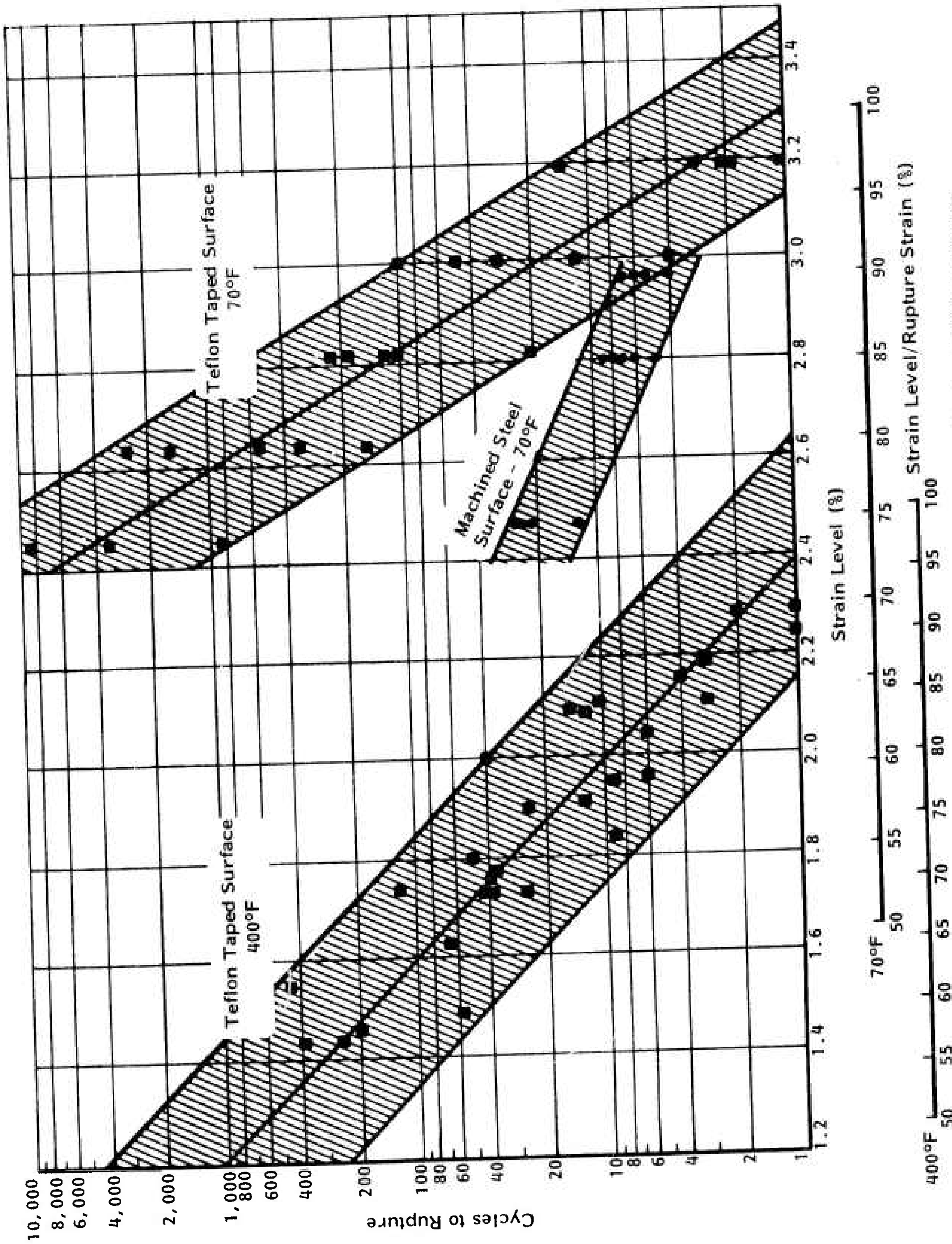

Figure 21. Cycle Lifetime of 400 Denier Kevlar 29 Yarn, 5 tpi, at 70°F and 400°F

At 400°F data were obtained on the Teflon taped surface only. The centerline of the two bands of data obtained on the Teflon surface were fitted to the data points using the method of least squares; the boundaries of each band were drawn to contain all data points and also to lie symmetrically about the centerline.

The large variation in the data at both temperatures, more than one order of magnitude, probably reflects both the unpredictable nature of abrasion damage and the variation in tensile properties from specimen to specimen. The band intercepts on the strain level axis correspond very closely to the range of rupture strain values obtained at each temperature, while the centerline of each band intersects this axis at a value of strain nearly equal to the average rupture strain. At 70°F, the strain level achieved varied by no more than ±0.02% from the nominal level. However, at 400°F the strain level was not as easily controlled because of the necessity of mounting specimens in the jaws removed from the Instron. Consequently, the strain level varied somewhat from specimen to specimen.

The vast improvement in cycle lifetime resulting from the increased smoothness of the Teflon surface is quite evident in Figure 21. At 75% of the first cycle rupture strain (approximately 2.5% strain) the lifetime at 70°F on the Teflon surface is on the order of 900 to 9000 cycles; on the machined steel surface, it is only 12-30 cycles. At 90% of the first cycle rupture strain (~3.0% strain), the lifetime on the Teflon surface ranges from 4 to 99 cycles; on the machined steel, from 4 to 7 cycles. Failures on both surfaces seem to be the result of abrasion, but it is obvious that the Teflon tape affords a considerable degree of protection.

Since the average rupture elongation of the Kevlar yarn decreases from 3.3% at 70°F to 2.5% at 400°F, comparisons of the cycle lifetime at these temperatures at the same absolute strain level are not valid. However, on the basis of strain level as a percentage of the first cycle rupture strain at each temperature, the effect of temperature on cycle lifetime can be evaluated. At 75% of the first cycle rupture strain, the lifetime at 70°F is 900-9000 cycles; that at 400°F, 5-80 cycles. At 90%, the lifetime at 70°F is 4-99 cycles; while at 400°F, it is 1-10 cycles. Cycle lifetime decreases from one to two orders of magnitude with an increase in temperature to 400°F.

Small changes in strain level result in very large changes in cycle lifetime on the Teflon surface at both test temperatures: an order of magnitude increase for a decrease in strain level of 0.25% at 70°F and 0.4% at 400°F.

The strain recovery, as a percentage of the applied strain, is summarized in Table VI. Each entry represents the average value for all specimens which reached the cycle level indicated. The amount of recovery, both at 70°F and at 400°F is remarkably independent of strain level over the range of strains studied, but decreases progressively with increasing number of cycles. The recovery is roughly 85% after one cycle and 66% after 9000 cycles at 70°F; it is about 78% after one cycle and 60% after 100 cycles at 400°F. The increase in temperature to 400°F is accompanied by an ~7% decrease in the recovered strain at all cycle levels.

Table VI: Recovered Strain in Cycled 400 Denier Kevlar 29 Yarn, 5 tpi, at 70°F and 400°F

Temp (°F)	Strain Level (%)	Strain Level % of Rupture Strain	Recovered Strain (% of applied strain) 1	5	10	20	100	500	2500	9000 Cycles
70	2.45	74	87	82	79		73	71	69	66
	2.64	80	87	81	79		74	69	68	
	2.82	85	85	81	79		75			
	3.00	91	85	80	78					
	3.19	97	84	78	76					
400	1.46	58	80	75	74	73	68			
	1.74	70	78	73	71	70				
	1.91	76	77	73	70					
	2.08	83	77	72						
	2.18	87	77							
	2.28	91	78							

The load level reached after successive cycles to the same strain falls only slightly over the lifetime of the specimen, thus the modulus increases during cycling to a value approximately equal to k times the original modulus where

$$k = \left[\frac{1}{\text{Strain Recovery}}\right]$$

d. Conclusions

The Kevlar 29 yarn is capable of withstanding many cycles of tensile strain at high strain levels if the surface to which it is attached is relatively friction-free. Although the cycle lifetime is considerably reduced at temperatures of 400°F, it remains sufficiently high at strain levels below 50% of the first cycle rupture strain at 70°F that it probably need not be of tremendous concern in the ultimate application of the material. Of greater concern is the effect of attachment surface roughness on cycle lifetime at 70°F.

Strain recovery from repeated tensile straining is better than 70% at temperatures up to 400°F and cycle levels up to 100.

SECTION IV

TORSIONAL STRESS-STRAIN BEHAVIOR OF KEVLAR FIBERS AND YARNS

1. Introduction

Although the basic element in the majority of textile structures is a twisted, bent fiber, torsional and bending properties of fibers are not always given due attention, probably because they are relatively difficult to measure, and once measured, results tend to be difficult to interpret and apply constructively. In this study of torsional properties of Kevlar fiber, efforts were made to minimize these potential problems. The essential portions of the work were performed using the FRL torsional measurement device, shown in Figure 22, which permits the generation of complete torsional stress-strain diagrams for single fibers in a comparatively straightforward manner. To add perspective and utility to the Kevlar 29 and Kevlar 49 data obtained, comparable data was also generated for nylon, Nomex, and polyester fibers.

In addition to the development of basic torsional fiber data, a heat setting study was made using 100 denier Kevlar 29 yarn, in whch the torsional recovery was measured after exposure of the twisted yarn to various temperatures. The net effect of elevated temperature exposure and twist level upon yarn strength was also evaluated. Although the torsional recovery and strength change data obtained and reported is specific to the particular yarn used, twist levels attained, and setting conditions employed, it provides a practical example of limitations that would be encountered in the heat setting of any Kevlar 29 yarn.

2. Calibration and Testing Techniques

Specimen preparation for the FRL torsional measurement device involves the cementing of upper and lower transverse mounting wires to a length of fiber, the spacing of the wires determining the gauge length. The upper wire is then placed over hooks suspended from the movement of a galvanometer, as shown in Figure 22. A tensioning weight, which also serves as a drive key, is hung over the lower mounting wire and slipped into a slot in the drive shaft of the instrument. Throughout this procedure, extreme care is required to ensure that the axis of the mounted fiber is concentric with the common axis of the galvanometer and drive shaft. During a test, as the fiber specimen is twisted, current is applied to the coil of the galvanometer to prevent rotation of the meter mechanism and pointer. The magnitude of this nulling current is recorded at regular increments of twist and later converted to units of torque and plotted versus twist level to yield a torsional stress-strain diagram.

Conversion of nulling current readings to specimen torque values requires the application of a calibration factor that was determined experimentally at the outset of the work by testing a Chromel R filament. Chromel R was known to have a torsional stress-strain curve with a long, linear, initial portion and its torsional shear modulus, G, was measured by the torsional pendulum method. A typical calibration curve is shown in Figure 23.

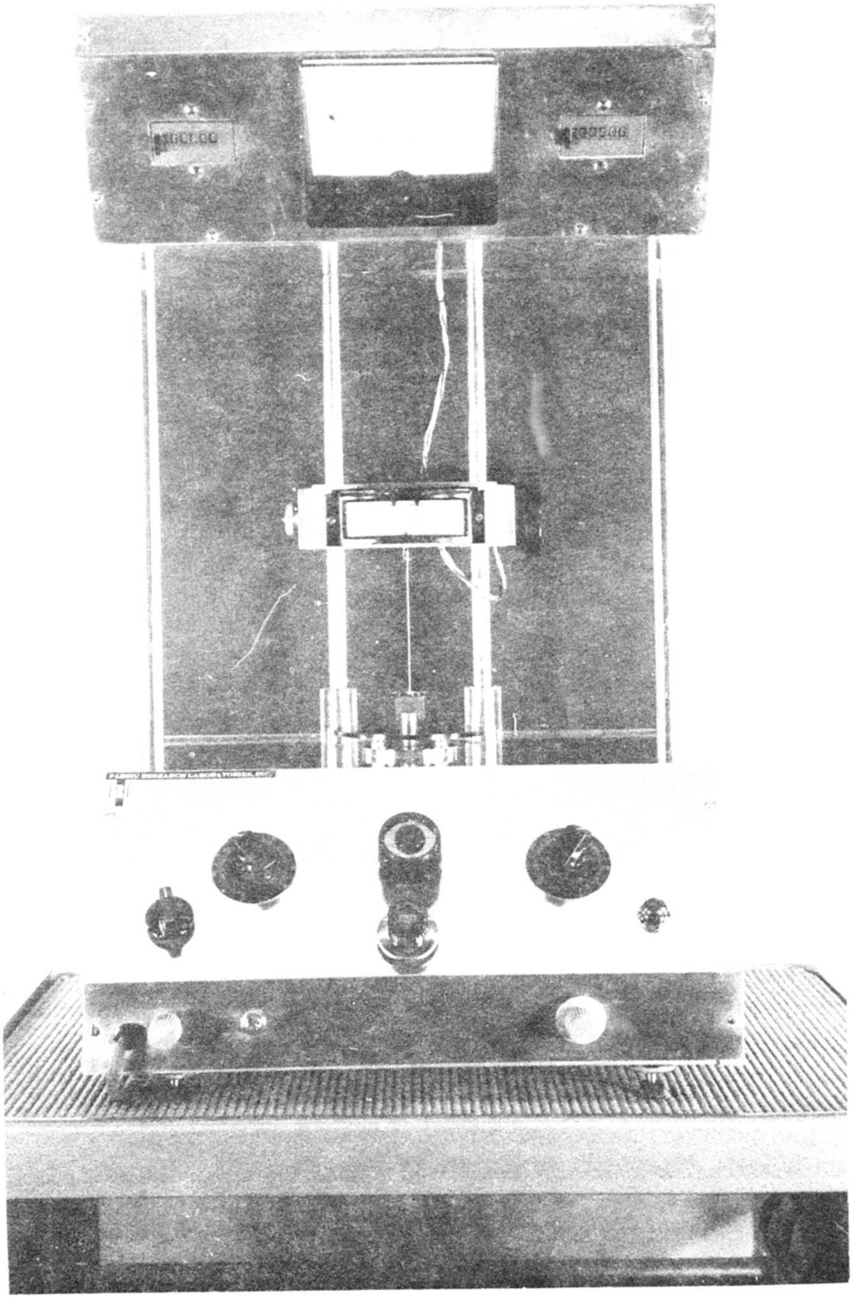

Figure 22. The FRL Torsion Measurement Device

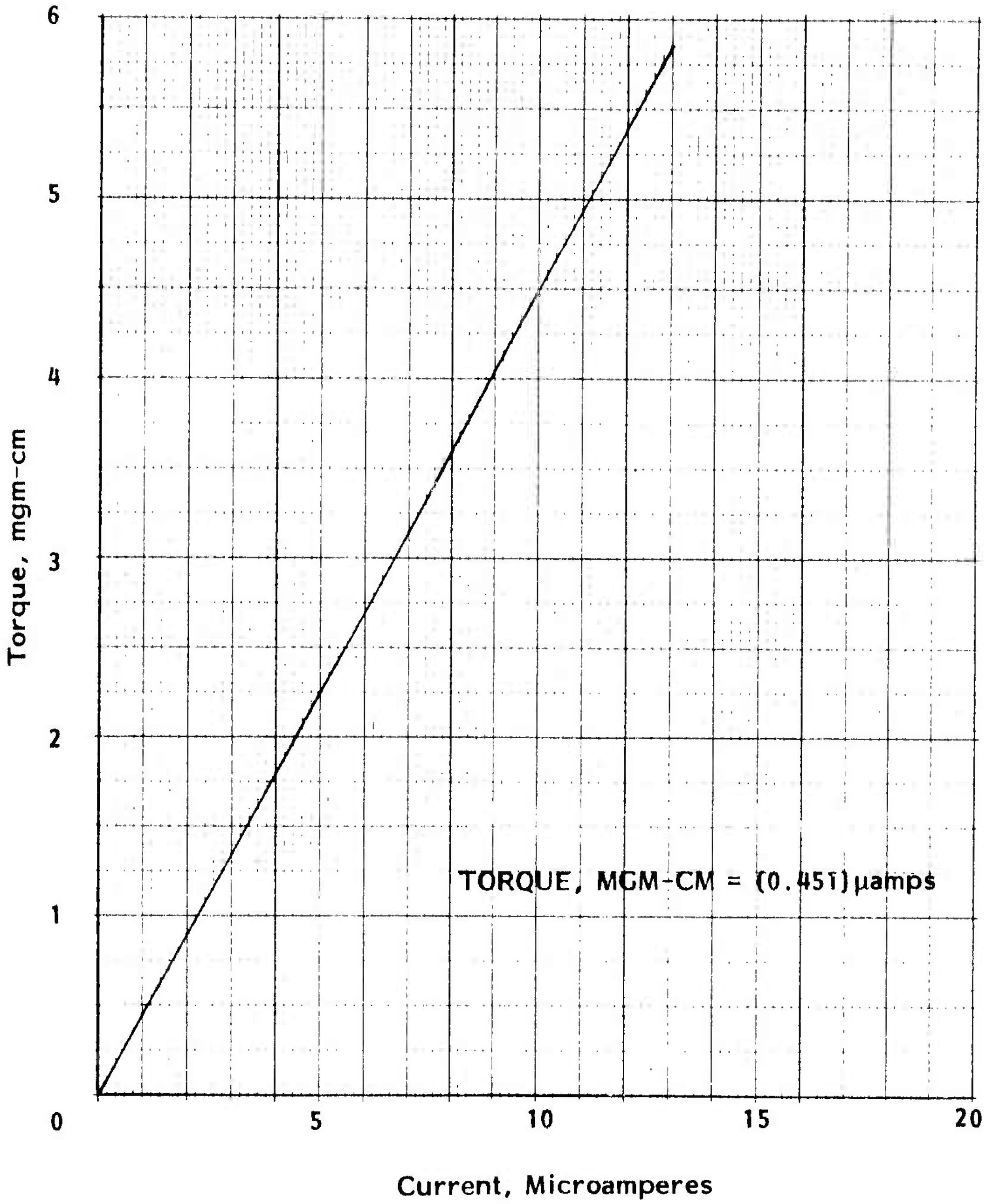

Figure 23. Torsion Device Calibration Curve Obtained Using 25 Micron Diameter Chromel R Wire and a Torsional Pendulum

In addition to the several torsional pendulums of Chromel R filament required during the course of instrument calibration, several more were assembled using Kevlar 29 fiber. Each torsional pendulum was made by cementing one end of a filament to a fixed hanger and the other end to a very light wire stirrup that cradled a round inertia rod. The wire stirrup allowed the inertia rod to be precisely centered on the fiber axis after the assembly was suspended from the fixed hanger. After centering the inertia bar, the pendulum was placed in a draft-free glass container. Torsional oscillation was induced without otherwise disturbing the hanging fiber by rotating a magnet underneath the steel inertia bar. The torsional rigidity, Γ, of the fiber was calculated from the relationship:

$$\Gamma = \frac{8\pi^3 IL}{T^2} \tag{1}$$

where I is the moment of inertia of the inertia rod about the fiber axis, L is the free fiber length, and T is the period of oscillation. The shear modulus, G, was obtained from the equation:

$$G = \frac{\Gamma}{S^2 \varepsilon} \tag{2}$$

where S is the cross-sectional area of the filament and ε is a shape factor that is equal to unity for round fibers such as the ones used. The shear modulus values obtained and other data pertinent to each pendulum are presented in Table VII.

The value of the torsional shear modulus of Kevlar 29 obtained using the torsional pendulum method was compared with that obtained on the FRL torsional measurement device by superimposing the straight line representing the pendulum-derived modulus onto a torsional stress-strain diagram plotted from data generated with the torsional device. This comparison is shown in Figure 25 and the agreement between the pendulum-determined modulus and the initial portion of the stress-strain diagram is quite good. There is a plausible explanation for the small disparity that does exist between the two curves. After several torsional pendulums had been assembled and the periods of oscillation timed, it became apparent that pendulums whose periods were relatively short, i.e., one to two seconds, yielded more repeatable results. The pendulums used for Kevlar 29, however, had periods from seven to ten seconds and it was demonstrated experimentally that they were affected to a proportionally greater degree by local magnetic disturbances and by air resistance. Such disturbances would most certainly increase the timed period and result in a lower calculated shear modulus. In order to shorten the period of a torsional pendulum, the specimen must be reduced in length, the inertia bar made smaller, or a greater diameter fiber used. However the fiber lengths and I-bar masses used in the Kevlar 29 tests have already been reduced to workable minimums and the fiber diameter is fixed. There is little possibility of improvement in the experimental accuracy.

After the torsional measurement device was calibrated, several preliminary tests were made to establish a satisfactory testing speed. Using 5 cm long fibers, a twisting rate of 16 turns/cm/min was found to be the practical upper limit. Above

Table VII: The Torsional Stiffness of Two Fibers Determined by the Use of a Torsional Pendulum

Fiber Type	Fiber Diameter (microns)	Fiber Length (cm)	Inertia Bar Mass (mg)	Inertia Bar Length (cm)	Pendulum Period (sec)	Shear Modulus, G (10^{10} dyne/cm^2)	Shear Modulus, G (10^6 psi)
Kevlar 29	12.0	2.75	11.3	1.70	10.4	1.35	0.20
	12.0	1.60	11.3	1.70	7.9	1.35	0.20
	12.0	1.25	11.3	1.70	7.2	1.26	0.18
					Avg	1.32	0.19
Chromel R	25.5	3.25	126.2	2.42	1.51	83.3	12.1
	25.5	3.00	343.2	3.40	3.37	82.8	12.0
	25.5	2.35	126.2	2.42	1.29	82.3	11.9
	25.5	2.28	343.2	3.40	2.87	86.9	12.6
					Avg	84	12.2

this rate, data acquisition and recording became somewhat unreliable. One-half this speed, 8 turns/cm/min, appeared to be an optimum testing speed and was used throughout the work. Within the range of 8 to 16 turns/cm/min, no strain rate effect was observed.

To prevent torsional buckling of the test specimen, a small tensile load must be applied. Prior experience had shown that such loading tends to increase the torque required to achieve a particular torsional deflection, and therefore the applied tensile load should be limited to the amount required to eliminate buckling. It was found experimentally that a minimal loading level of 0.9 gm was satisfactory for 1.5 denier Kevlar 29 and Kevlar 49 fiber (0.60 gpd) and for 2 denier fibers of nylon, Nomex, and polyester (0.45 gpd). Preliminary evidence that no torsional buckling occurred when specimens were tensioned with a 0.9 gm weight was provided by good agreement between the fiber retraction observed during testing and length changes calculated for various twist levels, based upon the geometry of the twisted fiber. If the observed retraction was significantly greater than that estimated, buckling would be suspected. To confirm the absence of buckling during the course of a test, photographs were taken of the weighted fiber end at discrete twist intervals. Measurement of retraction on each of the photographs obtained then made possible a plot of retraction versus twist level and any abrupt increase in retraction seen in this curve would indicate fiber buckling. This procedure was employed during tests of Kevlar 29 and Kevlar 49, which were the most susceptible to buckling of the five fibers tested, and the measurement verified that buckling had been successfully eliminated. The retraction-strain diagrams derived are shown in Figure 24, together with a theoretical plot calculated from an expression developed by Hearle [1] for the retraction of continuous filament yarns. This expression is based upon the fact that filaments at the outside of the twisted yarn are strained in tension, those in the center are in compression, and yarns positioned between these extremes are in an intermediate tensile or compressive state which is related to their position in the yarn. It must be assumed that a similar strain distribution is present in the cross-section of a torsionally strained single fiber, and the relatively good agreement between the experimental and theoretical curves lends credence to this. The difference that does exist between the curves at extreme levels of twist is probably attributable to a strain bias toward the compressive yield in the interior of the twisted Kevlar fiber, as a consequence of extremely low extensibility under tensile loads.

3. Torsional Stress-Strain Properties of Kevlar Fiber Compared to those of Nylon, Nomex, and Polyester

Six tests each of Kevlar 29 and Kevlar 49 fiber were made, twisting in the S direction, to accurately develop typical torsional stress-strain diagrams. Three tests each were made of nylon, Nomex, and polyester. In every instance the fiber specimens used were removed from low twist yarn (less than 0.5 turn/inch) and fiber diameter determinations were made using a projection microscope. Parent yarn designations and fiber diameters are recorded in Table VIII. All fibers tested, with the exception of Kevlar 49, were strained to a maximum of 140 to 150 turns/cm and then untwisted to the zero strain level. Kevlar 49 ruptures at a twist level of only 80 to 90 turns/cm so a limit of 70 turns/cm was used in tests of this fiber.

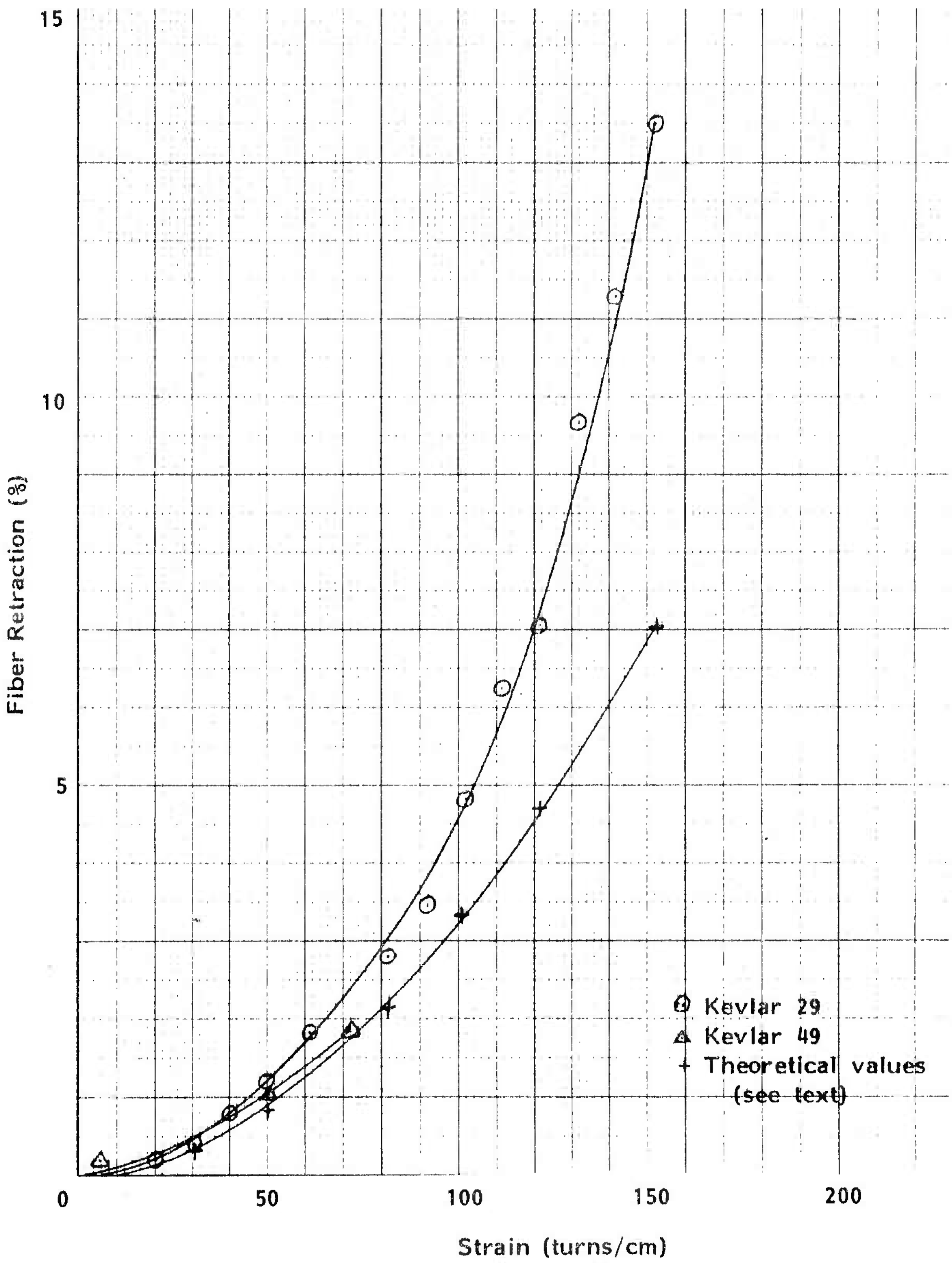

Figure 24. Length Retraction of 1.5 Denier Fibers as a Function of Torsional Strain

Stress-strain diagrams typical of those obtained for each of the five fibers are presented in Figures 25 through 29. Typical curves are presented rather than average curves since they represent yield points and other inflection points more accurately. Notice that the torsional stress-strain curves for Kevlar 29, nylon, Nomex, and polyester are all quite similar in form and correspond in general shape to tensile stress-strain curves for nylon, Nomex, and polyester fiber. They are totally unlike the tensile stress-strain diagram of Kevlar 29 fiber, which is essentially a straight line of high slope, indicative of a high tensile modulus. For Kevlar 49 the difference between the tensile and torsional behavior is not as extreme as for Kevlar 29.

The initial slope of the torsional stress-strain diagrams was measured to determine the torsional shear modulus, G, for each of the fibers tested. The values obtained are tabulated in Table VIII. Comparison of tensile moduli with the torsional shear moduli shown for each fiber provides further evidence of the highly anisotropic nature of Kevlar 29 and Kevlar 49. These comparisons can be readily made in familiar terms by calculating the effective Poisson's ratio from the expression:

$$\mu = \frac{E}{2G} - 1 \tag{3}$$

where μ is effective Poisson's ratio, E is the tensile modulus, and G is the shear modulus. Although this expression is strictly valid only for isotropic materials, the values of μ obtained nevertheless provide evidence of the extent of anisotropy: μ is equal to 18 for Kevlar 29, 37 for Kevlar 49, 6 for nylon, 6 for Nomex and 8 for polyester. For conventional polymeric materials, this value does not usually exceed 10. The extreme anisotropy of Kevlar is presumed to be the result of a high degree of drawing during fiber manufacture.

Following the initial testing described above, the torsional measurement device was modified to make possible the recording of both positive and negative torque, and a single specimen each of Kevlar 29, Kevlar 49, nylon, Nomex, and polyester was cycled through several levels of S and Z twist. Torsional stress-strain diagrams plotted from data generated in this way are shown in Figures 30 through 34. In the portion of each diagram representing the lowest twist level attained with each fiber, 20 turns/cm, it can be seen that the recovery portion of the curve is not markedly different from the twisting portion, indicating essentially elastic behavior. After twisting to higher increments of strain, complete recovery does not occur and the twisting and untwisting portions of the diagram for each fiber envelop a significant area that represents energy dissipated in overcoming internal fiber friction. The twisting portions of diagrams for cycles terminating above the elastic limit differ in successive cycles up to the termination point of the previous cycle. Beyond that point, the curve for each cycle approximates that shown in the typical diagrams presented previously. This aspect of the torsional behavior of the fibers tested renders repeated cycling of the same specimen a valid procedure for determining recovery from increasingly greater twist levels. Values of residual twist present after untwisting to the zero torque level from each maximum have been determined directly from the complete stress-strain diagram for each fiber (Figures 30 through 34) and are compiled in Table IX.

Table VIII: Torsional Moduli of Five Fibers Determined with the FRL Torsional Measurement Instrument

Parent Yarn	Nominal Fiber Denier	Fiber Diameter (microns)	Torsional Shear Modulus, G (10^{10} dyne/cm^2)	Torsional Shear Modulus, G (10^6 psi)
Kevlar 29, 1000 denier	1.5	12	1.86	0.27
Kevlar 49, 400 denier	1.5	12	1.62	0.24
DuPont nylon, 140-68-R28-924SD	2	17	0.31	0.04
DuPont Nomex, 200-100-0-430	2	--*	1.17	0.17
DuPont Dacron polyester, 70-34-056SD	2	16	0.54	0.08

*The cross-sectional shape of Nomex fiber is not round, but approximately that of an oval racetrack. The overall cross-sectional dimensions of the fiber tested were 21 by 10 microns.

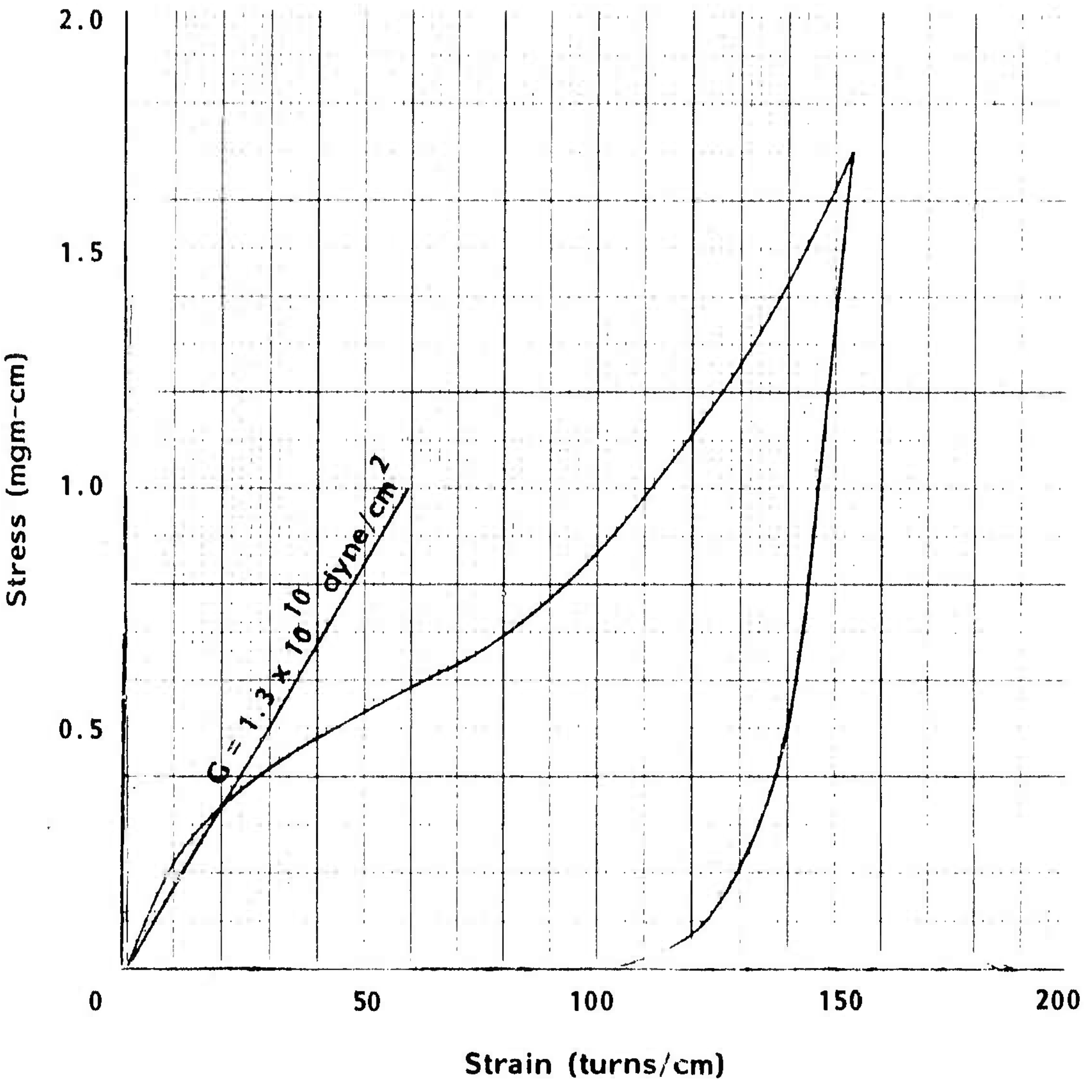

Figure 25. Typical Torsional Stress-Strain Diagram for 1.5 Denier Kevlar 29 Fiber

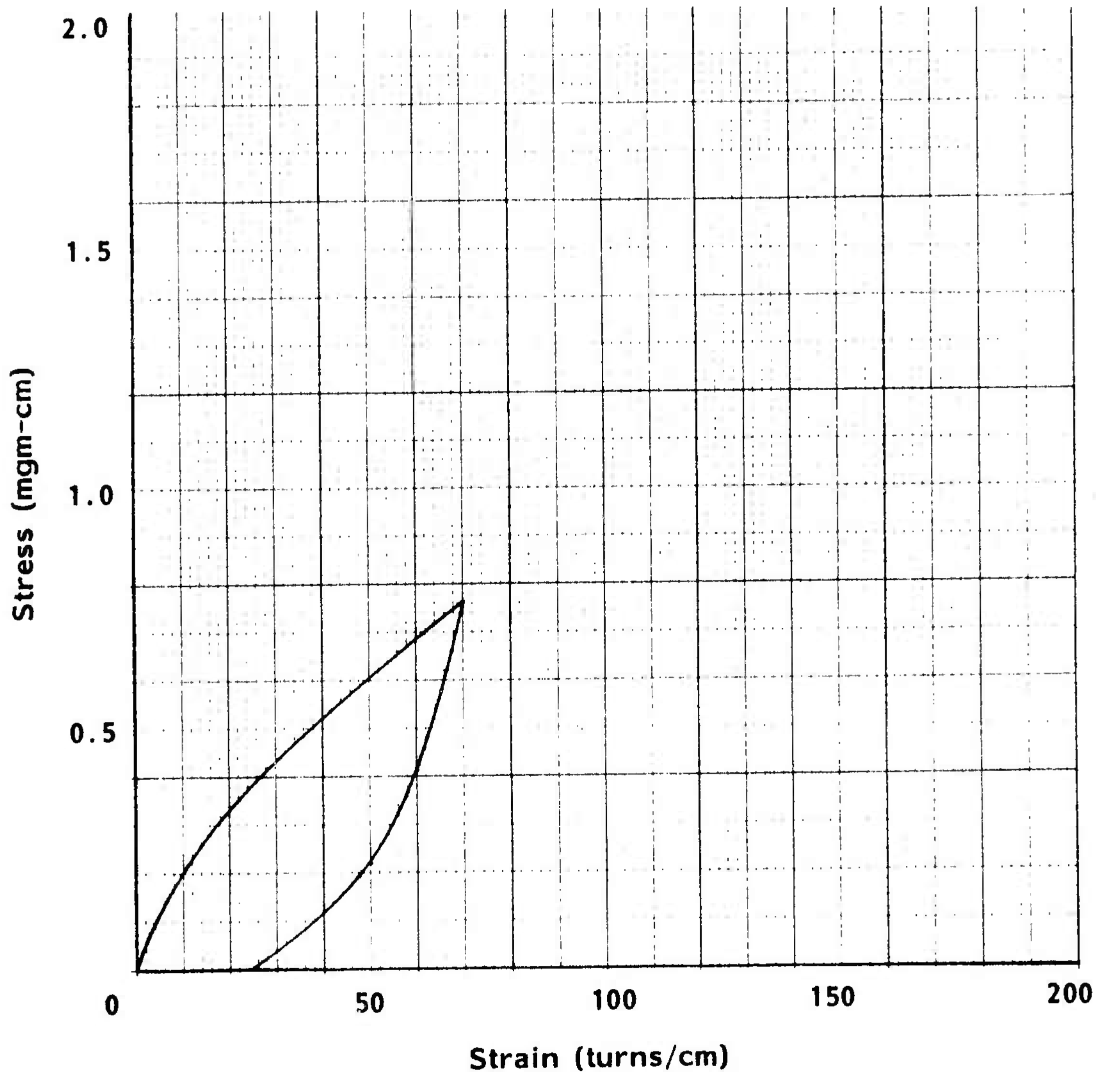

Figure 26. Typical Torsional Stress-Strain Diagram for 1.5 Denier Kevlar 49 Fiber

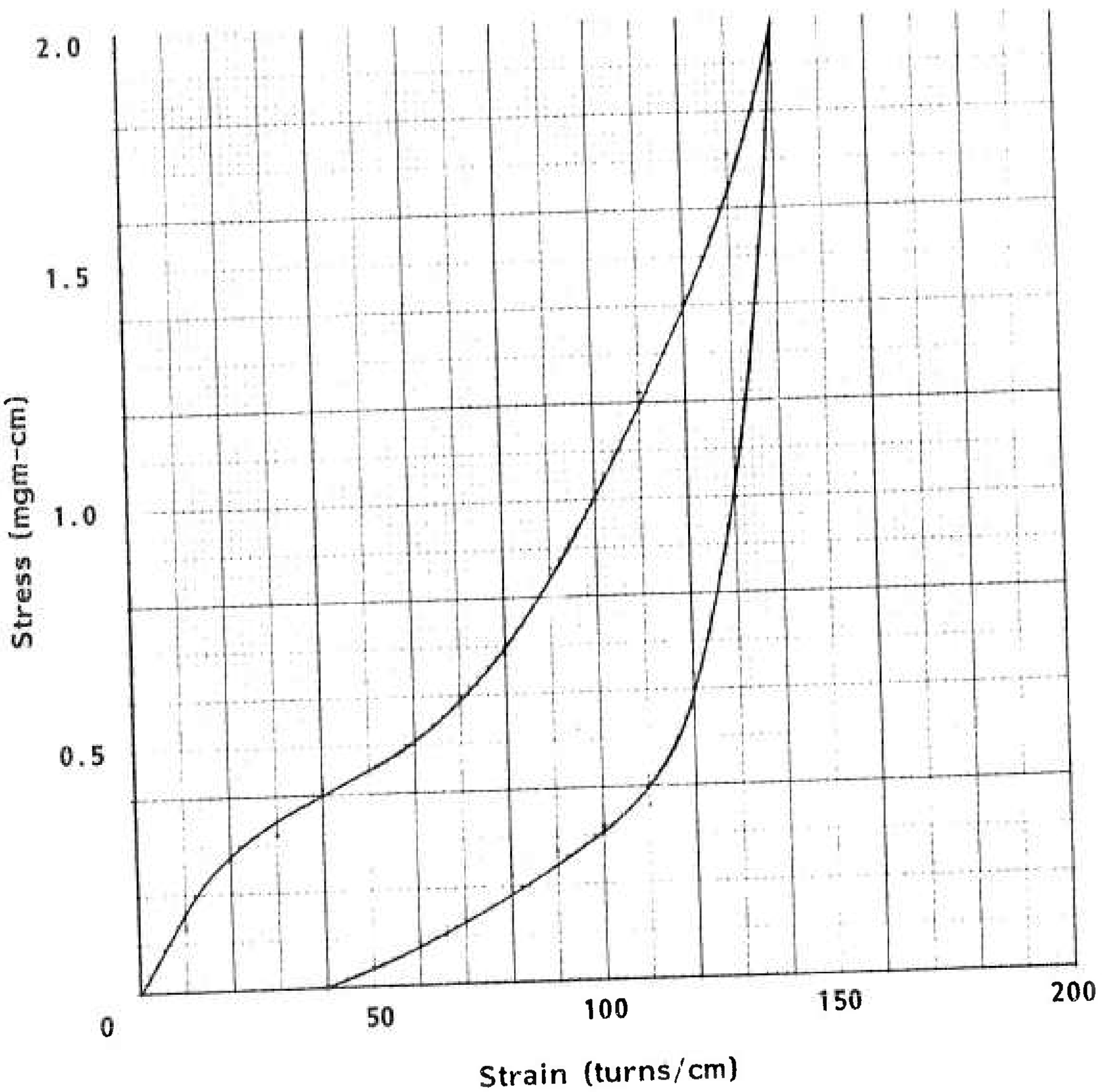

Figure 27. Typical Torsional Stress-Strain Diagram for 2 Denier Nylon Fiber

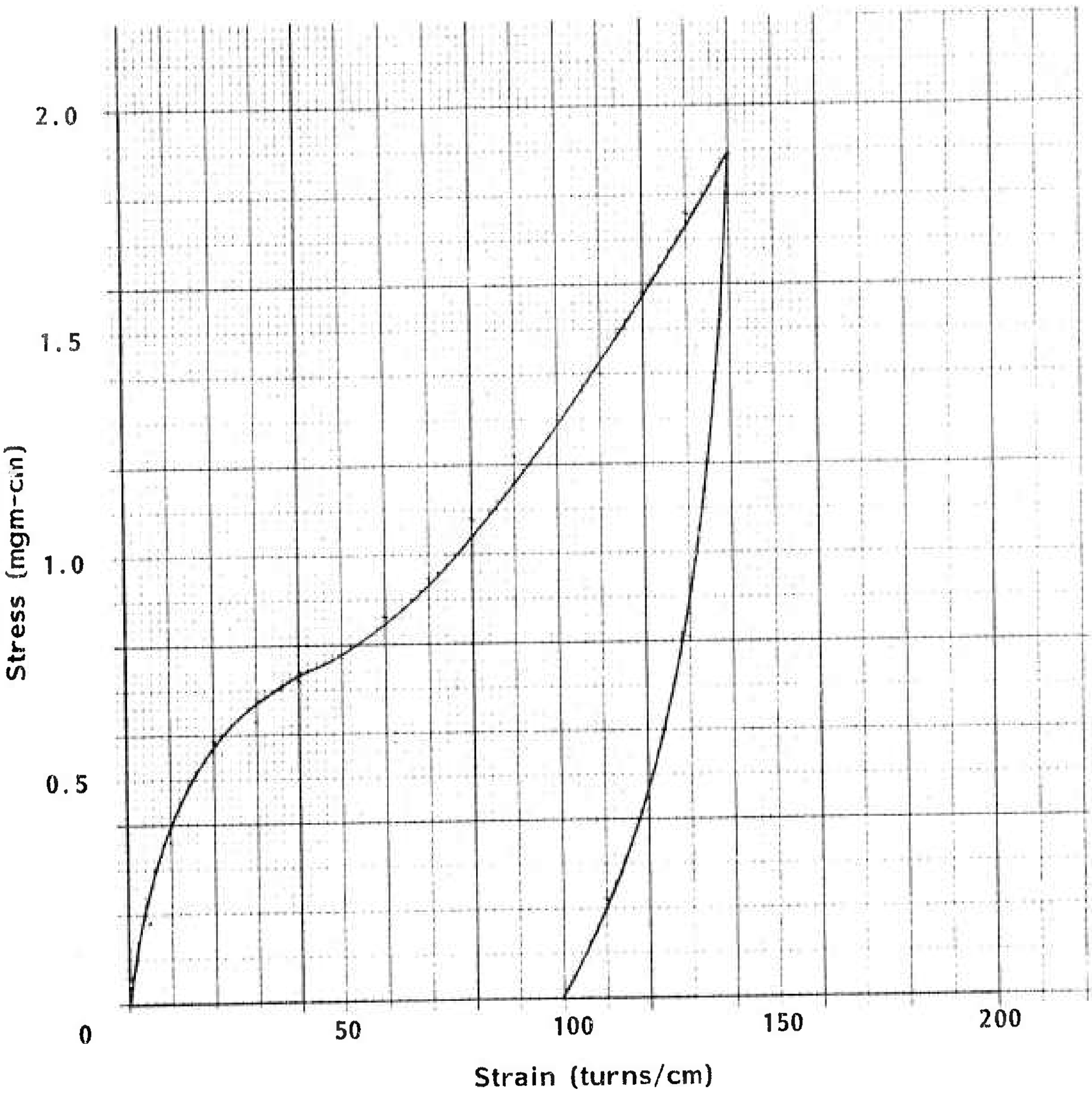

Figure 28. Typical Torsional Stress-Strain Diagram for Two Denier Nomex Fiber

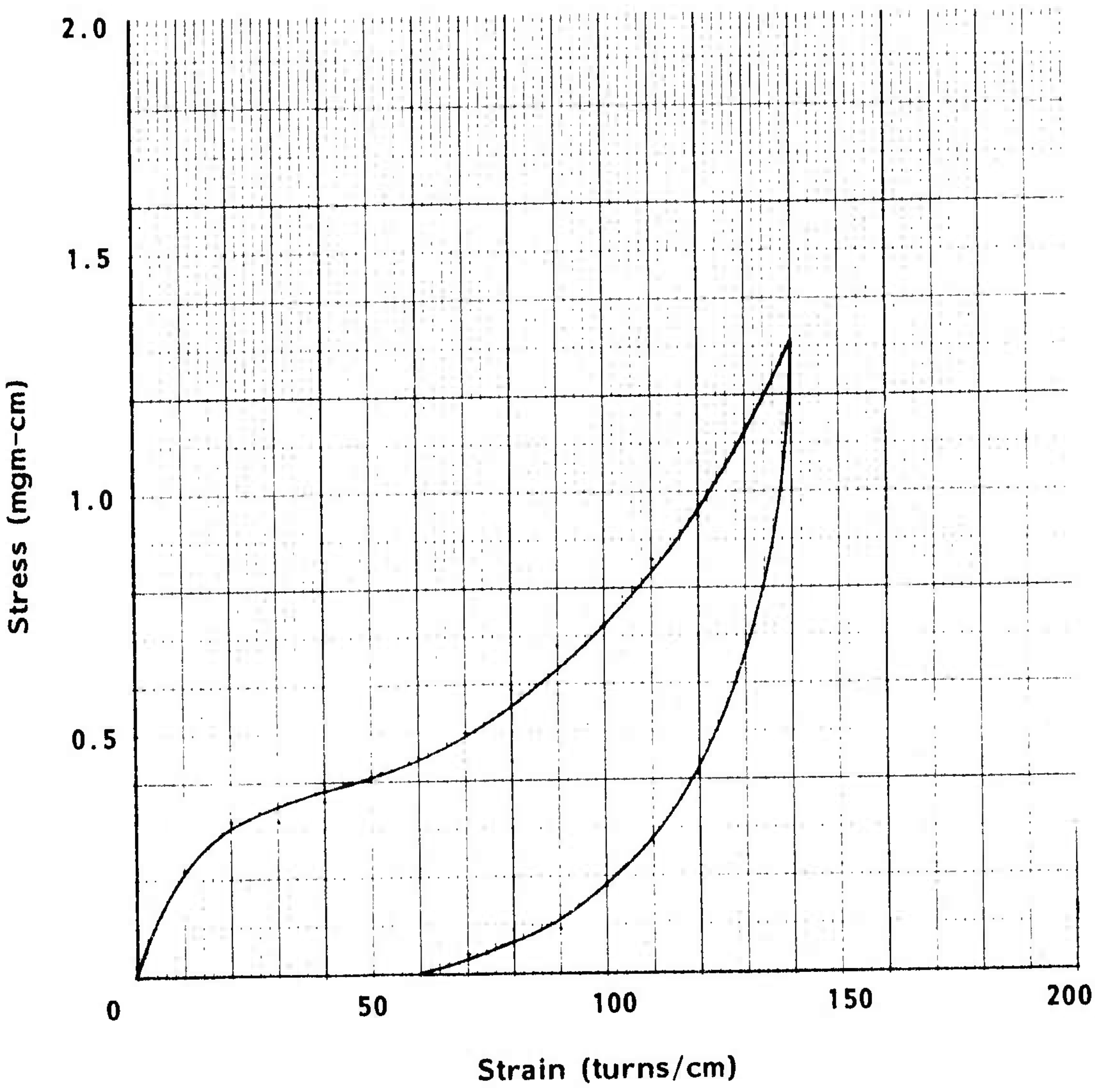

Figure 29. Typical Torsional Stress-Strain Diagram for 2 Denier Dacron Polyester Fiber

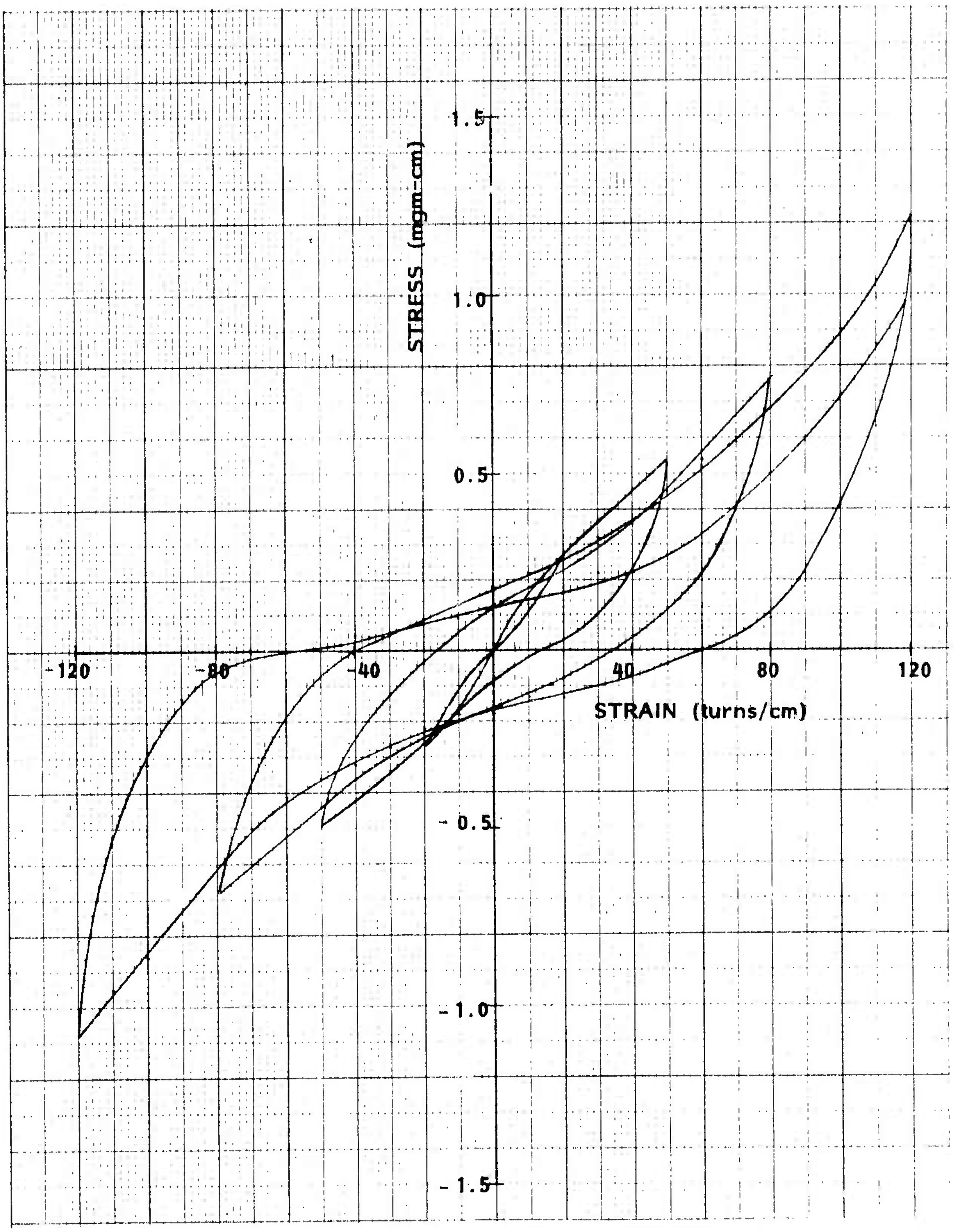

Figure 30. Torsional Stress-Strain Diagram for a Single Specimen of 1.5 Denier Kevlar 29 Fiber Cycled to Several Strain Levels (positive strain values represent S twist)

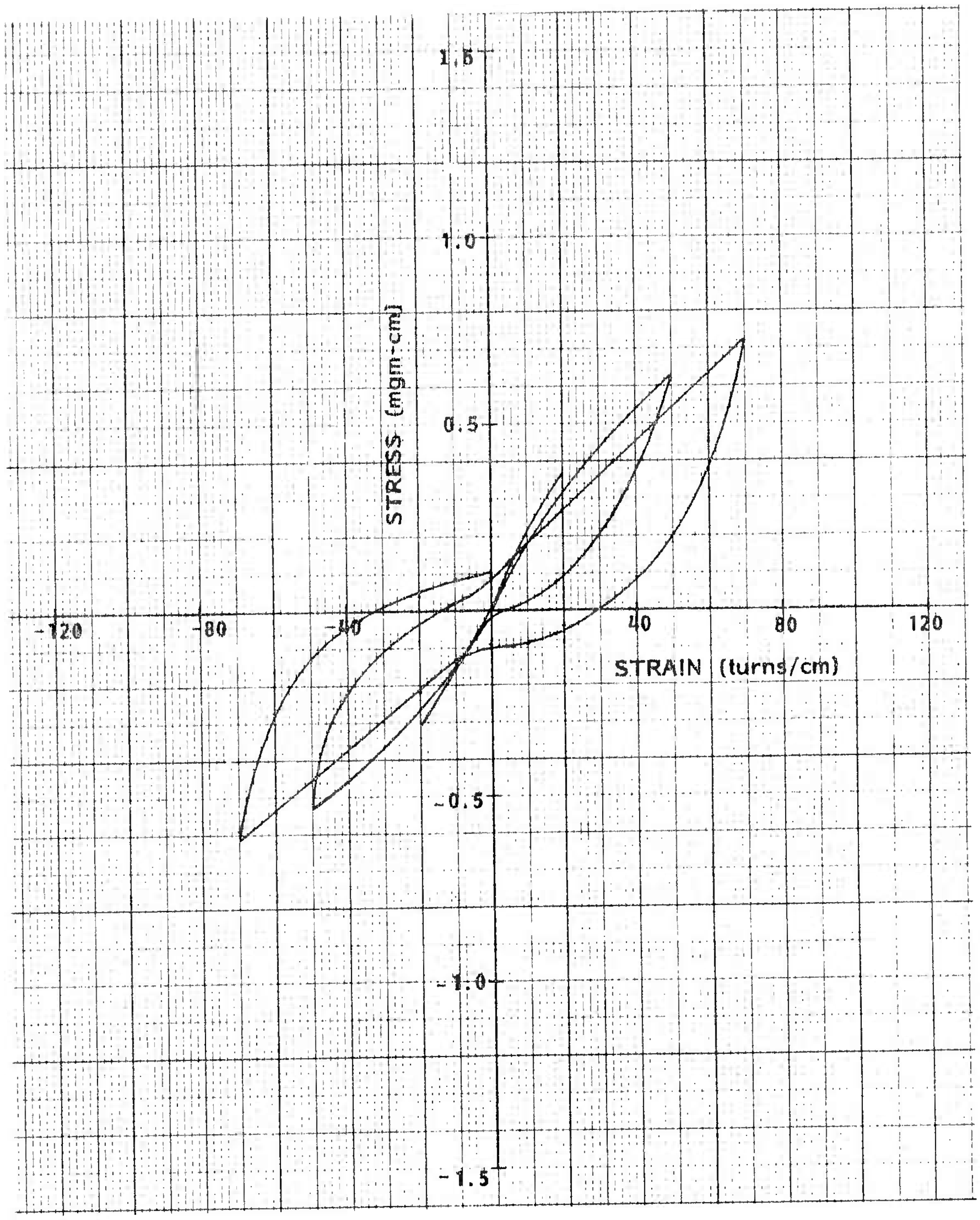

Figure 31. Torsional Stress-Strain Diagram for a Single Specimen of 1.5 Denier Kevlar 49 Fiber Cycled to Several Strain Levels (positive strain values represent S twist)

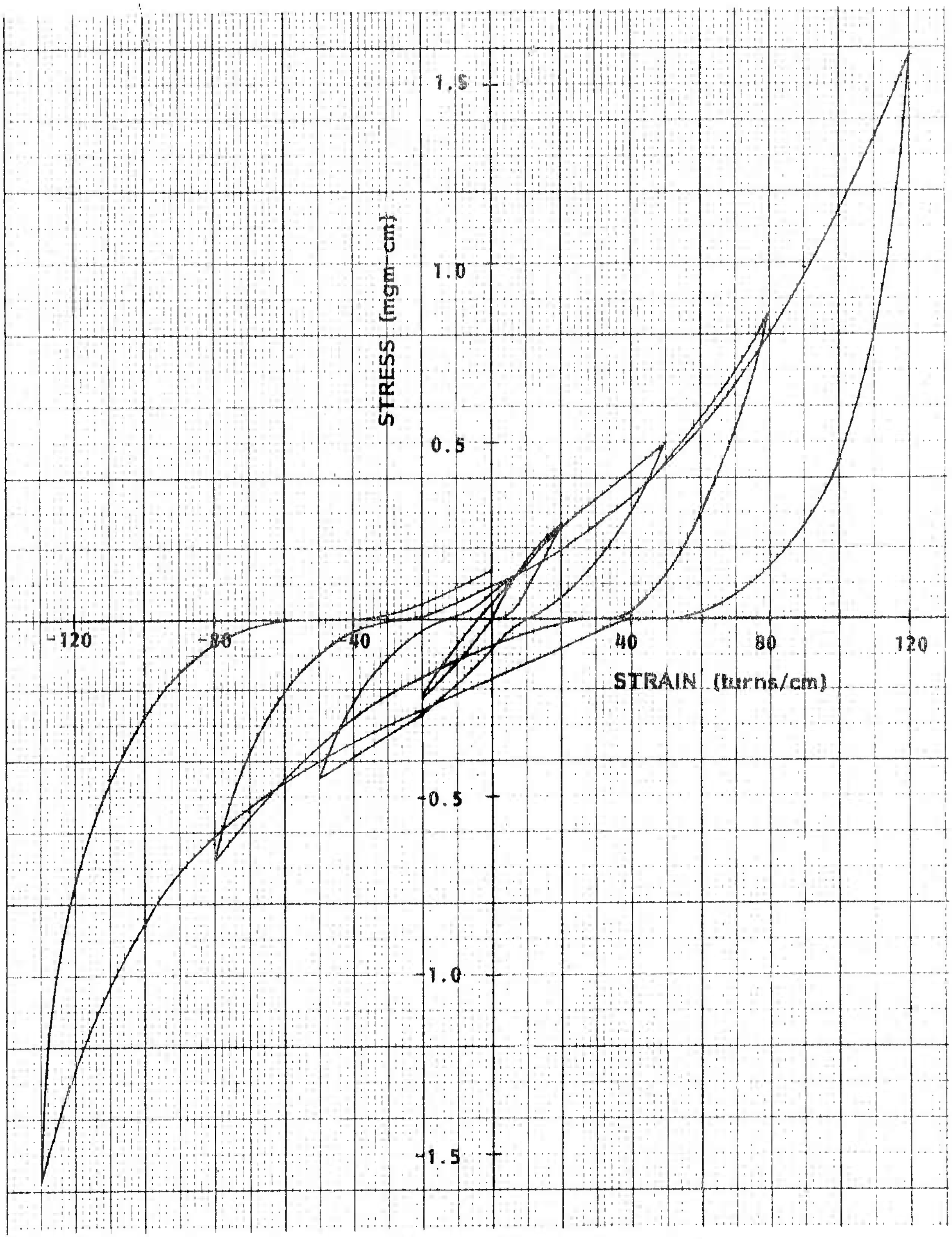

Figure 32. Torsional Stress-Strain Diagram for a Single Specimen of 2 Denier Nylon Fiber Cycled to Several Strain Levels (positive strain values represent S twist)

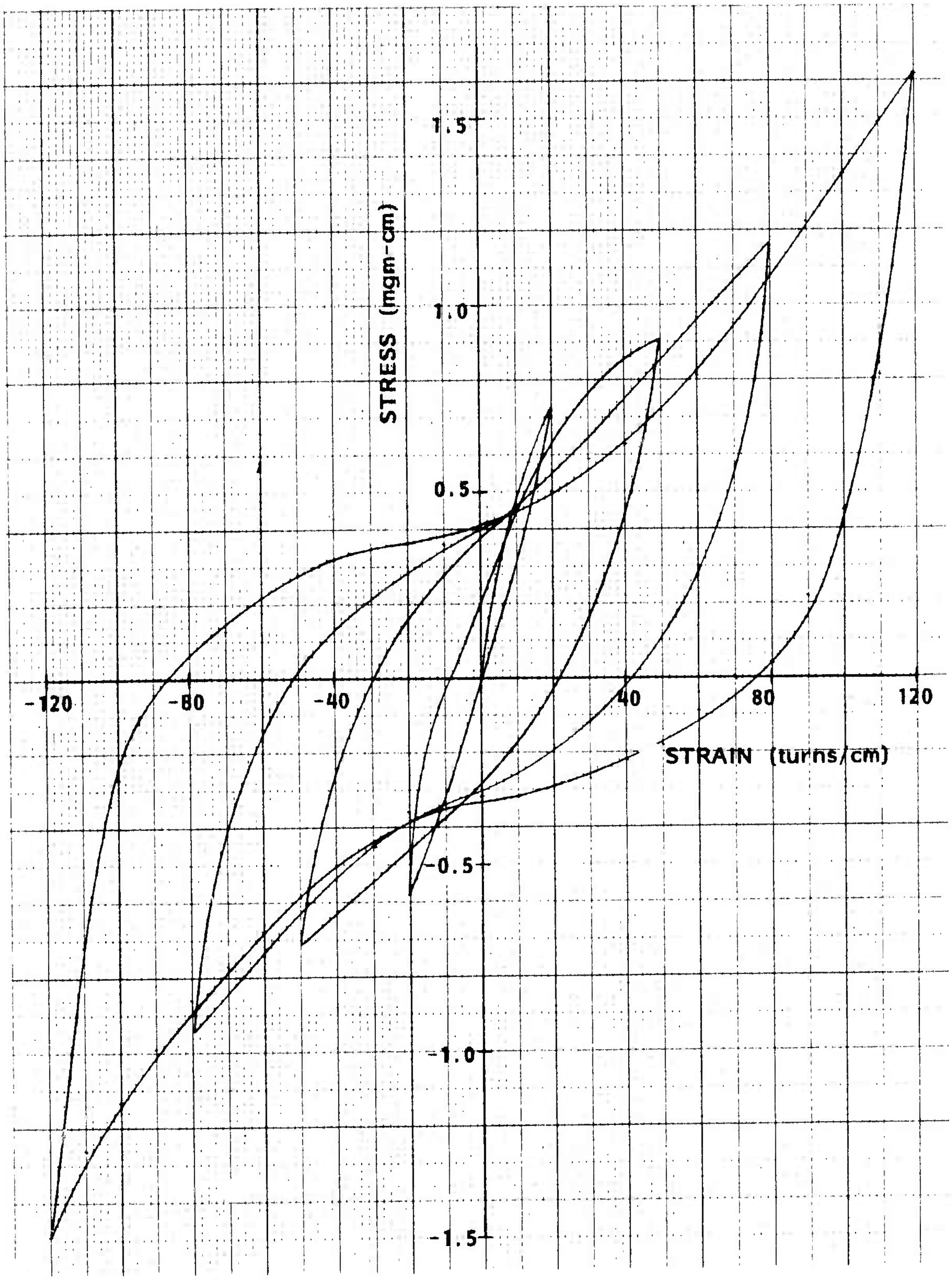

Figure 33. Torsional Stress-Strain Diagram for a Single Specimen of 2 Denier Nomex Fiber Cycled to Several Strain Levels (positive strain values represent S twist)

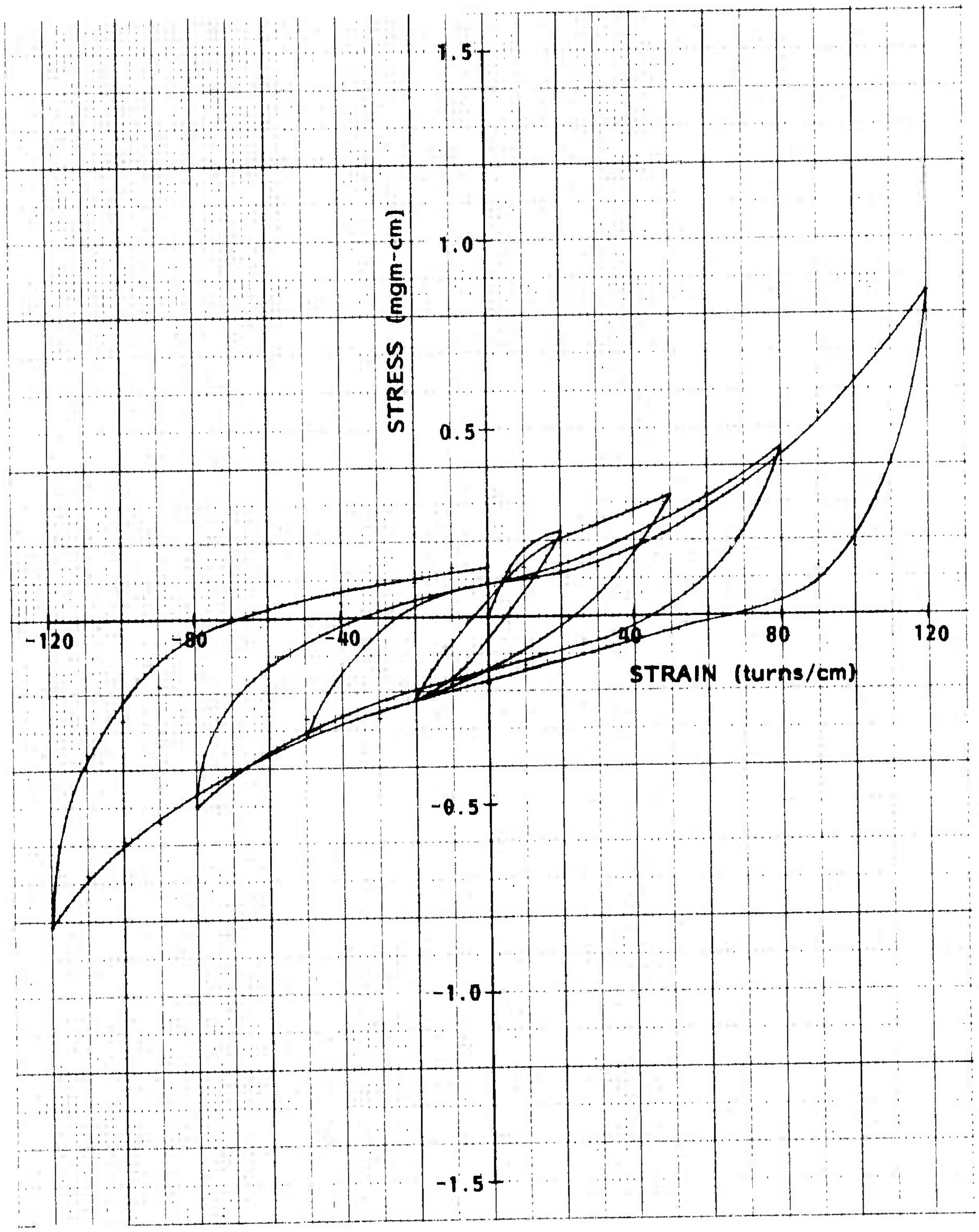

Figure 34. Torsional Stress-Strain Diagram for a Single Specimen of 2 Denier Dacron Polyester Fiber Cycled to Several Strain Levels (positive strain values represent S twist)

Table IX: Residual Torsional Strain in Single Fibers Measured after Deformation to Several Levels of Imposed Strain

Parent Yarn	Imposed Strain (turns/cm)	Residual Strain at Zero Torque (turns/cm)	Recovery (%)
Kevlar 29, 1000 denier	20	0	100
	50	14	72
	80	34	58
	120	60	50
Kevlar 49, 400 denier	20	0	100
	50	4	92
	70	30	57
DuPont nylon, 140-68-R28-924SD	20	3	85
	50	11	78
	80	34	60
	120	52	62
DuPont Nomex, 200-100-0-430	20	0	100
	50	22	56
	80	42	48
	120	76	37
DuPont Dacron polyester, 70-34-056SD	20	5	75
	50	24	52
	80	45	44
	120	67	44

This data is also presented in graphical form in Figure 35 to facilitate comparison of torsional recovery behavior among the five fibers. It is apparent in Figure 35 that no residual strain is present in Kevlar 29, Kevlar 49 and Nomex fiber upon return to the zero torque level after deformation to 20 turns/cm, although recovery from this strain level is incomplete for nylon and polyester. Also evident is a general similarity of shape among the curves representing Kevlar 29, nylon, Nomex, and polyester. The slopes of each of these curves are nearly the same above an initial strain level of 50 turns/cm. This suggests that, at these strain levels, similar recovery mechanisms operate in each of the fibers. However, absolute values of recovery do differ from fiber to fiber throughout the range of initial strains imposed because of differences in behavior at lower strain levels. The initial strain-residual strain diagram of Kevlar 49 differs distinctly from those of the other four fibers studied, having a prominent inflection point at 40 to 50 turns/cm of initial strain. Below this point, Kevlar 49 exhibits the greatest torsional recovery of the five fibers, but above it shows the least torsional recovery of the group. In fact, above 50 turns/cm, deformations are essentially plastic and no indication of elastic recovery behavior exists, since at strain levels above the inflection point, an increase of 10 turns/cm of initial strain increases the residual strain by 10 turns/cm.

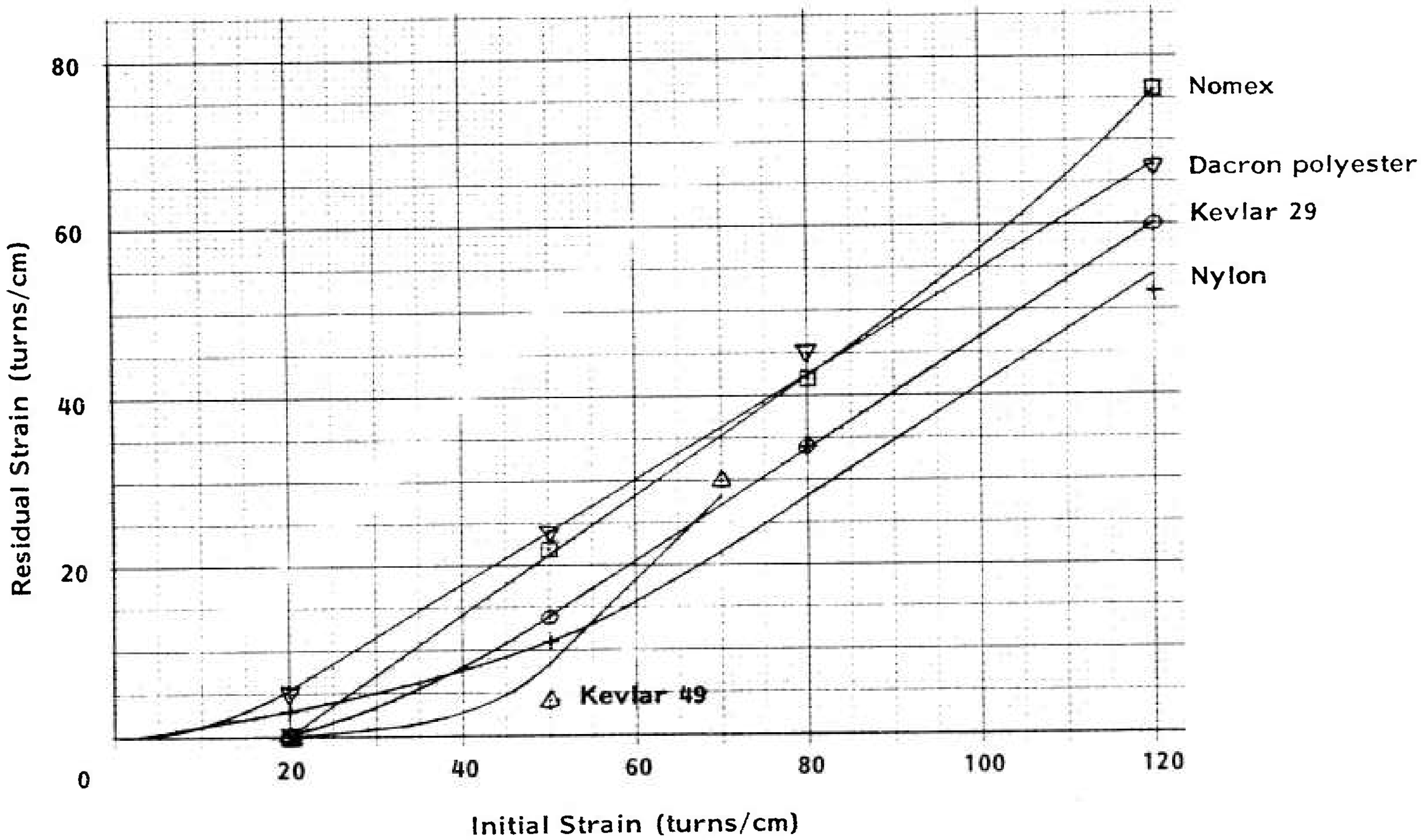

Figure 35. Torsional Strain Recovery of Several Fibers Measured at Zero Torque Level

4. Effect of Previous Exposure to an Extreme Twist Level upon the Tensile Properties of Kevlar 49 Fiber

Photographs taken using a JEOL Model JSM-15 scanning electron microscope provided evidence of permanent damage to Kevlar 49 fiber that had been twisted to 70 turns/cm, which is just below the level of torsional failure for this fiber. To obtain a measure of the degree of damage incurred when the fiber is twisted to this level and then completely untwisted, a number of samples prepared in this way were tested in an Instron tensile tester. The results of these tests, together with average control data obtained from previous tensile tests of the same fiber as it is removed from yarn, are presented in Table X. The loss in tensile properties observed in the twisted-untwisted fiber specimens is not extreme: the modulus decreased 9%, a small but significant amount, tenacity decreased 36%; and rupture elongation decreased 26%. Even though it was previously strained in torsional shear to a point just below failure, the fiber has retained a high degree of tensile integrity. This finding is consistent with data previously reported (AFML-TR-74-65, Part II) concerning the effect of relatively low levels of twist on the tensile strength of Kevlar 29 fiber. Fibers removed from yarn containing 5.5 turns/cm (14 turns/inch) of twist showed a tenacity loss of 25% when compared with fibers removed from untwisted yarn. However, single fibers, when twisted individually to approximately the same twist level, did not suffer any significant loss in tensile properties, indicating that the presence of twist alone was not a contributing factor to the strength loss.

5. Effect of Elevated Temperature Exposure on the Torsional Recovery of Kevlar 29 Yarn

Twist in Kevlar 29 yarn cannot be effectively set in a steam box as is the case with most polymeric yarns, but during the course of the high temperature tensile testing program conducted last year, it was observed that exposure to temperatures of 400°F or more did set twist in Kevlar yarn. More recently, during the fiber bending study reported in another section of this report, it was noted that exposures to temperatures of 400°F and 500°F for one minute set previously imposed bending deformations to the extent that recovery was limited to the 10 to 20% range, the exact figure being dependent on imposed curvature. Recognizing that exposure to temperatures in this range also induces a small but significant strength loss in Kevlar yarn, an experiment was devised that included the use of the FRL torsional measurement device to obtain an accurate determination of the relative effectiveness of several temperature levels used to set twist in Kevlar 29 yarn and a series of tensile tests was made to establish the net tenacity change in the twisted yarn that had been set at each temperature level. The resulting data define the counteracting torsional recovery-temperature and tenacity change-temperature relationships and is expected to provide a basis for selection of setting temperatures in future work.

The yarn used in the heat setting study, 100 denier Kevlar 29, was selected primarily to accommodate the torque capacity of the FRL torsional measurement device, which is 6 to 7 mg-cm. This torque range was chosen during the design stage to permit generation of torsional stress-strain diagrams, up to the point of

Table X: Tensile Properties of Kevlar 49 Fiber - Twisted 70 turns/cm, Then Untwisted (1.0 inch specimen length)

	Initial Modulus (gpd)	Average Modulus Change (%)	Rupture Elongation (%)	Average Elongation Change (%)	Rupture Tenacity (gpd)	Average Strength Change (%)
Control (average)	989		2.7		26.2	
Twisted, untwisted	891		2.2		18.3	
	886		1.7		13.3	
	939		2.1		18.7	
	918		1.9		15.9	
	886		2.1		17.1	
	872		2.2		18.1	
	884		2.4		20.0	
	969		1.4		12.5	
	867		1.9		16.3	
Average	901	- 9	2.0	-26	16.7	-36

rupture, for single fibers of one or two denier. Conveniently, 6 to 7 mg-cm of torque applied to 100 denier Kevlar 29 yarn resulted in 2.4 turns/cm or 6 turns/inch of twist, which is a normal level of twist for continuous filament textile yarns. However, because torsional stress-strain data reported in the preceding section for Kevlar 29 fiber was generated using specimens taken from 1000 denier yarn delivered approximately one year before the lighter yarn, and since Kevlar fiber tensile properties have been shown to vary significantly among yarn packages of different merge numbers, several torsion tests for fiber from the 100 denier yarn were made before the setting study was begun. Although no significant difference in initial modulus was recorded, fiber from the 100 denier yarn is notably stiffer than fiber from the 1000 denier yarn above a twist level of 20 turns/cm. The yield point seen at approximately this twist level in Figure 36, which is typical of four torsional stress-strain diagrams developed for fiber taken from 100 denier yarn, is less pronounced than that observed for fiber from 1000 denier yarn in Figure 25. A single fiber specimen taken from 100 denier yarn was also cycled to increasing levels of alternating S and Z twist and the stress-strain diagram shown in Figure 37 was obtained. Figure 37 is essentially the same as Figure 30 for fiber from 1000 denier yarn cycled through the same twist levels, the only difference being the greater modulus obtained above a strain level of 20 turns/cm for fiber from 100 denier yarn.

Four setting temperatures were selected for study, 200, 300, 400, and 500°F, and the time of exposure was one minute in each case. At the outset, several torsional stress-strain diagrams for 100 denier Kevlar 29 yarn were generated by recording torque values at twist increments up to a maximum of 2.4 turns/cm. The twisting and untwisting portions of a typical curve are shown in Figure 38. The effect of exposure to each temperature on the untwisting portion of the torsional stress-strain diagram was then determined according to the following scheme. A yarn specimen was twisted to a level of 2.4 turns/cm, and then removed from the torsional measurement device using a fixture designed specifically for this purpose. The fixture prevented the yarn from untwisting and was also used to support the twisted yarn during exposure in a hot air oven. After exposure, the specimen was reinserted in the test device and the untwisting portion of the stress-strain diagram was generated. A minimum of three tests for each temperature level was made to obtain typical curves of the type plotted in Figure 38 which clearly show the relative effectiveness of each setting temperature, particularly if the points where the residual torques measured after setting and before untwisting are noted, and if torsional strain recovery values at the zero stress level are compared. Both of these measures of torsional recovery, or setting effectiveness, have been compiled in Table XI. Note that torsional strain recovery decreases with increasing setting temperature and is close to zero when a setting temperature of 500°F is used.

Following completion of torsional recovery measurements, groups of ten yarns each were twisted to 2.4 turns/cm and set at each of the selected temperatures. After setting, these specimens were allowed to untwist to a zero torque state, the level of twist remaining varying with the setting temperature as reported in Figure 38 and Table XI. The set yarns were then tested in an Instron tensile tester and the results tabulated in Table XII. From this data a plot of tenacity versus residual twist was made for the heat-set yarns (see lower graph on Figure 39). This plot, however,

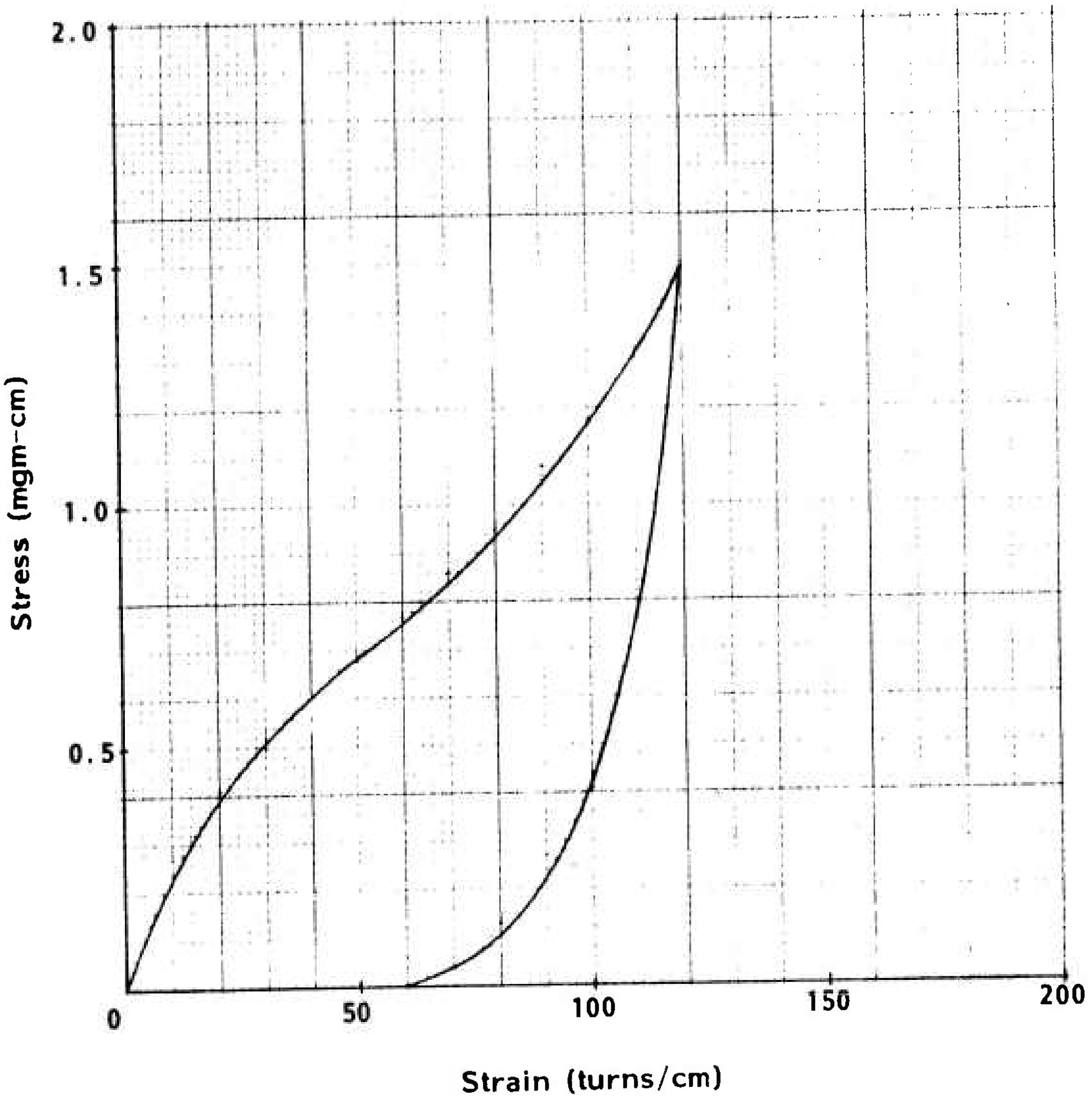

Figure 36. Typical Torsional Stress-Strain Diagram for 1.5 Denier Kevlar 29 Fiber Removed from 100 Denier Yarn

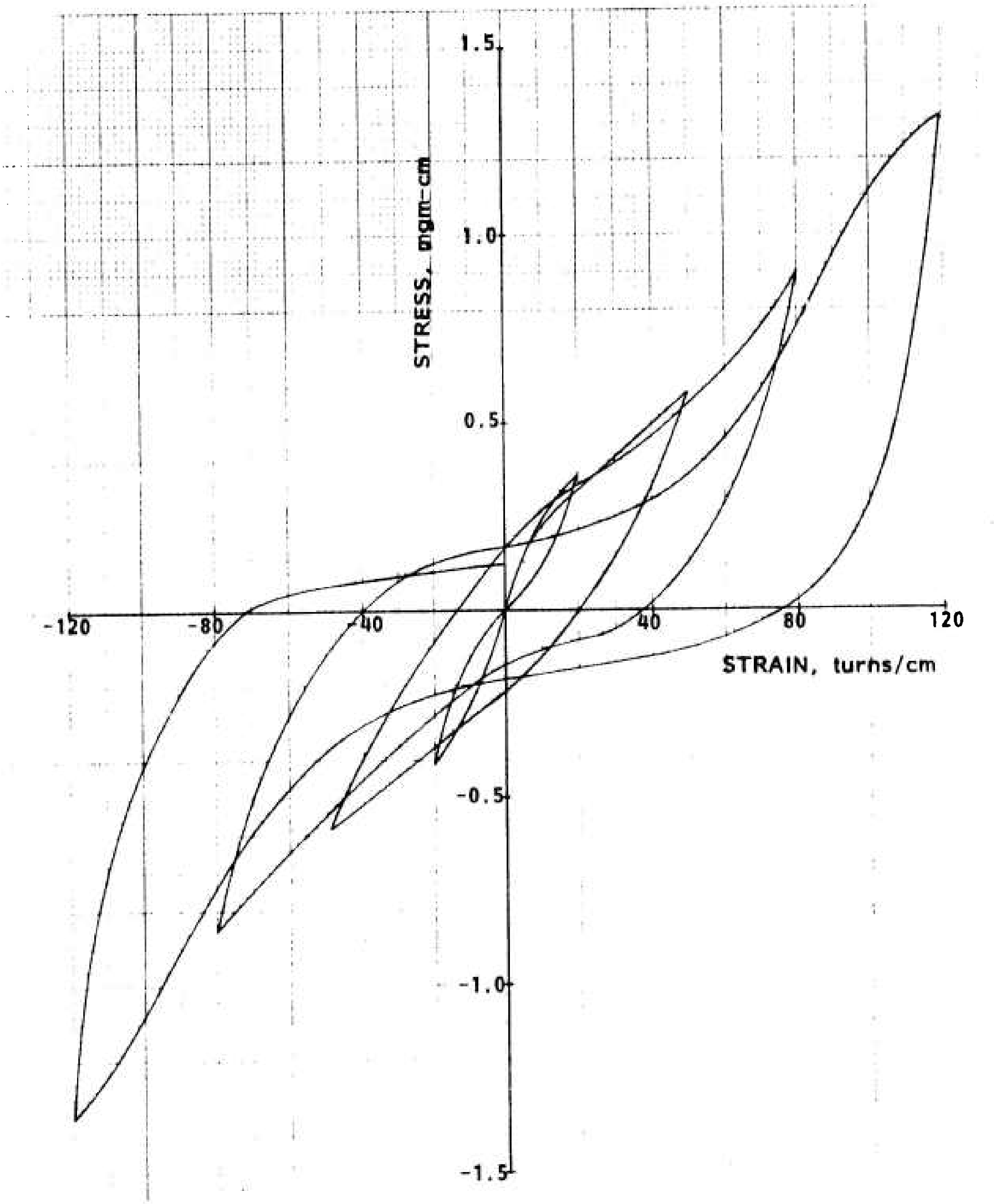

Figure 37. Torsional Stress-Strain Diagram for a Single Specimen of 1.5 Denier Kevlar 29 Fiber Taken from 100 Denier Yarn and Cycled to Several Strain Levels (positive strain values represent S twist)

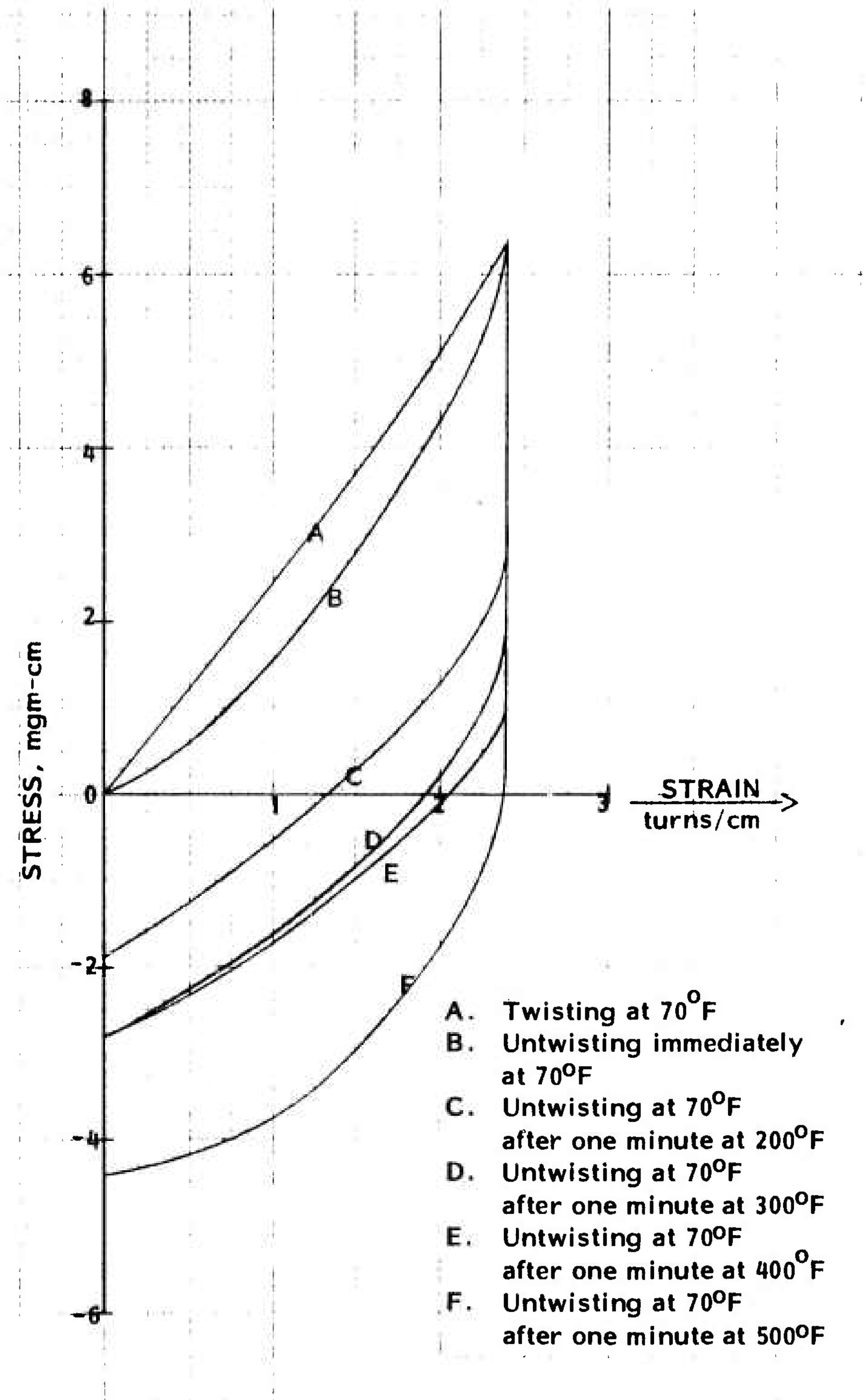

Figure 38. The Effect of Elevated Temperature Exposure on the Torsional Recovery Characteristics of 100 Denier Kevlar 29 Yarn

Table XI: Relative Effectiveness of Four Temperatures to Set Twist in 100 Denier Kevlar 29 Yarn

	Residual torque measured after setting and before untwisting; expressed as a percent of the torque measured before setting	Torsional strain recovery measured at the zero stress level (%)
70°F - control	----	100
		100
		100
One minute at 200°F	46.3	40.0
	41.0	43.3
	47.8	43.3
One minute at 300°F	25.2	20.0
	26.7	23.3
	26.2	23.3
One minute at 400°F	21.4	13.3
	20.3	13.3
	19.2	13.3
One minute at 500°F	3.5	3.3
	0.0	0.0
	2.0	3.3
	4.7	3.3

Table XII: Tenacity (gpd) of 100 Denier Kevlar 29 Yarn Twisted to 2.4 turns/cm (6 turns/inch), Heat Set for One Minute at Each of Several Temperature Levels, and Allowed to Recover Before Tensile Testing

Test No.	Set at 200°F recovered to 1.3 turns/cm (3.3 turns/inch)	Set at 300°F recovered to 1.9 turns/cm (4.8 turns/inch)	Set at 400°F recovered to 2.1 turns/cm (5.3 turns/inch)	Set at 500°F recovered to 2.4 turns/cm (6.0 turns/inch)
1	22.1	22.5	22.1	21.2
2	23.0	22.3	20.6	20.6
3	22.1	22.5	21.9	20.6
4	21.2	23.1	20.3	21.0
5	22.7	22.7	21.4	20.8
6	23.4	22.5	21.6	21.4
7	21.2	23.0	22.7	21.4
8	23.5	20.6	21.9	21.0
9	23.0	20.6	22.5	21.2
10	22.5	23.1	22.1	21.6
Average	22.5	22.3	21.7	21.1
Standard Deviation	0.8	0.9	0.8	0.3
Coefficient of Variation (%)	3.6	4.1	3.5	1.6

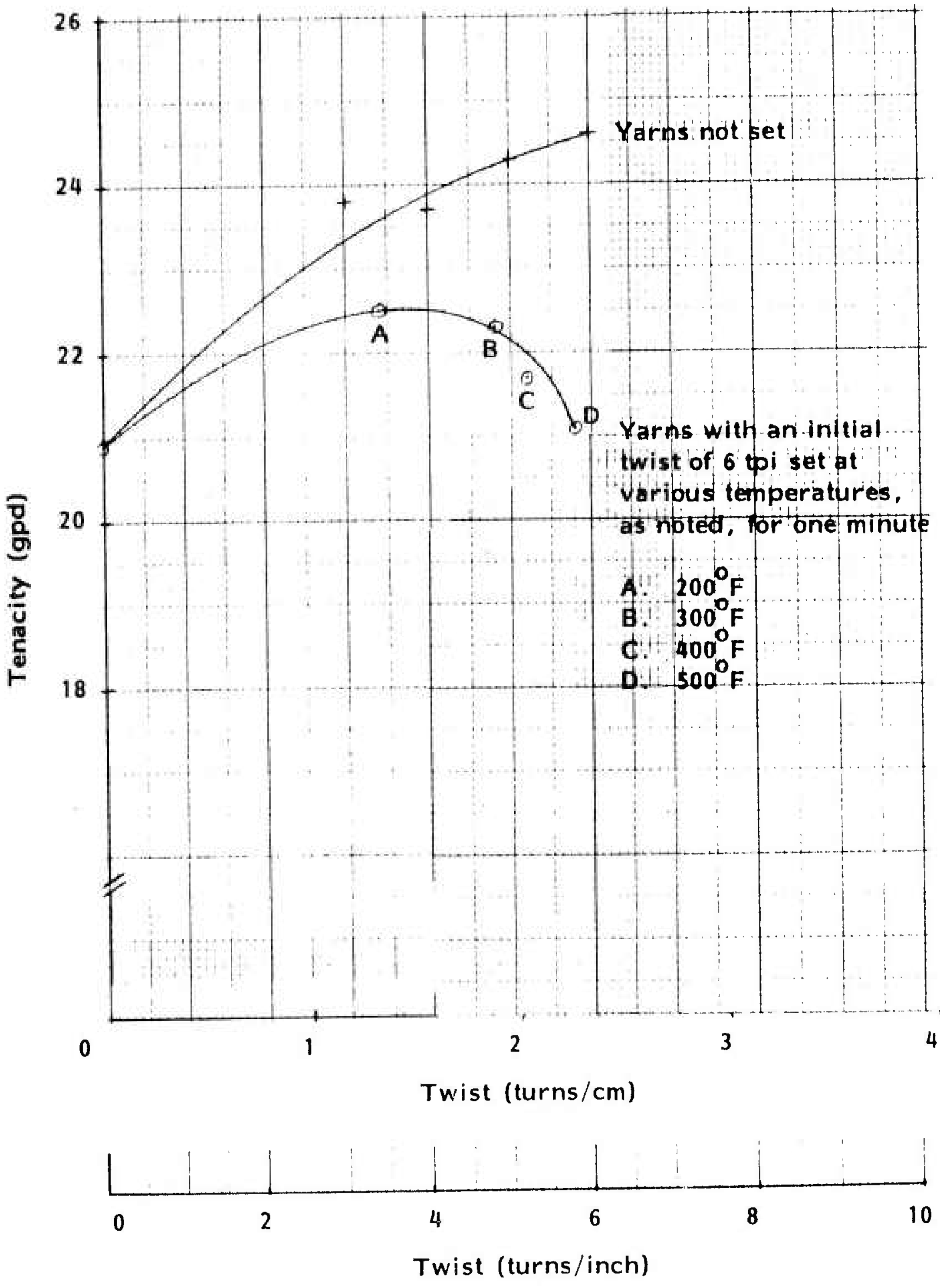

Figure 39. Effect of Twist, Both Heat-Set and Not Set, on the Tensile Strength of 100 Denier Kevlar 29 Yarn

represents total tenacity changes attributable to two factors, exposure to heat and changes in twist level: to apportion the contribution of each requires more information Groups of the same 100 denier yarn were therefore twisted to various levels between zero and 2.4 turns/cm and each of these specimens were carefully mounted in an Instron tensile tester without loss of twist. The tenacities obtained in this way (see Table XIII) when plotted as a function of twist and compared to a corresponding plot for twisted and heat-set yarn, provide a basis for gauging the proportion of tenacity change caused by high temperature exposure alone. Tenacity-twist level diagrams for both heat-set and non-set yarn are given in Figure 39. It is interesting to note that, although tenacity loss increases with setting temperature, the tenacity level of twisted, heat-set yarn remains greater than yarn taken from the producer's package (zero twist) even after setting for one minute at 500°F.

Although torsional recovery in the Kevlar 29 yarn studied can be effectively prevented if the setting temperature employed is great enough, tenacity losses increase with increasing setting temperature. It is apparent that selection of setting temperatures for future work will therefore involve some degree of compromise. Figure 40, in which torsional recovery and tenacity are both plotted as a function of setting temperature, provides the essential information required to select a setting temperature on that basis. For example, it is probable that a tenacity loss of 8% would be acceptable in some applications involving the 100 denier Kevlar 29 yarn that was the subject of this study. This is seen to be the magnitude of strength loss to be expected after one minute of exposure to a setting temperature of 300°F, and the torsional recovery following such an exposure will amount to 22%.

6. Changes in Torsional Stress-Strain Characteristics Induced by Heat Setting Kevlar 29 Yarn

In the preceding subsection, one of several changes to the torsional stress-strain diagram of Kevlar 29 yarn caused by exposure of the yarn to elevated temperatures was examined in detail. However, in addition to changing the strain level at which zero stress occurs, exposure to elevated temperature alters the torsional stress-strain diagram in other interesting ways. As an aid to understanding these changes, a series of microphotographs was taken as a heat-set yarn specimen was tested in torsion.

Figure 41 is a torsional stress-strain diagram obtained by twisting 100 denier Kevlar 29 taken directly from the producer's package to 2.4 turns/cm (6 turns/inch) in the S direction, untwisting, twisting to 2.4 turns/cm in the Z direction and again untwisting. A corresponding diagram for heat-set yarn (Figure 42) was generated by twisting a similar yarn specimen to 2.4 turns/cm S, then heat-setting it with a one minute exposure at 300°F; immediately after setting, the yarn was untwisted, then twisted to 2.4 turns/cm Z. From this point it was untwisted through the zero strain level and retwisted back to 2.4 turns/cm S. Comparison of Figures 41 and 42 makes obvious several changes to the torsional stress-strain diagram of the yarn caused by heat-setting. Perhaps most conspicuous is the fact that the zero strain level no longer coincides with the zero stress level. Also, after setting, the internal frictional force at the zero strain level, represented by the difference between the ordinates of the two portions of the curve at that point, is quite large, although it is zero in the case of the control yarn taken directly

Table XIII: Tenacity (gpd) of 100 Denier Kevlar 29 Yarn at Several Levels of Twist: Not Heat Set

Test No.	From package, No Twist	1.2 turns/cm (3.0 turns/inch)	1.6 turns/cm (4.0 turns/inch)	2.0 turns/cm (5.0 turns/inch)	2.4 turns/cm (6.0 turns/inch)
1	19.7	24.2	23.4	24.0	24.7
2	20.3	24.4	24.4	24.7	24.2
3	21.4	25.1	23.2	24.2	24.4
4	20.7	24.0	23.8	24.0	24.4
5	21.3	23.8	23.1	24.7	24.7
6	21.4	23.8	24.2	24.2	25.1
7	21.3	22.9	23.8	25.1	24.7
8	21.2	23.6	23.8	23.4	24.9
9	21.1	22.7	23.2	23.4	24.0
10	20.8	23.1	24.0	24.9	25.3
Average	20.9	23.8	23.7	24.3	24.6
Standard Deviation	0.6	0.7	0.4	0.6	0.4
Coefficient of Variation (%)	2.6	3.0	1.8	2.4	1.6

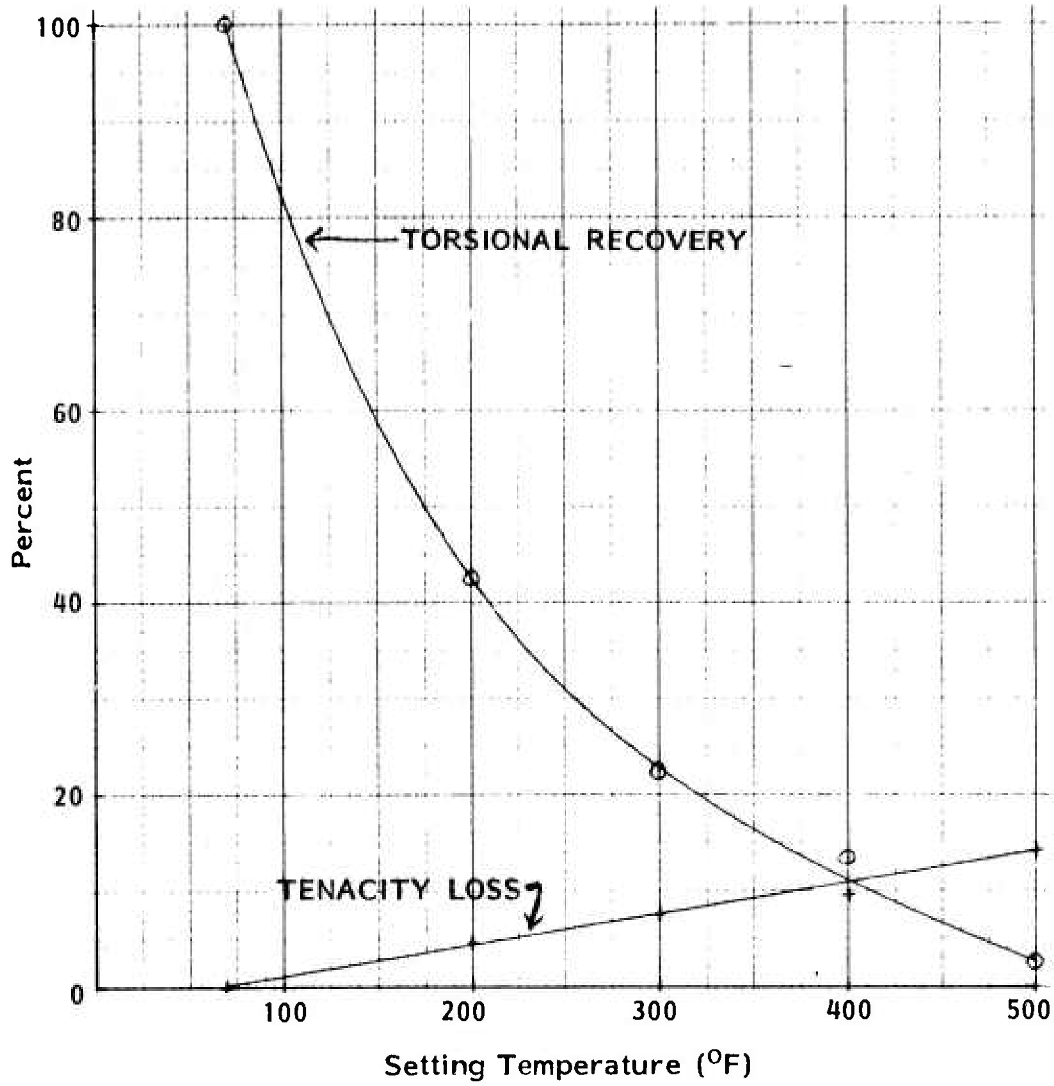

Figure 40. Torsional Recovery and Tenacity Loss as a Function of Setting Temperature for 100 Denier Kevlar 29 Yarn. Setting time was one minute, and initial twist level was 2.4 turns/cm (6.0 turns/inch)

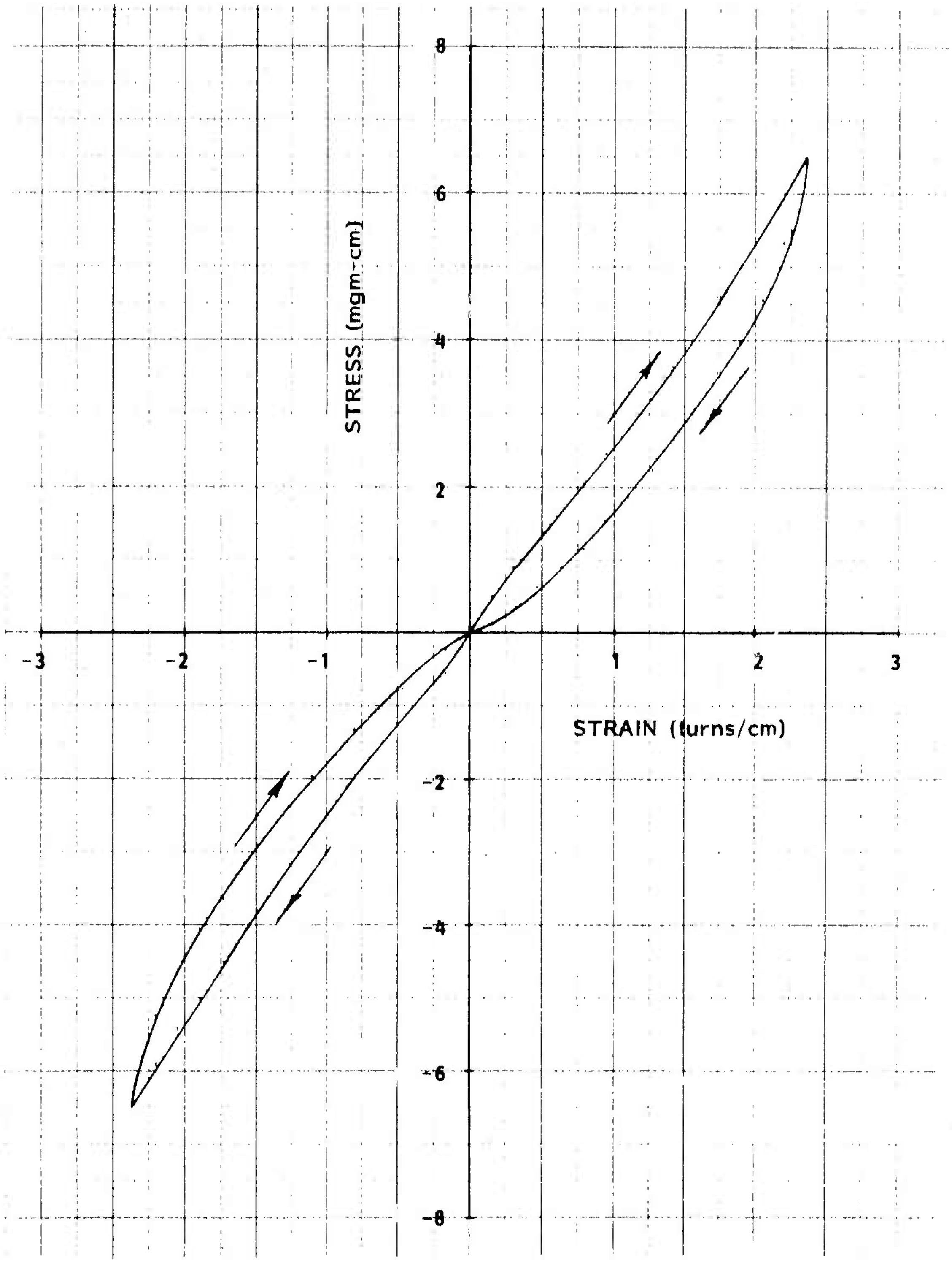

Figure 41. Torsional Stress-Strain Diagram for 100 Denier 29 Yarn Strained in both the S (+) and Z (-) Directions

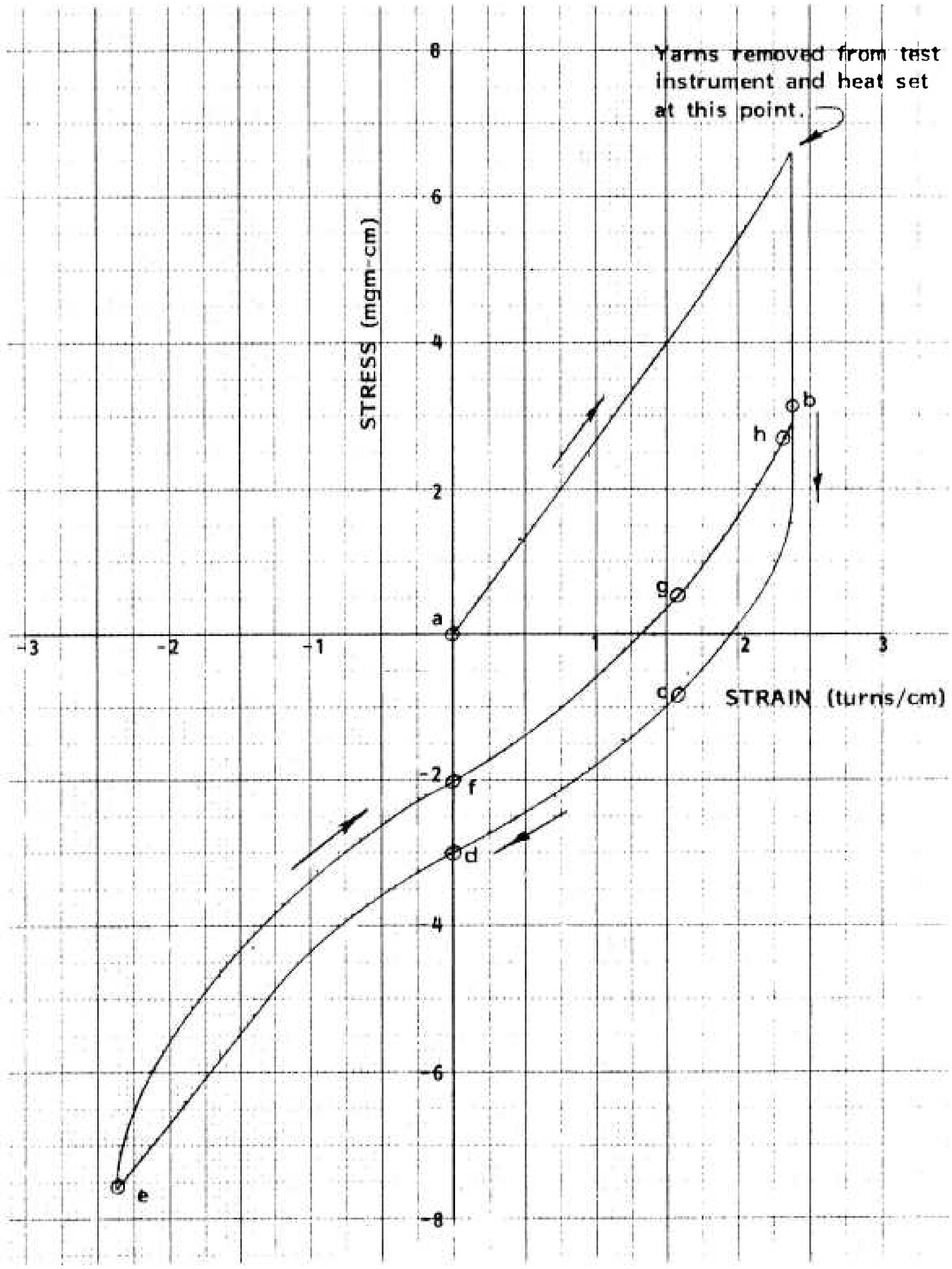

Figure 42. Torsional Stress-Strain Diagram for 100 Denier Kevlar 29 Yarn Strained in both the S (+) and Z (-) Directions after being Heat-Set at 300°F for one Minute. Letters show points at which accompanying photographs were taken.

from the producer's package. Internal friction is, in fact, greater throughout the entire stress-strain cycle after the yarn has been heat set. Another major modification to the diagram is the lesser slope at most strain levels after heat setting, indicative of reduced torsional stiffness.

The shift of the torsional stress-strain diagram downward so that negative stress values occur over a greater portion is an easily understood, inherent consequence of setting S twist (positive strain) in the yarn. The reduction in torsional stiffness that occurs between approximately -1.5 turns/cm and +1.5 turns/cm undoubtedly represents a material property change that is a consequence of the one minute exposure at 300°F. However, changes in the torsional stress-strain diagram resulting from increased interfiber friction within the yarn are less easily explained, and it was for this reason that a series of microphotographs of heat-set yarn was taken during a torsion test. Although photographs were taken at twenty-two intervals, the eight shown in Figure 43, a through h, illustrate the most prominent changes that occur in the appearance of the yarn as it is cycled in torsion. Letters a through h have been placed on the stress-strain diagram in Figure 42 to identify the point in the cycle at which each photo in Figure 43 was obtained. Examining the photographs and the diagram together, one can correlate changes in yarn appearance with changes in internal friction. At a, the fiber appears as it comes from the producer's package with little or no twist and we know from the complete stress-strain diagram for yarn in this state (Figure 41) that the internal friction opposing torsion is zero. At b, the yarn has been heat-set and now has 2.4 turns/cm of S twist. At c, the yarn has just passed through its now preferred state (zero stress level) and is at 1.6 turns/cm S. The yarn diameter has increased at d, a point of zero twist, and several fibers, now set in a helical configuration, are buckling away from the main body of the yarn. After twisting and untwisting through e, the point of maximum Z twist, the yarn is returned to another point of zero twist, f. Fiber to fiber frictional forces within the set yarn at zero twist are not zero, as with the unset yarn, as indicated by the stress level f-d. After twisting to g, one sees an increased stress level g-c, indicative of greater total frictional forces within the yarn at this point. The cycle is completed at h, the maximum S twist level again having been attained.

From the torsional stress-strain diagram for heat-set Kevlar 29 yarn, it is evident that internal frictional forces opposing twisting are greatest when the yarn is close to its preferred state, the zero stress level. Photographs show the yarn diameter to be near or at a minimum at this point and fiber to fiber contact appears to be greatest. At the point of no twist, fiber diameter is at a maximum and fiber to fiber forces opposing twisting have been lessened but are not zero. The only circumstance in which this is so is that of unset yarn at zero twist when all fibers are parallel to the body of the yarn and are in a relaxed state. The number of fiber to fiber contact points is apparently lessened when yarn set with S twist is untwisted and then Z twisted because the yarn diameter at e, the point of maximum Z twist, is greater than at b, the point of equivalent S twist. Although greater yarn diameter is assumed to be indicative of fewer fiber to fiber contact points, the stress required to overcome internal friction is not at a minimum at the zero strain level, where yarn diameter is the greatest. This is probably because

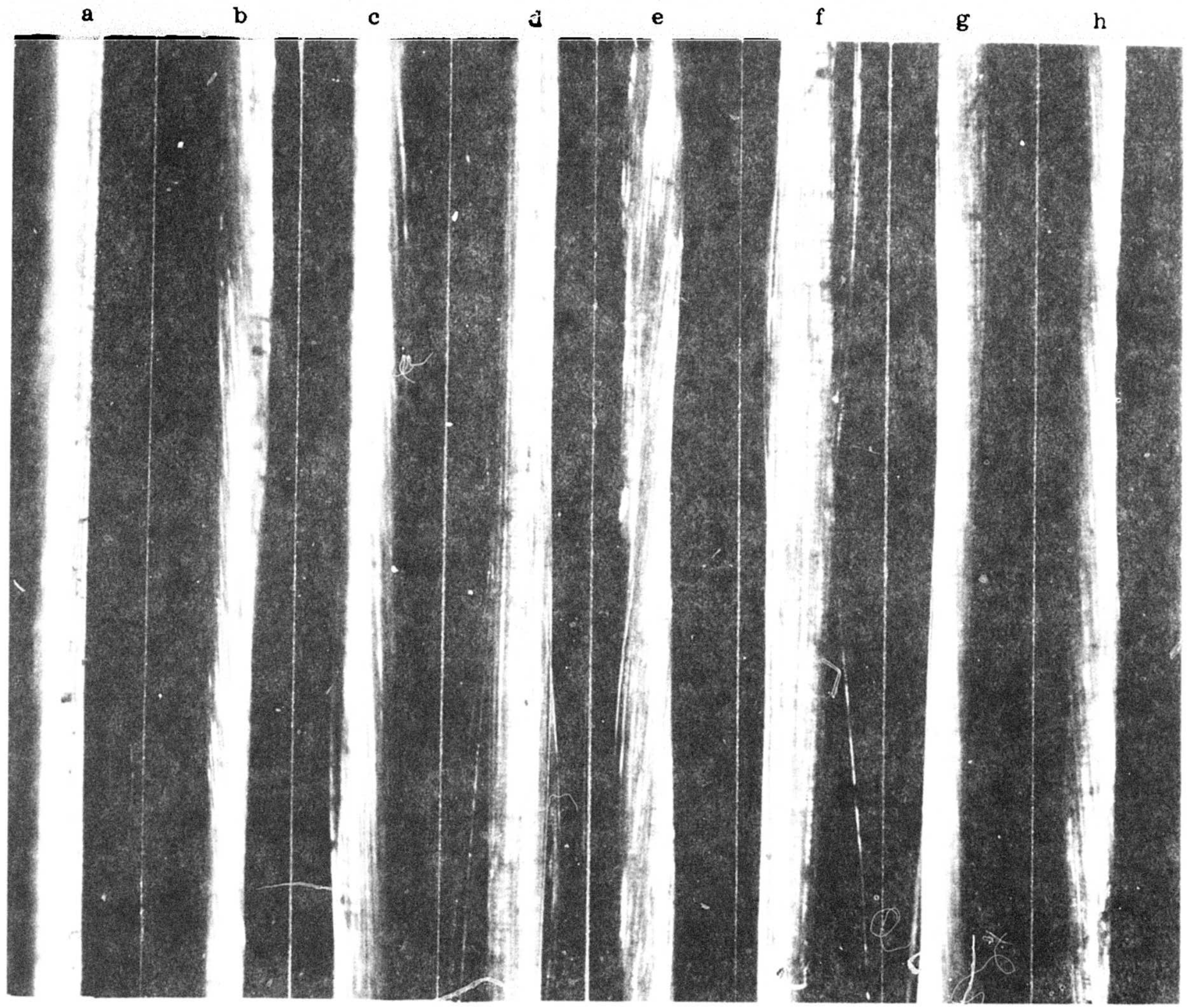

Figure 43. Microphotographs (~65X) of 100 Denier Kevlar 29 Yarn Taken at Several Intervals During a Torsion Test

normal forces at each contact point are increased at zero twist, due to the helical set in each fiber. Note that the torsional stress required to overcome internal friction is less on the Z twist side (-) of the diagram, as indicated by the vertical width of the enclosed area.

The greatly altered torsional properties of 100 denier Kevlar 29 yarn that has been heat set are not solely the result of molecular changes within the material. The nature of fiber to fiber contact within the yarn is greatly changed by setting, and this has a significant effect on the torsional behavior of the yarn structure as a whole.

SECTION V

BENDING RECOVERY OF KEVLAR FILAMENTS

1. Introduction

During the course of earlier work at FRL aimed at determining the ultimate strains which various filamentous materials can sustain in bending, it was discovered that Kevlar filaments could survive apparent surface bending strains as high as 100% without fracturing [2]. Furthermore, recovery of the Kevlar filaments from bending at high radii of curvature was far from complete. Generally, materials such as Kevlar, which exhibit low elongation to rupture and linear stress-strain diagrams in tension are considered brittle both in tension and bending. The Kevlar, on the other hand, behaves in bending similarly to the more usual polymeric materials. The mechanism by which Kevlar filaments survive severe bending is undoubtedly axial compressive yielding and the associated shifting of the neutral plane from the central plane of the filament toward that part of the filament cross-section in tension; such shifting of the neutral axis results in reduced surface tensile strains. The complete stress-strain diagram for the Kevlar materials is thought, therefore, to have the character indicated in Figure 44, exhibiting a yield in axial compression and subsequent plastic flow.

In an effort to further extend knowledge of the basic mechanical properties of the Kevlar fibers, measurements were made of their recovery from bending over a range of imposed curvatures both at 70°F and after short-term exposure to elevated temperature. The effect on the bending recovery of an extended period of time in the bent state, during which bending stresses may relax, has also been determined. Knowledge concerning such bending recovery behavior will contribute directly toward an understanding of the stabilization and heat setting of Kevlar structures containing bent filaments, including twisted yarns and woven and braided structures. In addition, it may be possible to deduce approximate values of the compressional parameters of the fibers such as compressive yield strain and post-yield compressive modulus by matching the measured bending recovery characteristics with those predicted from a theoretical analysis.

2. Experimental Procedure

Kevlar filaments were wound around mandrels of various diameters under a slight (0.05g) winding tension, and after a specified period of time, released to recover elastically. The recovered curvature of the filament was then determined as a function of the imposed curvature according to a procedure described by Freeston and Platt [3].

The apparatus used to wind the filaments is illustrated in Figure 45. The mandrel is held in a drill chuck attached to a hand crank which also drives a counter via a chain and sprocket. With this arrangement the filament can be wound a precise number of turns around the mandrel. After the specified time period the unwound portion of the filament is cut to remove the tensioning weight, releasing

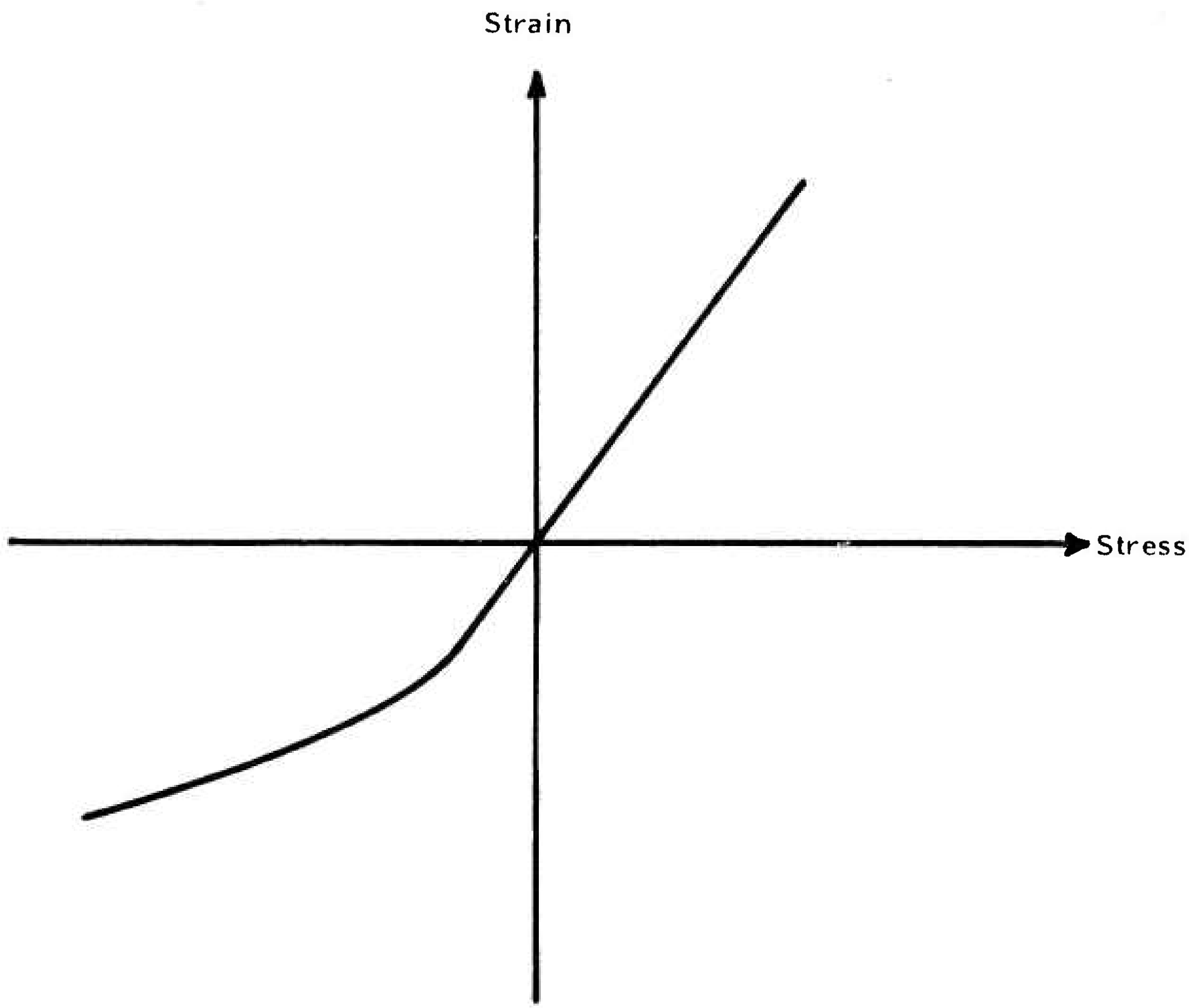

Figure 44. Anticipated Shape of Kevlar Stress-Strain Diagram

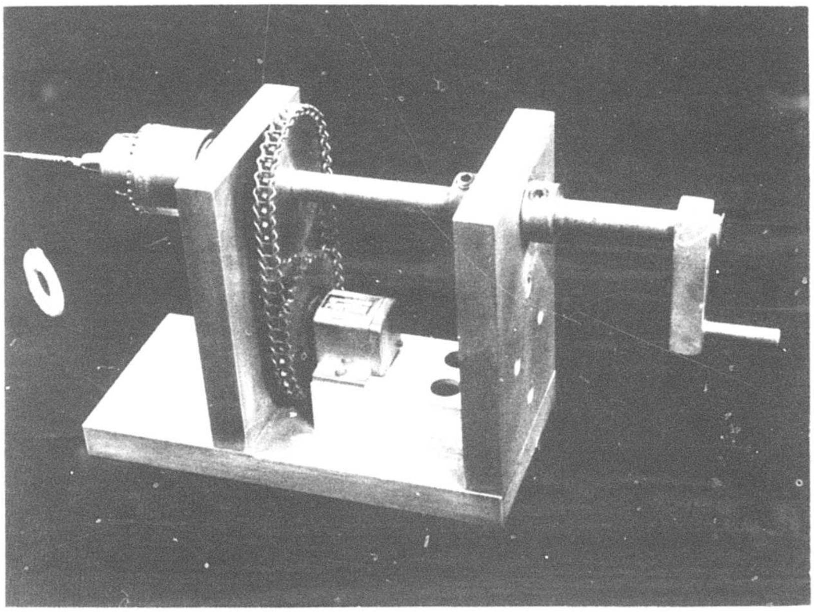

Figure 45. Filament Bending Recovery Test Fixture

the filament to recover freely. (Slight jostling of the winding is sometimes necessary to overcome frictional restrictions.) The number of turns remaining in the filament are then counted after unwinding it from the mandrel. During the tests the test fixture is mounted at a slight angle α, to the horizontal to cause some separation of the individual turns; the winding thus deviates from a 90° helix by an amount α.

The imposed curvature $1/\rho_1$, is given by the expression:

$$1/\rho_1 = \frac{2}{(D+d)} \tag{1}$$

where D is the mandrel diameter and d, the diameter of the fiber (0.00047 inch for the Kevlar). The displacement angle α used throughout this series of measurements was ~3.2° resulting in a correction factor, $\sin^2(90°-\alpha) = 0.9969$, negligibly different from one.

The recovered curvature $1/\rho_2$ can be expressed as a function of the initial curvature and initial and recovered number of turns in the windings, n_1 and n_2 respectively, as follows:

$$1/\rho_2 = \frac{n_2}{n_1} (1/\rho_1), \tag{2}$$

which can be derived by considering that the same length of filament is involved in both the initial and final windings. The bending recovery E is given by the expression:

$$E = \frac{1/\rho_1 - 1/\rho_2}{1/\rho_1} = \left(1 - \frac{n_2}{n_1}\right) \tag{3}$$

The effect of duration of the imposed bending strains was determined by restraining the filaments in the wound state for various lengths of time before allowing them to recover. Measurements were made after immediate release, and after 5 minute , on both materials; additionally after 16 hours, and in two selected cases, after 6 months on the Kevlar 29 only. In each case the immediate recovery was determined; no measurements were made after extended recovery periods. The recovered number of turns were counted to the nearest half turn. A sufficiently large number of turns was imparted to the filaments initially that the calculation of recovered curvature was precise to the nearest integral value.

Short term exposures of the wound filaments to elevated temperatures from 400-700°F were carried out by inserting the chuck holding the wound mandrel with tensioning weight in place in a hot-air oven. The total elapsed wound time of these specimens was 5 minutes; the specimens were inserted in the oven two minutes after winding, exposed for one or two minutes, and then allowed to cool for the remainder of the five minutes. The mandrels were cool to the touch within a few seconds after being removed from the oven.

3. Experimental Results and Discussion

The recovered curvature of Kevlar 29 filaments after various lengths of time before release from the wound state are given in Table XIV; the recovered curvature as a function of imposed curvature is plotted in Figure 46. Similar data for Kevlar 49 is contained in Table XV and plotted in Figure 47. The individual values of recovered curvature represent the average of multiple determinations except for those Kevlar 29 filaments held in the wound state for 6 months. The associated values for bending recovery for Kevlar 29 and Kevlar 49 are plotted in Figures 48 and 49 respectively; these diagrams were constructed using Eq 3 and pairs of points from the solid lines in Figures 46 and 47 rather than by simply connecting the individual data points.

In Figures 46 through 49 a scale of maximum apparent bending strain is shown to aid in the interpretation of the range of curvature values imposed. This strain is given by the ratio of the fiber radius to the imposed radius of curvature,

$$\varepsilon_{app} = \frac{d}{2\rho_1},$$

and is called apparent strain because it does not take into account shifting of the neutral axis from the central plane of the fiber cross-section.

Marked transition regions in the slopes of the recovered curvature curves are apparent in Figures 46 and 47; these are presumably related to the yield strain in axial compression. At imposed curvatures below those necessary to produce some yielding in the filament cross-section, recovery from bending should, if the material is perfectly elastic, be complete. Since the recovery from tensile loading is nearly complete for these materials, internal friction is probably responsible for restricting complete recovery in the initial regions of these curves. Extrapolation of the post-transition linear region to the complete recovery axis of those curves obtained after immediate recovery results in a value of apparent strain of 1.0% for the Kevlar 29 and 0.6% for the Kevlar 49.

The recovery of the Kevlar 29 is slightly more complete than that of the Kevlar 49 both after immediate release and when released after 5 minutes. This trend is in the direction to be expected from what is known of the comparative stress-strain properties of the two Kevlar materials: the Kevlar 29 has the lower tensile and initial compressive modulus and higher elongation to break [4], and thus bending to a particular curvature is less severe. However, the Kevlar 29 is more sensitive to the 5 minutes elapsed wound time before recovery than the Kevlar 49, suggesting a greater degree of stress decay in the Kevlar 29. As the time before release is increased to 16 hours and 6 months for the Kevlar 29 filament, the recovery becomes poorer, approaching more nearly the zero recovery line. As stress within the filament decreases with increasing wound time, less energy is available for recovery.

Table XIV: Bending Recovery of Kevlar 29 Filaments at 70°F

Time Before Release	Mandrel Diameter, D (inch)	Imposed Curvature, $1/\rho_1$ (inch^{-1})	Number of Turns: Imposed, n_1	Number of Turns: Recovered, n_2	Recovered Curvature, $1/\rho_2$ (inch^{-1})	Bending Recovery, E (%)
~0	0.101	20	30	3-4	2-3	~90
	0.052	38	30	4.2	5	86
	0.039	51	40	5.5	7	86
	0.032	61	50	6.2	8	88
	0.024	81	40	7.3	15	82
	0.020	97	50	11.2	22	78
	0.016	121	30	8.7	35	71
	0.0135	142	30	8.5	41	72
5 minutes	0.101	20	30	4-5	3	~85
	0.052	38	30	5.5	7	82
	0.039	51	40	7.5	9.5	81
	0.032	61	40	7.3	11	82
	0.024	81	40	10.8	22	73
	0.020	97	50	16.4	32	67
	0.016	121	30	11.0	44	63
	0.0135	142	30	11.3	54	62
16 hours	0.101	20	20	5.8	6	71
	0.052	38	20	7.7	15	61
	0.032	61	20	7.1	22	64
	0.024	81	20	9.2	38	53
	0.020	97	20	10.7	52	46
	0.016	121	20	10.3	62	49
	0.0135	142	30	16.0	76	46
6 months	0.025	78	20	14.0	55	30
	0.016	121	20	15.5	87	23

Table XV: Bending Recovery of Kevlar 49 Filaments at 70°F

Time Before Release	Mandrel Diameter, D (inch)	Imposed Curvature, $1/\rho_1$ (inch^{-1})	Number of Turns: Imposed, n_1	Number of Turns: Recovered, n_2	Recovered Curvature, $1/\rho_2$ (inch^{-1})	Bending Recovery, E (%)
~0	0.101	20	30	4–5	3	~85
	0.052	38	30	7.1	9	76
	0.039	51	40	9.8	12	75
	0.032	61	30	8.9	18	70
	0.024	81	40	12.9	26	68
	0.020	97	50	18.8	37	62
	0.016	121	30	11.6	47	61
	0.0135	142	30	13.1	62	56
5 minutes	0.201	10	20	1–2	0.5–1	~96
	0.101	20	30	5–6	3–4	~82
	0.052	38	30	7.6	10	75
	0.039	51	40	10.9	14	73
	0.032	61	30	10.7	22	64
	0.024	81	40	13.5	28	66
	0.020	97	40	16.0	39	60
	0.016	121	30	12.2	49	59
	0.0135	142	30	13.9	66	54

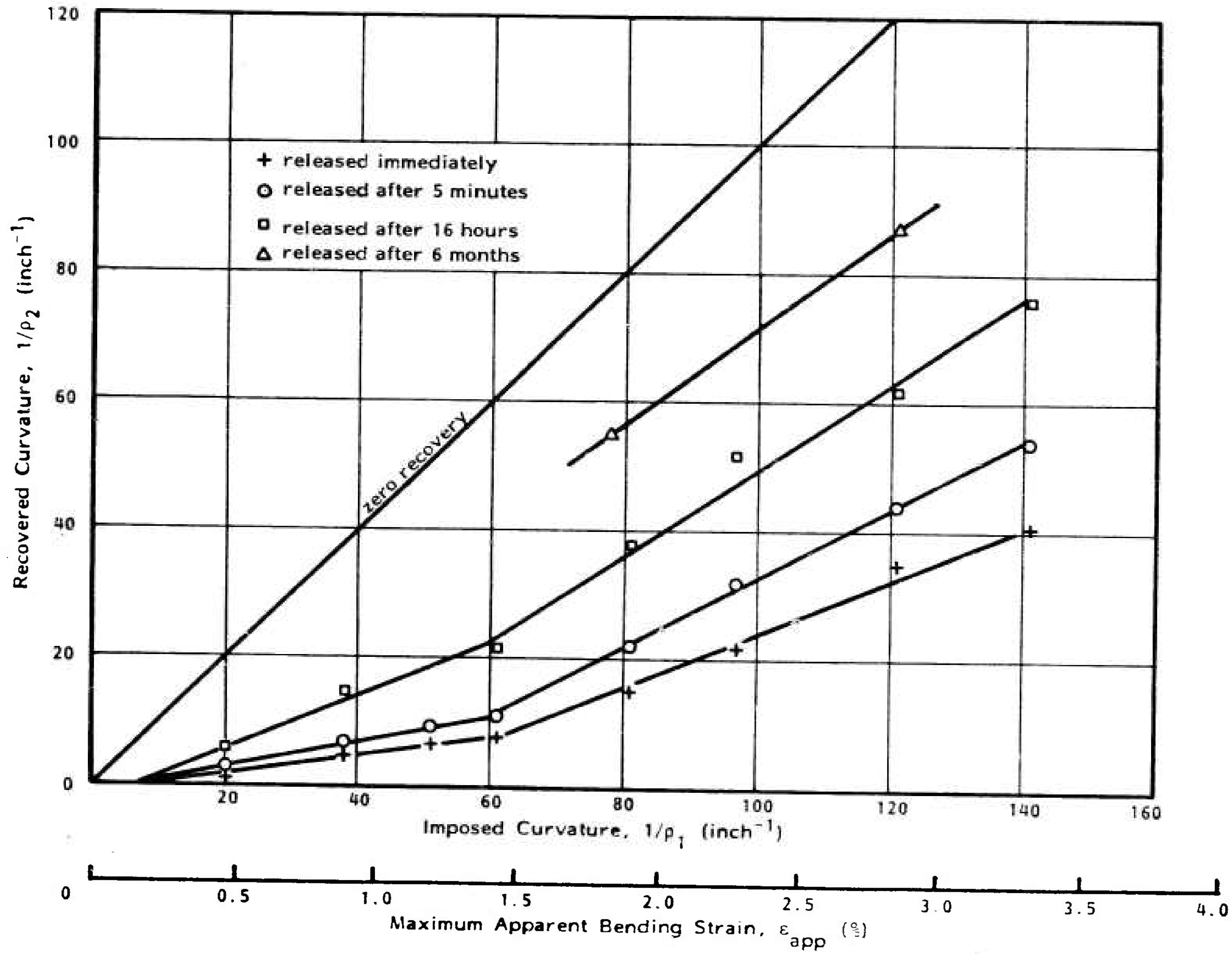

Figure 46. Recovered Curvature as a Function of Imposed Curvature for Kevlar 29 Filaments at 70°F after Various Times Before Release

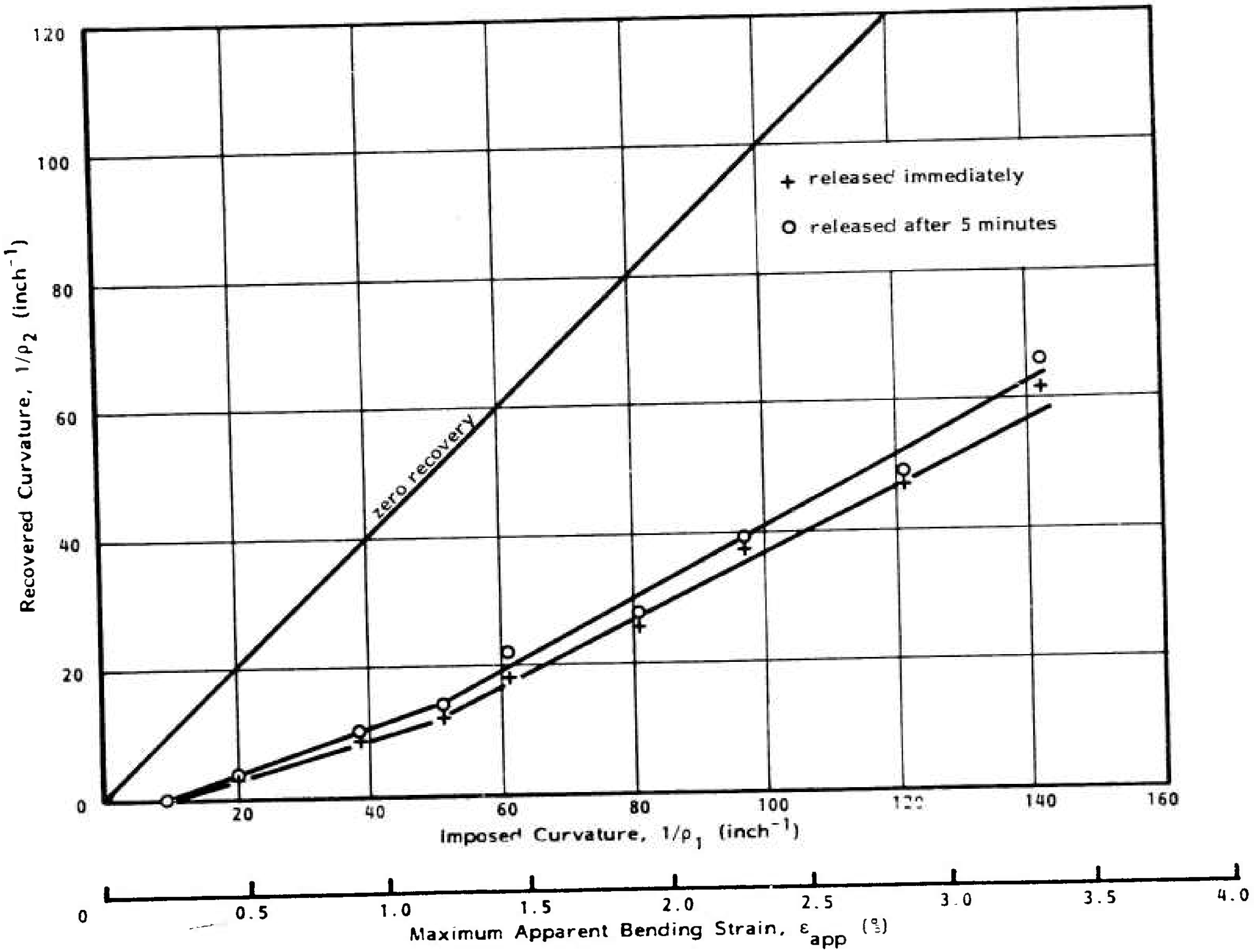

Figure 47. Recovered Curvature as a Function of Imposed Curvature for Kevlar 49 Filaments at 70°F after Various Times Before Release

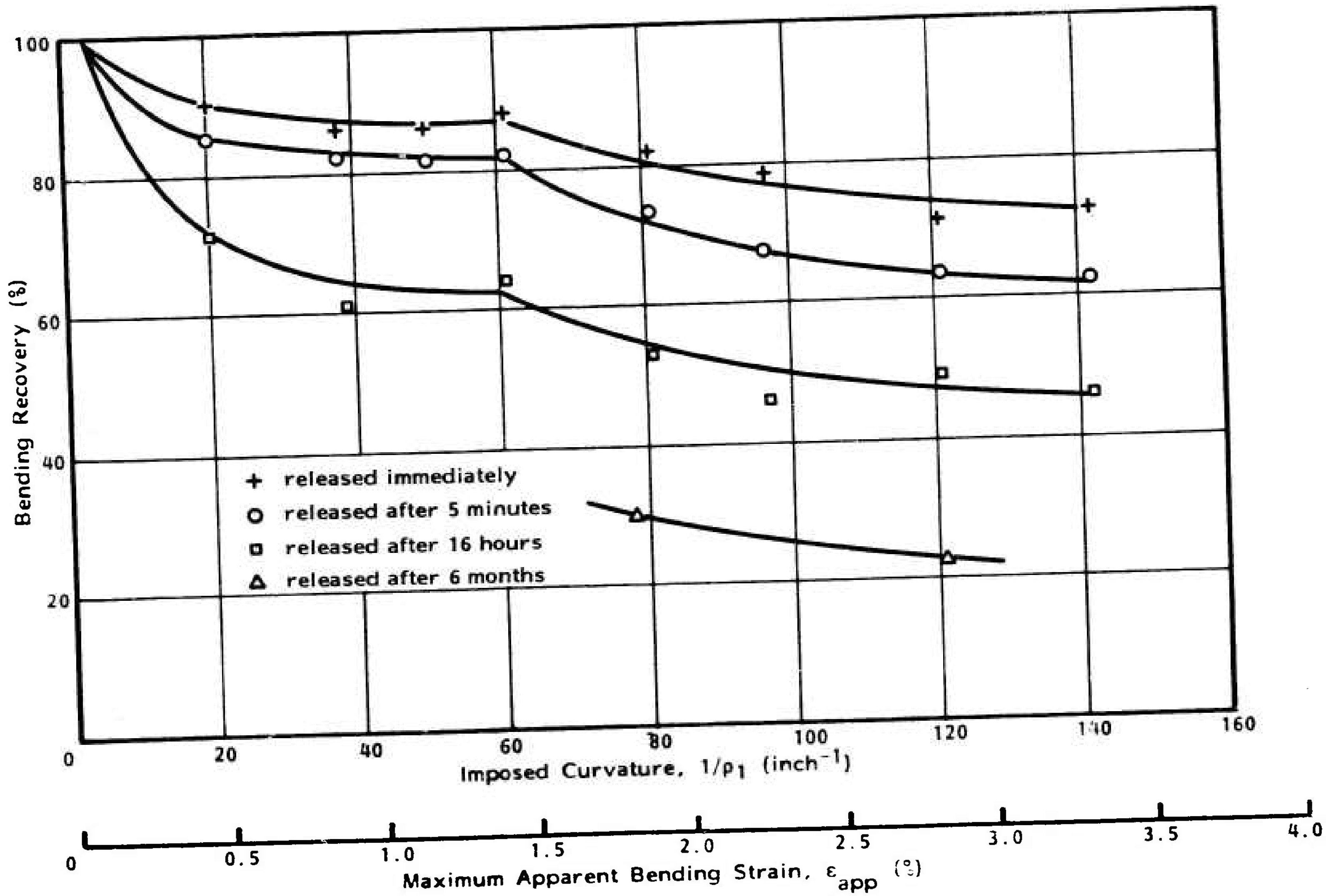

Figure 48. Bending Recovery of Kevlar 29 Filaments as a Function of Imposed Curvature at 70°F after Various Times Before Release

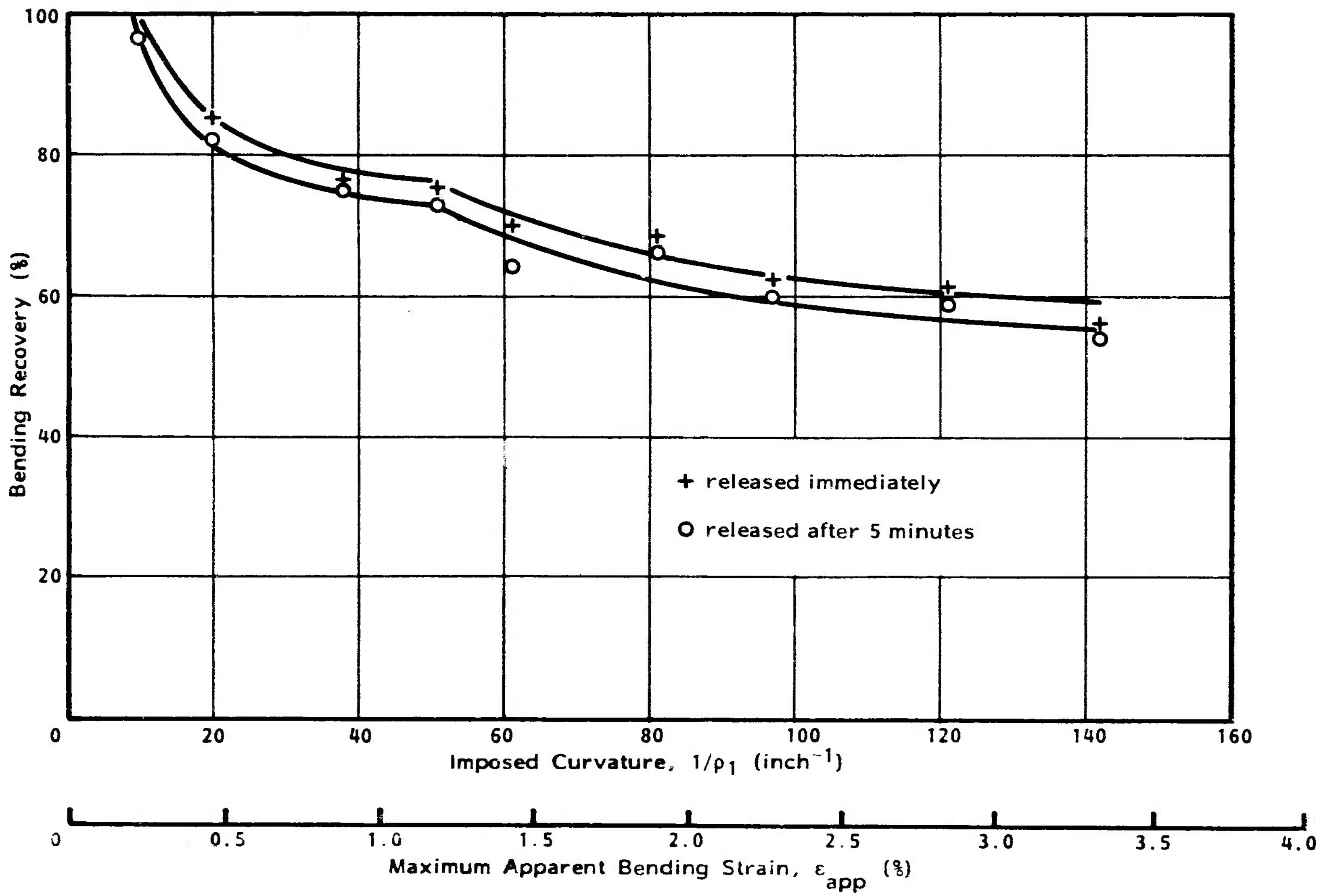

Figure 49. Bending Recovery of Kevlar 49 Filaments as a Function of Imposed Curvature at 70°F after Various Times Before Release

The bending recovery of Kevlar 29 after short-term exposures to temperatures of 400, 500, 600 and 700°F are given in Table XVI and plotted in Figures 50 and 51. The bending recovery of Kevlar 49 after exposure to 400 and 700°F is given in Table XVII and Figures 52 and 53. The response of the two fibers at 70°F and 400°F are compared in Figure 54. The data in Table XVI shows essentially no differences in recovery after one or two minutes at 400°F for the Kevlar 29, hence all succeeding measurements were made after one minute exposures at temperature. The Kevlar 29 recovers ~20% after a one-minute exposure at 400°F. Recovery decreases progressively as the exposure temperature is increased to 700°F where essentially no recovery occurs. After one-minute exposures at both 400°F and 700°F, the Kevlar 49 recovers more than the Kevlar 29, a trend consistent with the lesser degree of stress decay observed with this material at 70°F. Thus, stresses imposed by bending can be significantly reduced in both Kevlar 29 and Kevlar 49 filaments by short-duration exposures at 400°F.

4. Theoretical Analysis of Bending Recovery

Equations have been formulated aimed at predicting theoretically the bending recovery of filaments with the particular stress-strain profile of the Kevlar filaments. This analysis is patterned after that of Freeston and Platt [3] but includes the effect of translation of the neutral axis from the central plane of the filaments. Numerical solution of these equations is not yet complete.

5. Compressive Yield Strain

Numerical solution of the theoretical equations describing the bending recovery of Kevlar filaments requires knowledge of both the tensile and compressive moduli, the compressive yield strain, and the post-yield compressive modulus of the fiber. The tensile modulus is available from single fiber tensile tests [4] and the initial compressive modulus has been determined from measurements of the bending modulus made on the Searle double pendulum [4]. Direct measurement of the yield strain in compression of a fiber as fine as the Kevlar would be extremely difficult. However, bent Kevlar fibers consistently show visual evidence of compressive buckling (see Figure 69a). The fiber strain at which the onset of this buckling occurs, as computed from the fiber curvature, is thought to be a direct indication of the compressive yield strain. Consequently efforts were made to bracket that value of apparent bending strain at which buckling first becomes evident using FRL's scanning electron microscope. Kevlar fibers in which a loose overhand knot has been tied were vacuum metallized and mounted on a special stage designed and constructed by FRL which allows tensioning of specimens in the SEM. While being observed, the knot was pulled progressively tighter in small increments until buckling was just visible on the inside of the bend, Figure 55. The curvature of the knot was progressively monitored at a lower magnification.

Partly because of the time-consuming nature of the measurement and partly because of the many experimental difficulties encountered in preparing and mounting the individual specimens, only a few successful measurements were made. The bracketing values of apparent yield strain are given in Table XVIII. Although the scatter in these measurements is large, they are in good general agreement with those obtained by extrapolation of the recovered curvature diagrams for the two

Table XVI: Bending Recovery of Kevlar 29 Filaments after Exposure at Various Temperatures (time before release, 5 minutes)

Exposure Temp (°F)	Time at Temp (min)	Mandrel Diameter, D ($inch^{-1}$)	Imposed Curvature, $1/\rho_1$ ($inch^{-1}$)	Number of Turns: Imposed, n_1	Number of Turns: Recovered, n_2	Recovered Curvature, $1/\rho_2$ ($inch^{-1}$)	Bending Recovery, E (%)
400	1	0.201	10	8	6.5	8	19
		0.101	20	20	17.1	17	14
		0.059	33	20	14.6	25	27
		0.052	38	20	15.5	30	24
		0.039	51	20	15.3	39	23
		0.028	70	20	16.5	58	17
		0.024	81	20	16.2	66	19
		0.020	97	20	17.0	83	15
		0.016	121	20	17.6	107	12
400	2	0.101	20	20	17.2	17	14
		0.052	38	20	14.7	28	26
		0.039	51	20	16.0	40	20
		0.024	81	20	16.6	68	17
		0.020	97	20	17.1	83	15
500	1	0.052	38	20	16.5	31	17
		0.024	81	20	17.5	71	12
		0.016	121	20	18.5	112	7
600	1	0.052	38	20	17.5	33	12
		0.024	81	20	17.7	72	12
		0.016	121	20	19.0	115	5
700	1	0.052	38	20	17.3	33	13
		0.024	81	20	18.8	77	6
		0.016	121	20	19.7	119	2

Table XVII: Bending Recovery of Kevlar 49 Filaments after Exposure at Various Temperatures (time before release, 5 minutes)

Exposure Temp (°F)	Time at Temp (min)	Mandrel Diameter, D ($inch^{-1}$)	Imposed Curvature, $1/\rho_1$ ($inch^{-1}$)	Number of Turns: Imposed, n_1	Number of Turns: Recovered, n_2	Recovered Curvature, $1/\rho_2$ ($inch^{-1}$)	Bending Recovery, E (%)
400	1	0.101	20	20	10.5	10	48
		0.052	38	20	12.6	24	37
		0.039	51	20	13.1	33	35
		0.028	70	20	15.4	54	23
		0.024	81	20	15.5	63	23
		0.020	97	20	15.7	77	22
		0.016	121	20	16.9	102	15
700		0.052	38	20	15.0	29	25
		0.024	81	20	17.5	71	13
		0.016	121	20	18.0	109	10

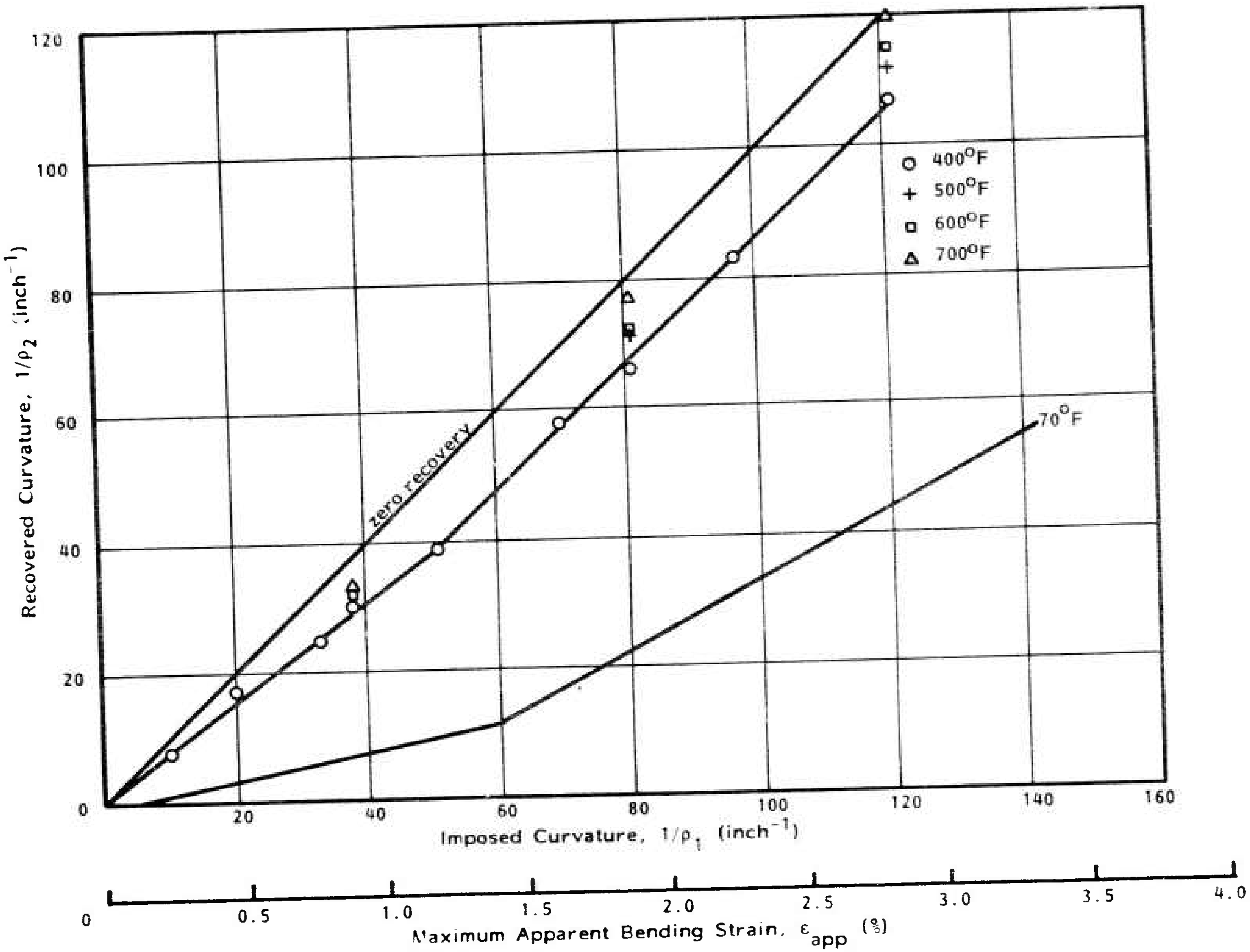

Figure 50. Recovered Curvature as a Function of Imposed Curvature for Kevlar 29 Filaments after 1 Minute Exposure at Various Temperatures - Released after 5 Minutes

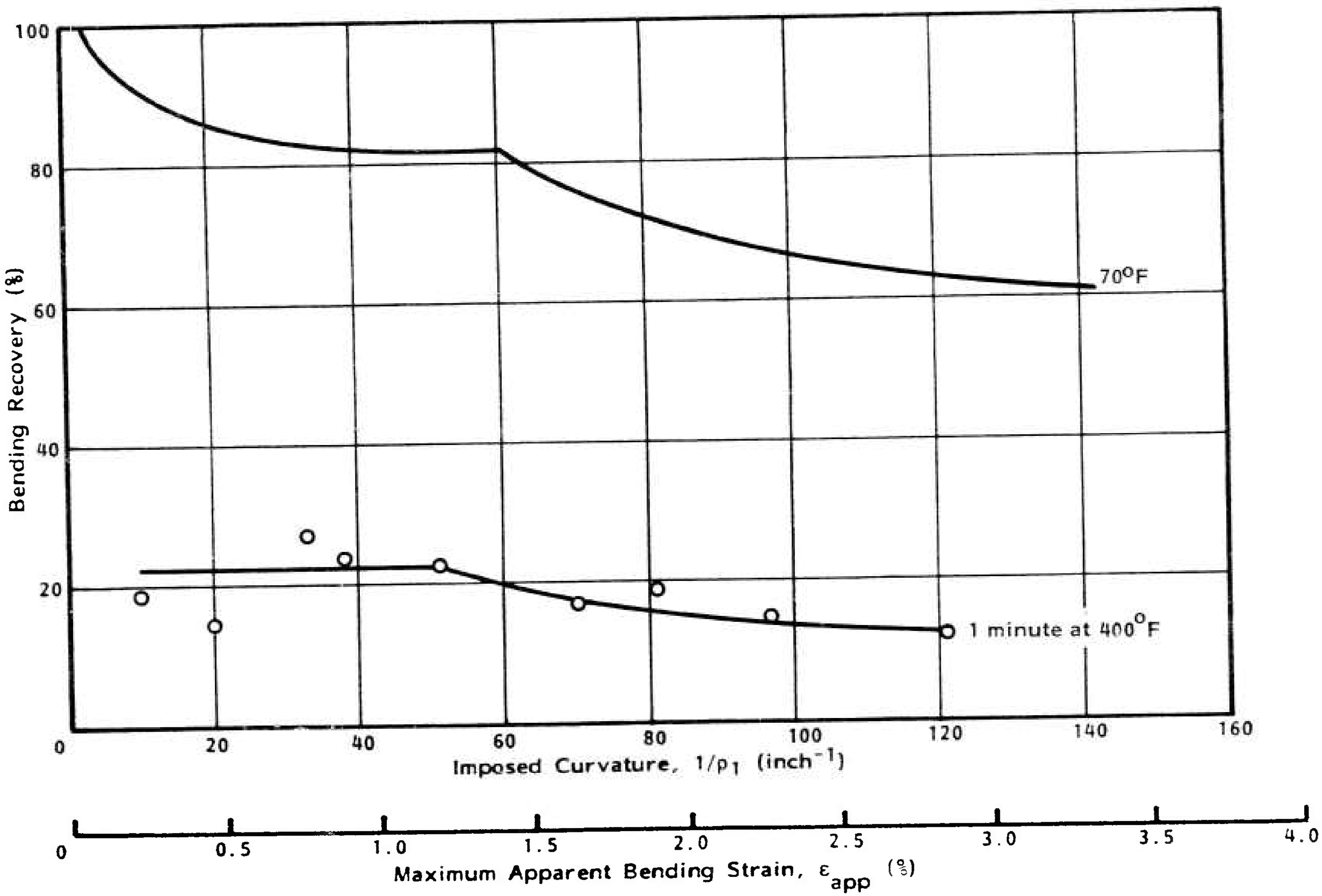

Figure 51. Bending Recovery of Kevlar 29 Filaments after 1 Minute Exposure at 400°F as a Function of Imposed Curvature - Released after 5 Minutes

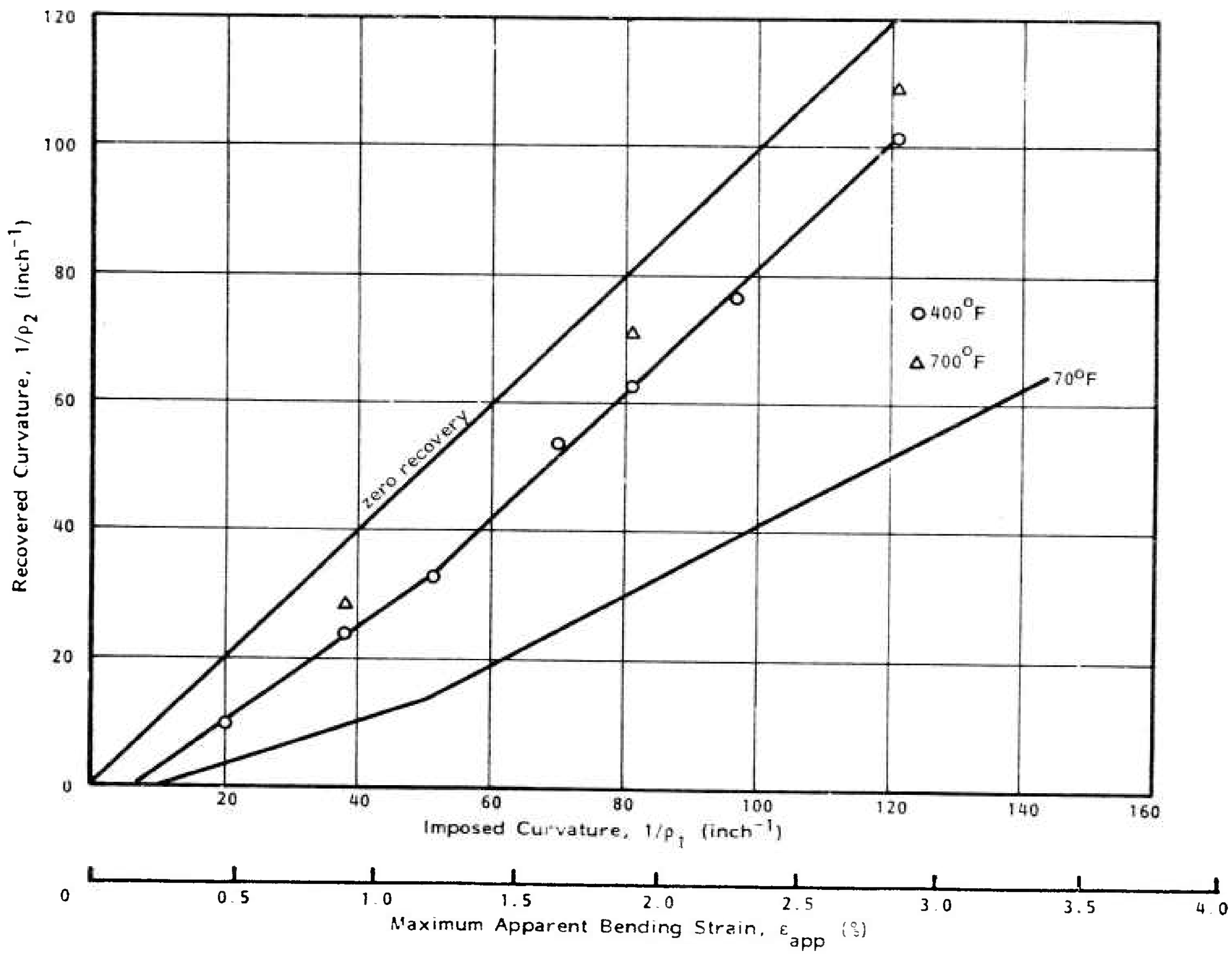

Figure 52. Recovered Curvature as a Function of Imposed Curvature for Kevlar 49 Filaments after 1 Minute Exposure at Various Temperatures - Released after 5 Minutes

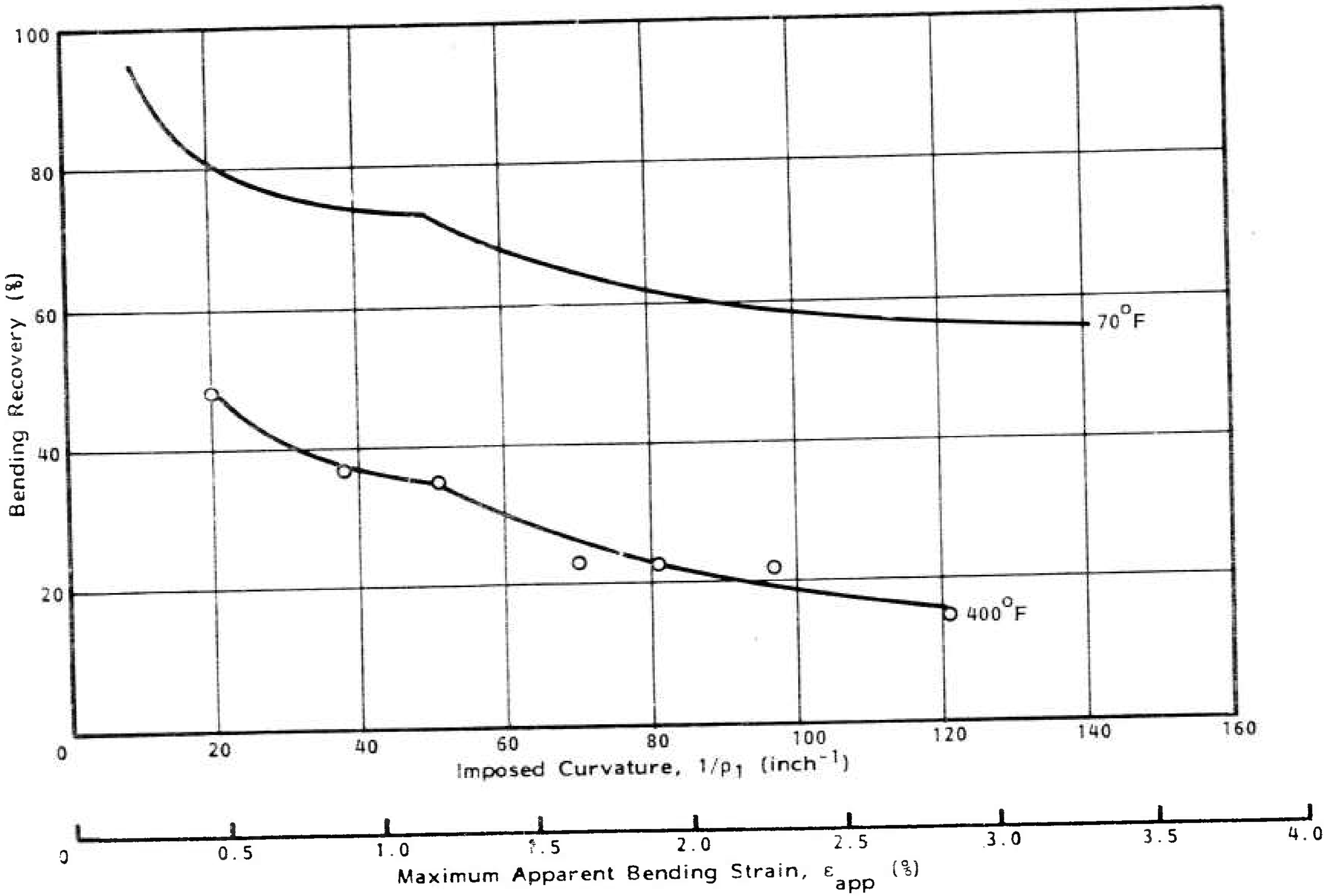

Figure 53. Bending Recovery of Kevlar 49 Filaments after 1 Minute Exposure at 400°F as a Function of Imposed Curvature - Released after 5 Minutes

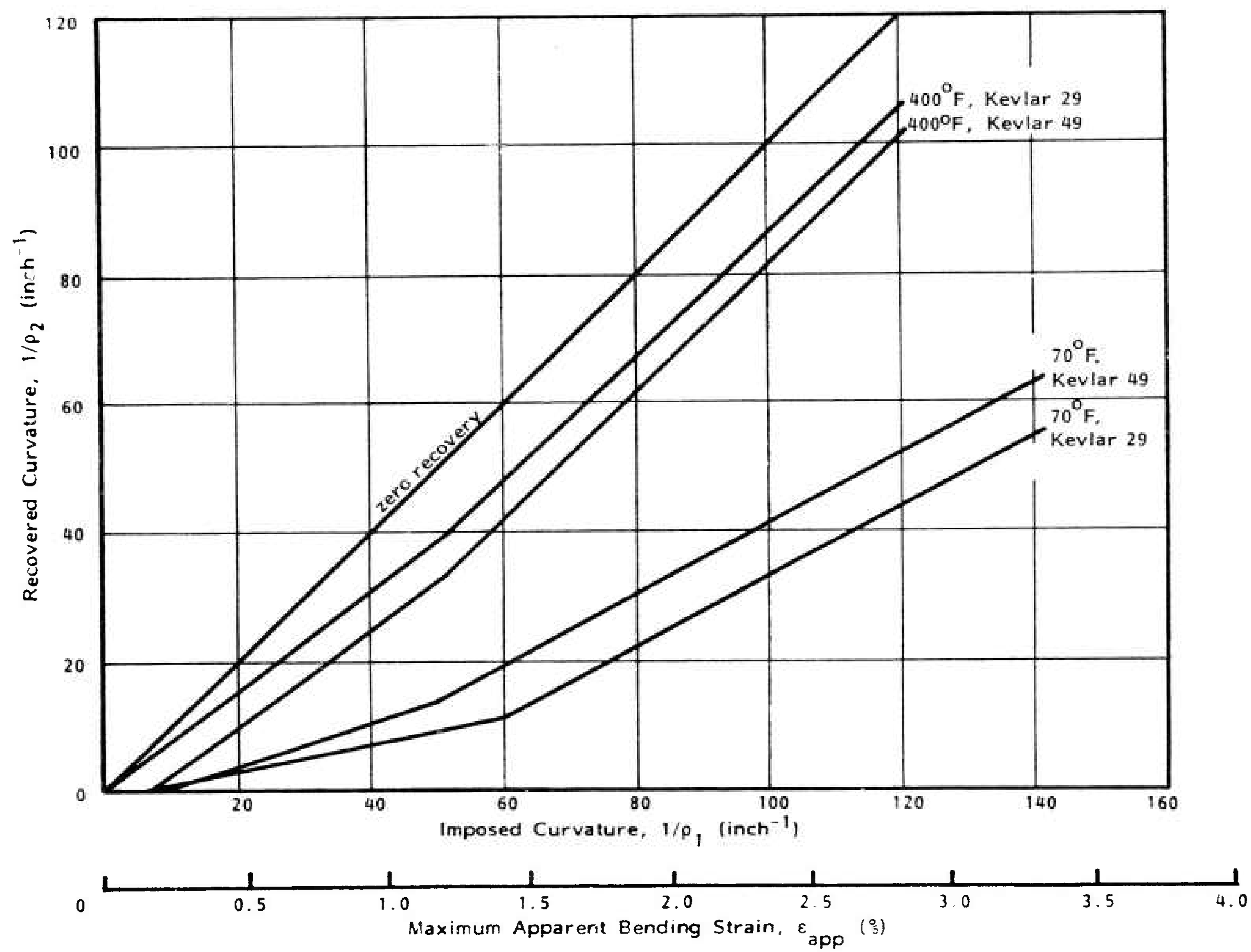

Figure 54. Recovered Curvature as a Function of Imposed Curvature for Kevlar 29 and Kevlar 49 Filaments at 70°F and 400°F - Released after 5 Minutes

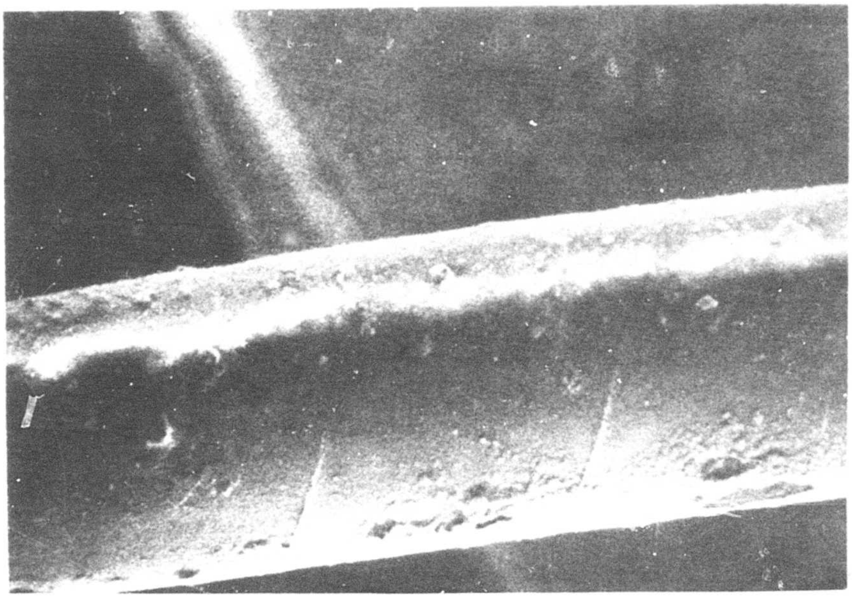

Figure 55. Onset of Compressive Buckling in a Bent Kevlar Fiber (3000X)

materials, namely 1.0% for the Kevlar 29 and 0.6% for the Kevlar 49. The values in Table XVIII, while substantiating the relationship between compressive buckling and yielding, do not provide a single, accurate estimate of the compressive yield strain as had been hoped. The large range in the measured values is the result of either an insufficiently refined experimental technique, or a significant deviation in this property from specimen to specimen, or both. A larger number of measurements than has been made would be required for a more precise average value of this quantity.

Table XVIII: Bending Strain at Onset of Compressive Buckling in Knotted Kevlar Fibers

Material	Apparent Bending Yield Strain (%) No Buckling		Buckling
Kevlar 29	1.46		1.62
	0.79		0.84
	1.07		1.22
	----		0.91
		Average	1.15
Kevlar 49	----		0.78

6. Conclusions

Both Kevlar 29 and Kevlar 49 fibers show good recovery from short-term bending at 70°F: 60-80% for the Kevlar 29 and 55-75% for the Kevlar 49 over a range of imposed curvatures sufficient to cause some compressional yielding. Decreased recovery, or setting, is observed in those specimens held in the bent state for extended periods of time; recovery of the Kevlar 29 after 16 hours in the bent state is on the order of 50%; after 6 months, 20-30%.

The stresses imposed by bending are largely relaxed at 400°F for both materials. After one minute at 400°F, the recovery of Kevlar 29 drops to ~10-20% and that of Kevlar 49 to 15-30%. This finding, which indicates that these materials may be heat set, provided a starting point for the heat setting study discussed in a previous section of this report. Although heat setting of Kevlar 29 yarn was shown to be feasible, strength losses resulting from elevated temperature exposure accompany the gains achieved by setting.

Estimates of the apparent yield strain in compression of the two fibers center around 1% for the Kevlar 29, slightly less for the Kevlar 49.

SECTION VI

MECHANICAL PROPERTIES OF FABRICS IN A RADIANT HEAT ENVIRONMENT

1. Introduction

Fabrics intended for use in high heat flux situations must be nonflammable, dimensionally stable, and effective thermal barriers. Past work on such fabrics has centered on defining their flammability by measurements of ignition times and burning rates at various temperatures and in various oxygen concentrations, and their effectiveness as thermal barriers by determination of their heat transfer characteristics. An equally important facet of their protective capacity is their ability to continue to act as fabrics in a high heat flux environment, that is, to retain those characteristics of flexibility and strength which originally led to the choice of a fabric structure in the particular application. If a fabric becomes so weakened or embrittled by the application of heat that it disintegrates or tears during movement or slight stressing, it can no longer serve as a thermal barrier. The limits of usefulness of a variety of fabrics can be determined by studying their mechanical properties at various levels of heat flux. Measurements of the changes in tensile modulus, tensile and tearing strength and determination of bending hysteresis losses, while the fabric is subjected to high levels of radiant heat, should define the level and rate of embrittlement and degradation undergone by the fabric in such a situation. In an attempt to explore these changes, preliminary measurements of the tensile properties of two fabrics, a spun Durette and spun HT-4, have been made in various bilateral radiant heat flux environments as high as 1.25 cal/cm^2/sec supplied by two facing infrared heaters.

2. Experimental Procedure

The tensile test specimens are suspended between two vertical infrared heaters mounted in a chamber which rests on the crosshead of an Instron tensile test machine, and are gripped by split cylinder jaws fitted into specially designed jaw holders linked to the Instron load cell and crosshead, Figure 56a. The jaws are inserted in the jaw holders and, at the same time, between the heaters by means of a track and plunger system mounted on the chamber door, as shown in Figure 56b. This specimen mounting system allows both rapid and precisely timed insertion of a test specimen between heaters already at thermal equilibrium. Decomposition products are constantly withdrawn from the chamber during the testing and vented outside the building. At the end of a predetermined exposure time, a tensile test is carried out.

The quartz-faced radiant heater strips*, measuring 12 inches by 2 inches, are individually capable of supplying a unilateral heat flux up to approximately 1.5 cal/cm^2/sec; used as a facing pair, the heaters can irradiate a specimen placed between them at bilateral energy levels up to 3.0 cal/cm^2/sec. Measurements of the thermal output 1/4 inch from the surface of a single heater using a

*Solar Strip Heater, Hugo N. Cahnman Assoc., Kew Gardens, New York.

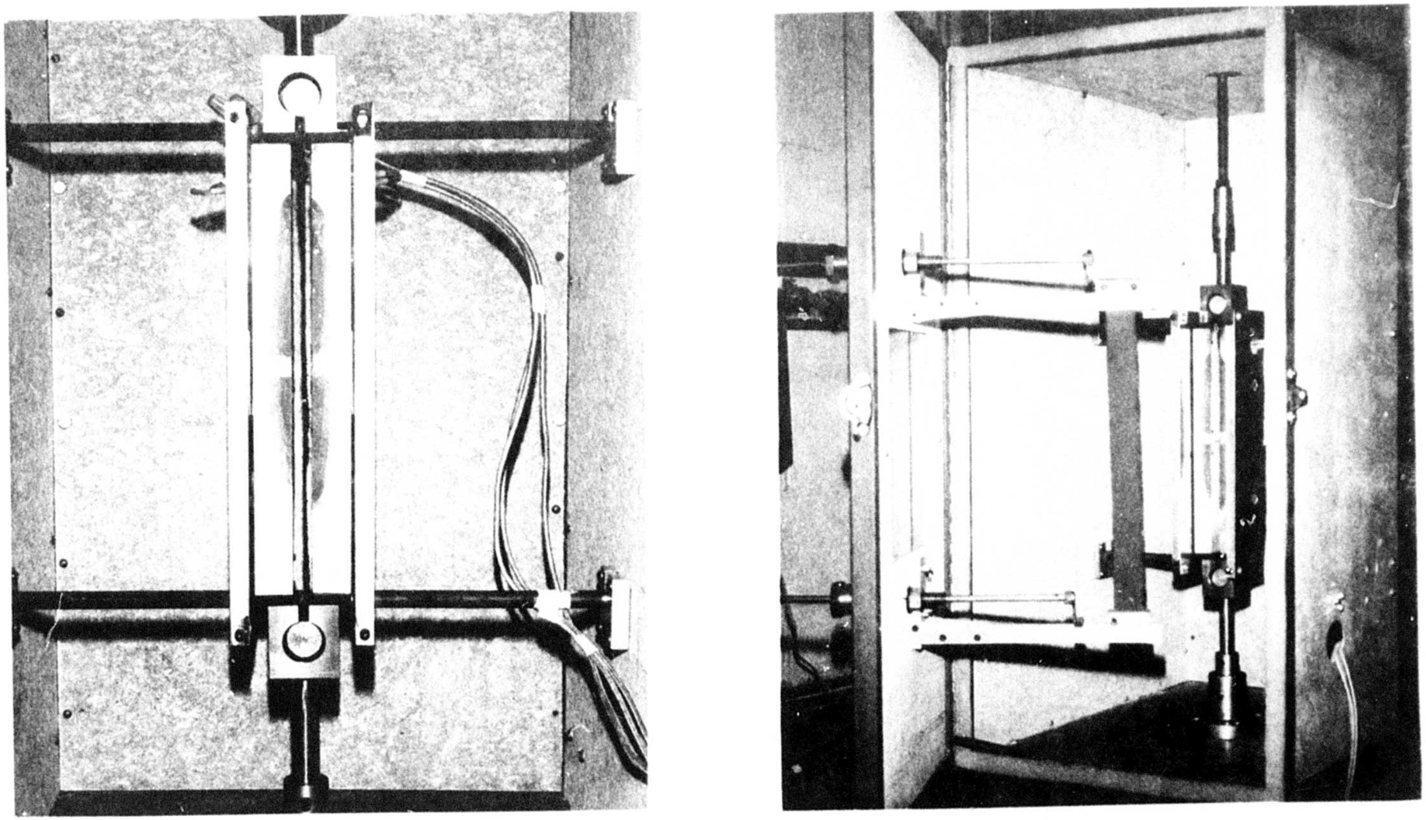

(a) (b)

Figure 56. Radiant Heaters and Test Chamber: (a) Specimen in Place Between Facing Heaters, (b) Track System for Inserting Test Specimen

water-cooled calorimeter indicated that the heat flux varies considerably with position across the heater surface, the average being ~60% of the power supplied to the heater. Since an averaging effect is likely to occur over the surface of a specimen placed between the heaters, the heat flux levels used in the tensile testing will be reported as ranging from 60 to 100% of the power supplied, the lower value indicating more closely the governing heat level and the higher value, a maximum above which no portion of the fabric was exposed.

The tensile tests were carried out on one-inch wide ravelled strips using a 13.5 inch gauge length and a crosshead speed of 20.0 inches per minute. The long gauge length was dictated by the heater configuration; the fast crosshead speed was necessary to minimize the test time in relation to exposure time.

3. <u>Experimental Results and Discussion</u>

Preliminary measurements of the tensile properties of a spun Durette and a spun HT-4 fabric have been made at several bilateral heat flux levels. These data indicate only the types of trends that can be expected with these two materials as incident heat flux and time of exposure are increased. Further work will be necessary to determine the fabric tensile properties under more precise and uniform conditions of impinging heat flux. A description of the two fabrics used in the investigation and their tensile properties at 70°F are given in Table XIX; both fabrics are flightsuit weight, 4.7 oz/yd^2. The properties in high thermal flux were determined in the warp direction for the Durette fabric and the filling direction for the HT-4 fabric since these corresponded to the directions of lowest yarn crimp in the respective fabrics. Both fabrics were tested in the scoured state.

Table XIX: Fabric Description and 70°F Tensile Properties of Durette and HT-4 Fabrics

Fabric Description	Initial Modulus (lb/in. width) Warp	Initial Modulus (lb/in. width) Fill	Rupture Elongation (%) Warp	Rupture Elongation (%) Fill	Rupture Load (lb/in. width) Warp	Rupture Load (lb/in. width) Fill
Durette, 4.7 oz/yd^2	834		20.1		69.3	
plain weave, 49 x 43	850		23.1		74.4	
	907		18.9		69.2	
	770		22.9		68.3	
	840		21.4		70.0	
Average	840		21.3		70.2	
HT-4, 4.7 oz/yd^2	1210	1590	16.1	10.5	113	112
plain weave, 54 x 47	1210	1530	15.8	11.6	110	108
	1210	1530	16.0	11.5	107	111
	1180	1470	15.7	11.5	102	105
	1190	1490	15.1	10.8	103	100
Average	1200	1520	15.7	11.2	107	107

The fabric strength retention, approximate rupture elongation and approximate initial modulus are plotted as a function of duration of exposure to heat flux of various levels in Figures 57 - 59 for the Durette and Figures 60 - 62 for the HT-4. Each data point represents the average of at least three determinations at the indicated conditions unless a (1) is noted by a particular entry on the graph, in which case a single determination was made. Since the actual test time during which the crosshead was moving was several seconds in most cases (0.45 x % rupture elongation), the rupture strength and elongation values are plotted against total time elapsed to specimen rupture; the modulus values are plotted against exposure times at the start of the test.

As shown in Figure 57, the Durette fabric loses over 80% of its strength during exposures of 10 seconds at a bilateral heat flux of 0.5-0.8 cal/cm^2/sec and 90% of its strength at exposures between ~30 seconds and 10 minutes. At a heat flux of 0.6-1.0 cal/cm^{2}sec, the strength loss is 97% at 2 seconds and essentially 100% by 10 seconds. The rupture elongation values plotted in Figure 58 show a general downward trend with increasing heat flux and time of exposure interrupted by regions of high flow at low load level for heat flux values of 0.6-1.0 and 0.7-1.2 cal/cm^2/sec. The initial modulus values, Figure 59, decrease rapidly to values only a small fraction of the original value, then show a gradually increasing trend. The Durette fabric does not become severely embrittled at high heat fluxes but does lose virtually all of its strength within seconds after exposure to bilateral heat fluxes exceeding 0.5-0.8 cal/cm^2/sec.

The HT-4 fabric retains a greater portion of its strength than the Durette fabric in a similar thermal environment. The strength of the HT-4 fabric, Figure 60, falls 70% after about 15 seconds at 0.5-0.8 cal/cm^2/sec and 80% within approximately 45 seconds; after 10 minutes at this heat flux, it still retains 15% of its strength. At a heat flux of 0.8-1.3 cal/cm^2/sec, the strength loss is 93% within 7 seconds and 100% at 30 seconds. The rupture elongation, Figure 61, shows a similar downward trend with no high-flow regions. The initial modulus, Figure 62, falls to less than half its original value within a few seconds at both levels of heat flux, but at 0.5-0.8 cal/cm^2/sec rises again to a level nearly equal to its original value; at 0.8-1.2 cal/cm^2/sec, the modulus falls to approximately zero at 30 seconds.

Because of the ~1.5 inches of the fabric strip length located outside of the high thermal flux region between the heaters both the rupture elongation and the modulus values measured directly from the Instron chart and based on a gauge length of 13.5 inches are somewhat in error. However, it can be shown that the magnitude of this error is not more than 1.5/12.0, or 12.5%, of the measured value when the measured fabric modulus in the heated region E_T is less than approximately twice the modulus in the unheated region E_O. If $E_T < E_O$, as is the case for all data obtained thus far, the measured values of rupture elongation will be somewhat low and those for modulus, somewhat high.

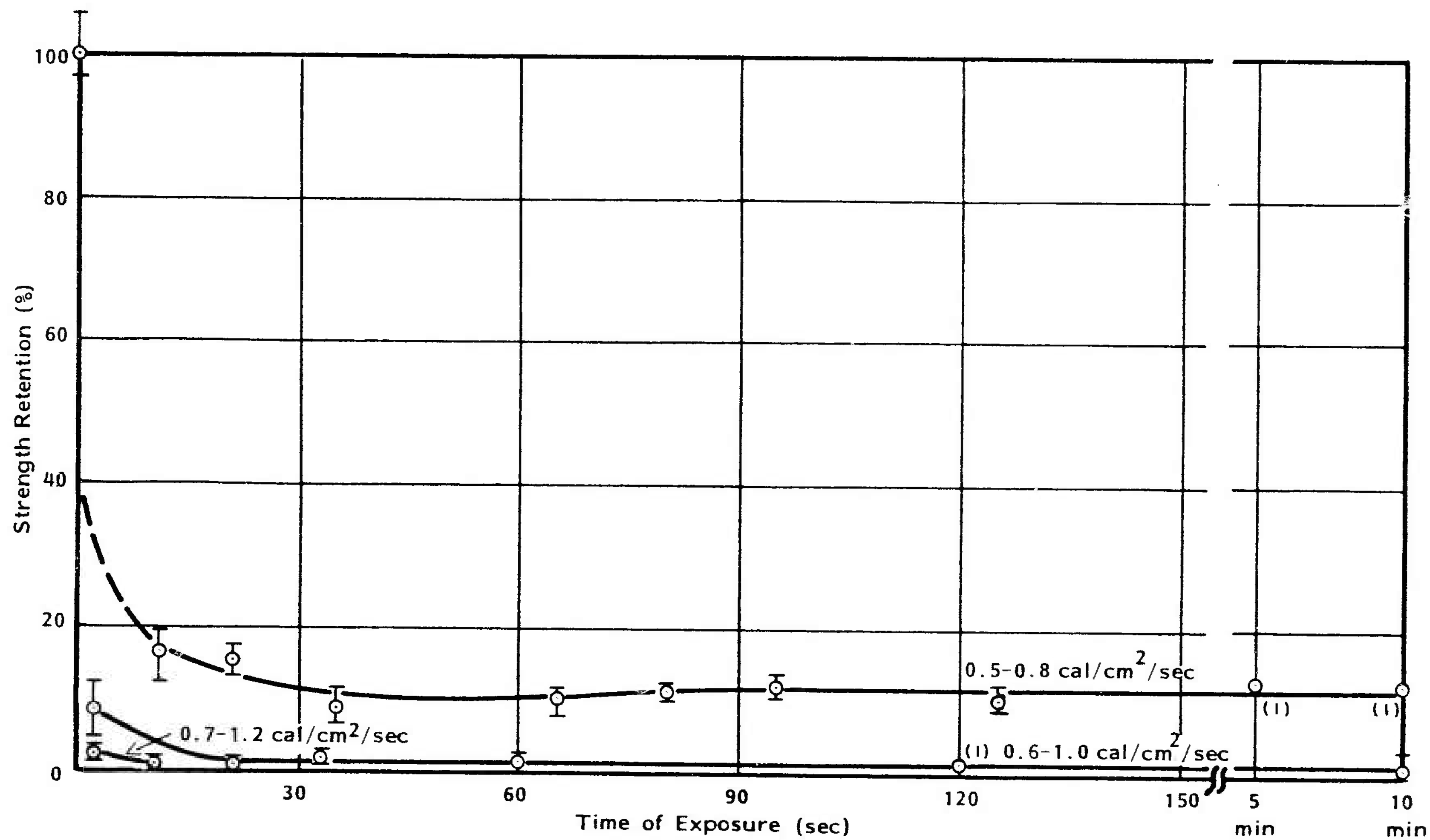

Figure 57. The Effect of Bilateral Radiant Heat Flux and Duration of Exposure on the Strength Retention of Durette Fabric (4.7 oz/sq yd)

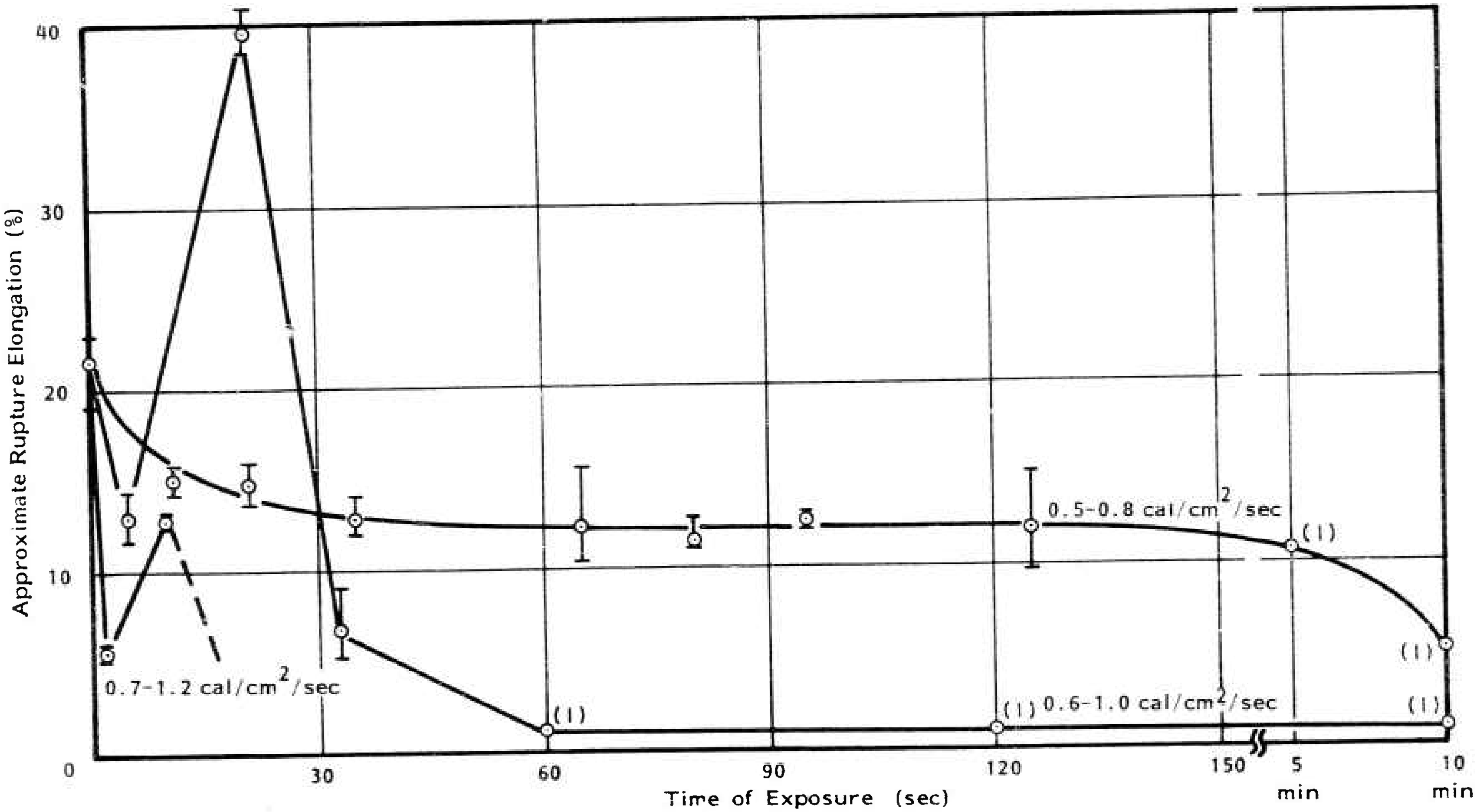

Figure 58. The Effect of Bilateral Radiant Heat Flux and Duration of Exposure on the Rupture Elongation of Durette Fabric (4.7 oz/sq yd)

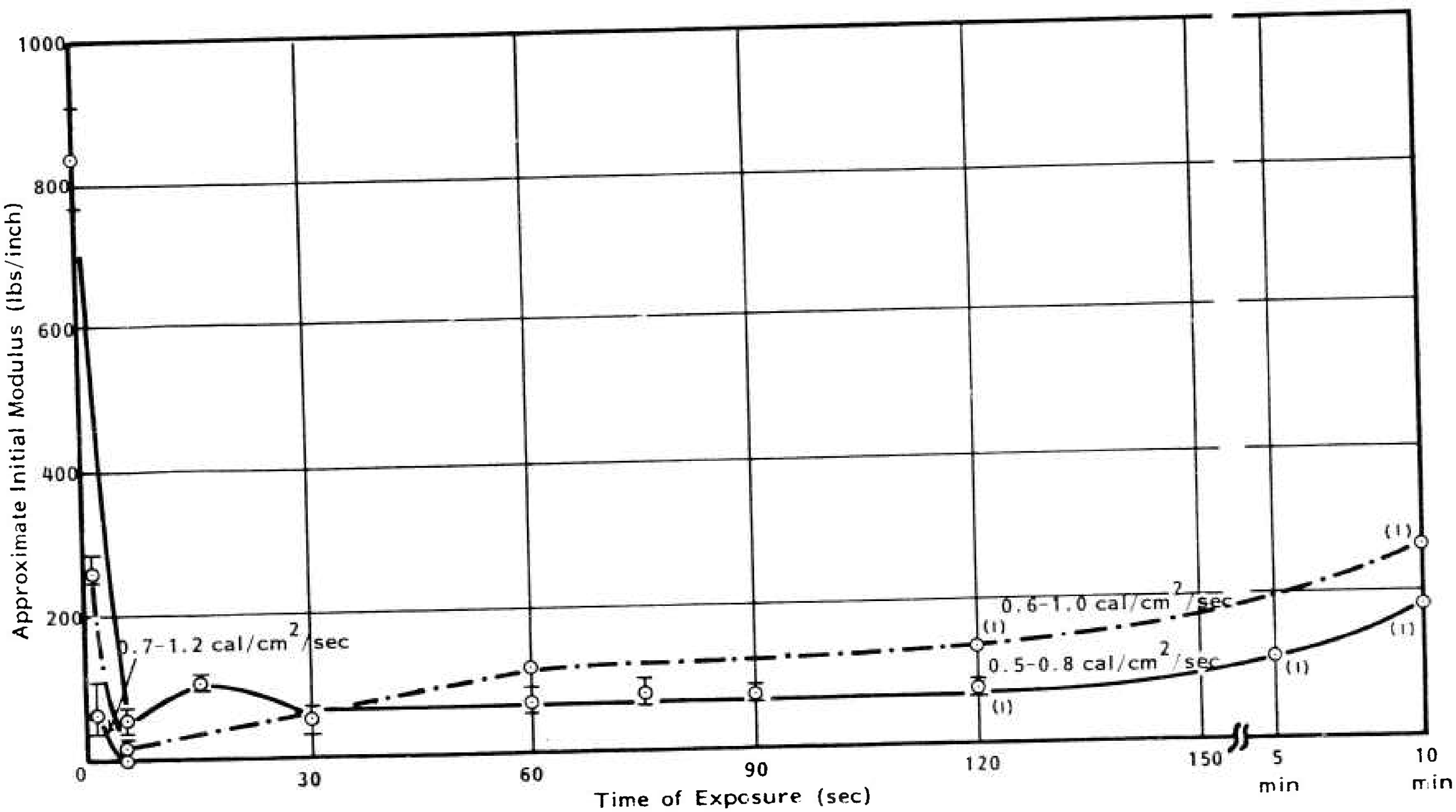

Figure 59. The Effect of Bilateral Radiant Heat Flux and Duration of Exposure on the Initial Modulus of Durette Fabric (4.7 oz/sq yd)

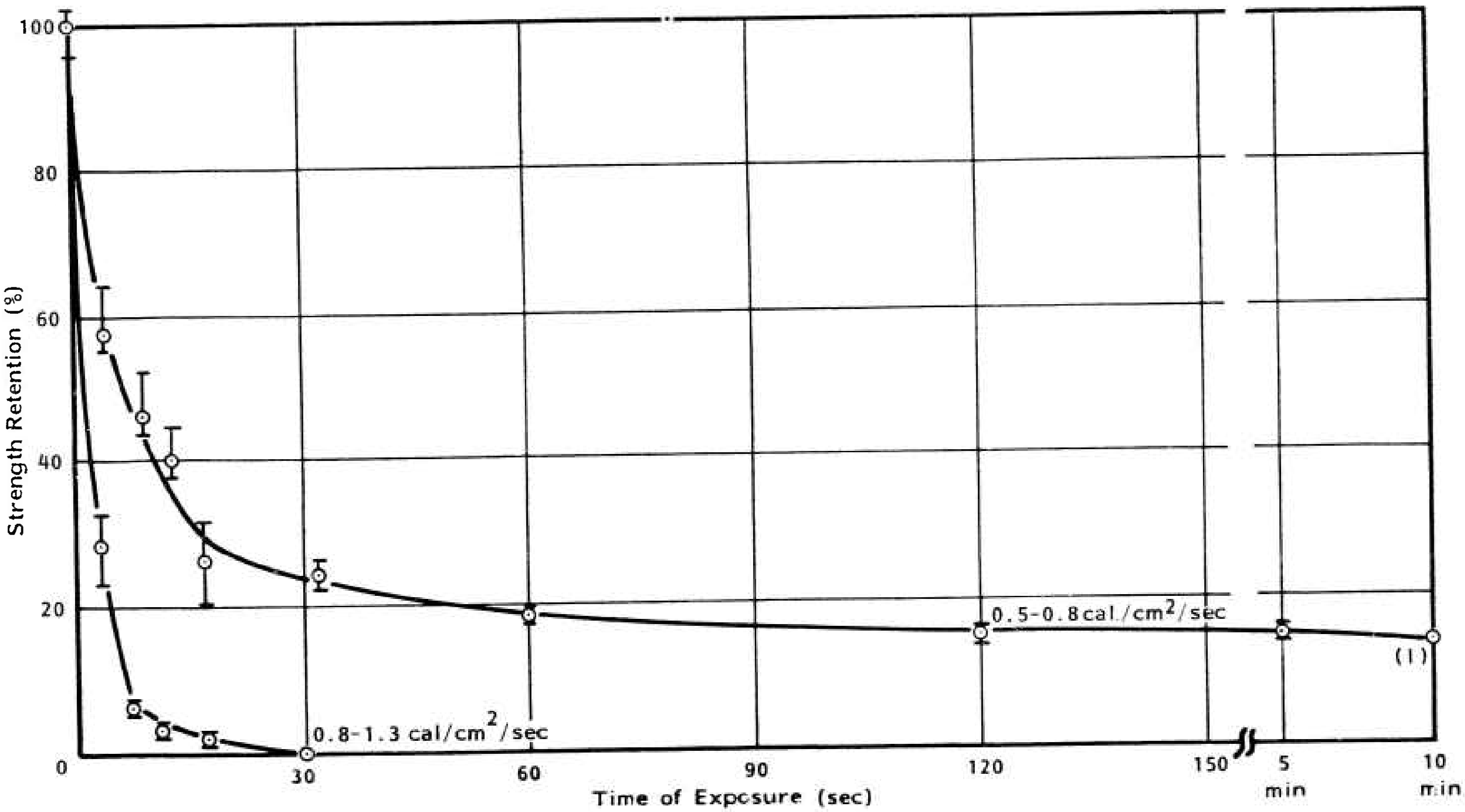

Figure 60. The Effect of Bilateral Heat Flux and Duration of Exposure on the Strength Retention of HT-4 Fabric (4.7 oz/sq yd)

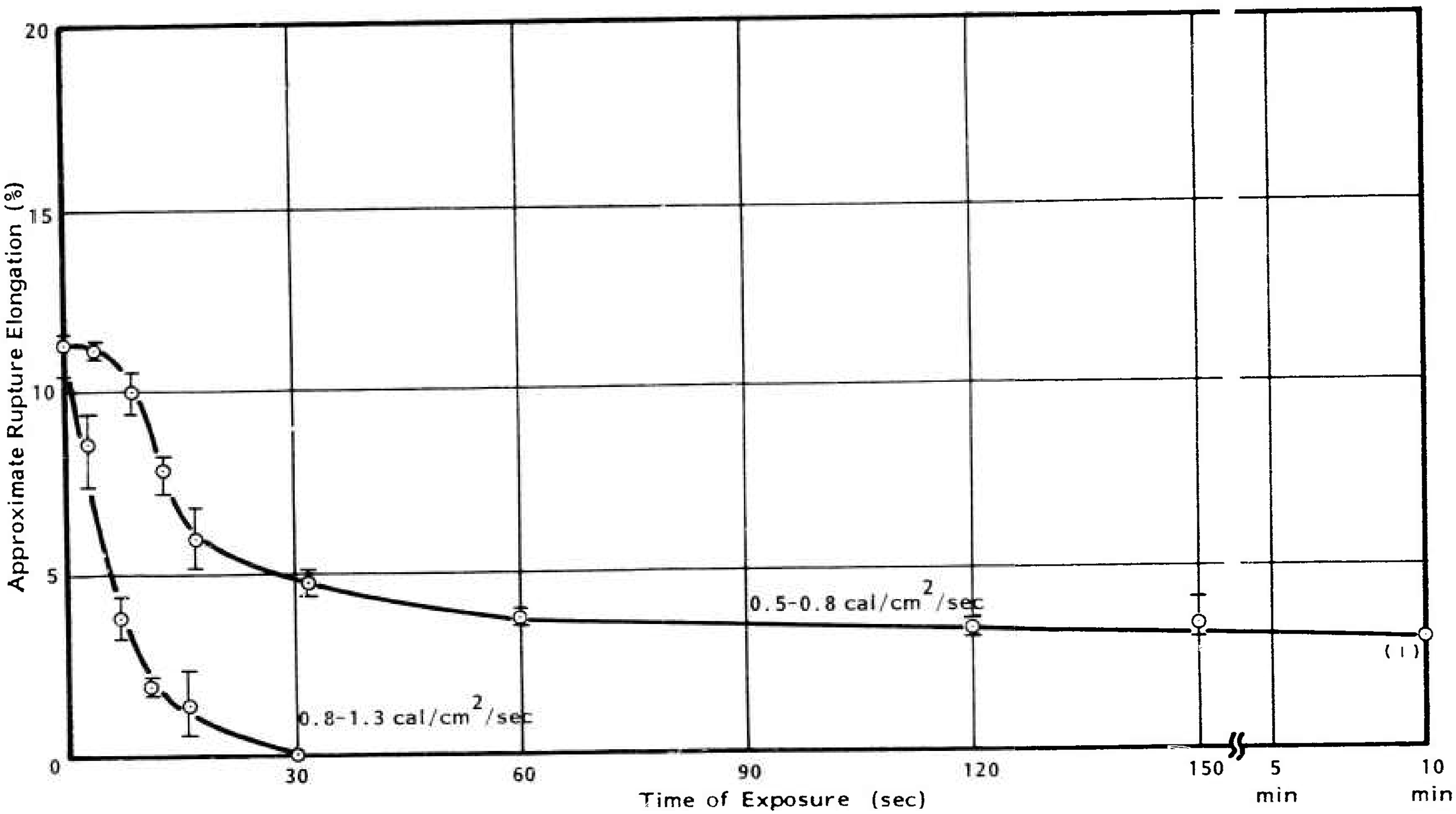

Figure 61. The Effect of Bilateral Radiant Heat Flux and Duration of Exposure on the Rupture Elongation of HT-4 Fabric (4.7 oz/sq yd)

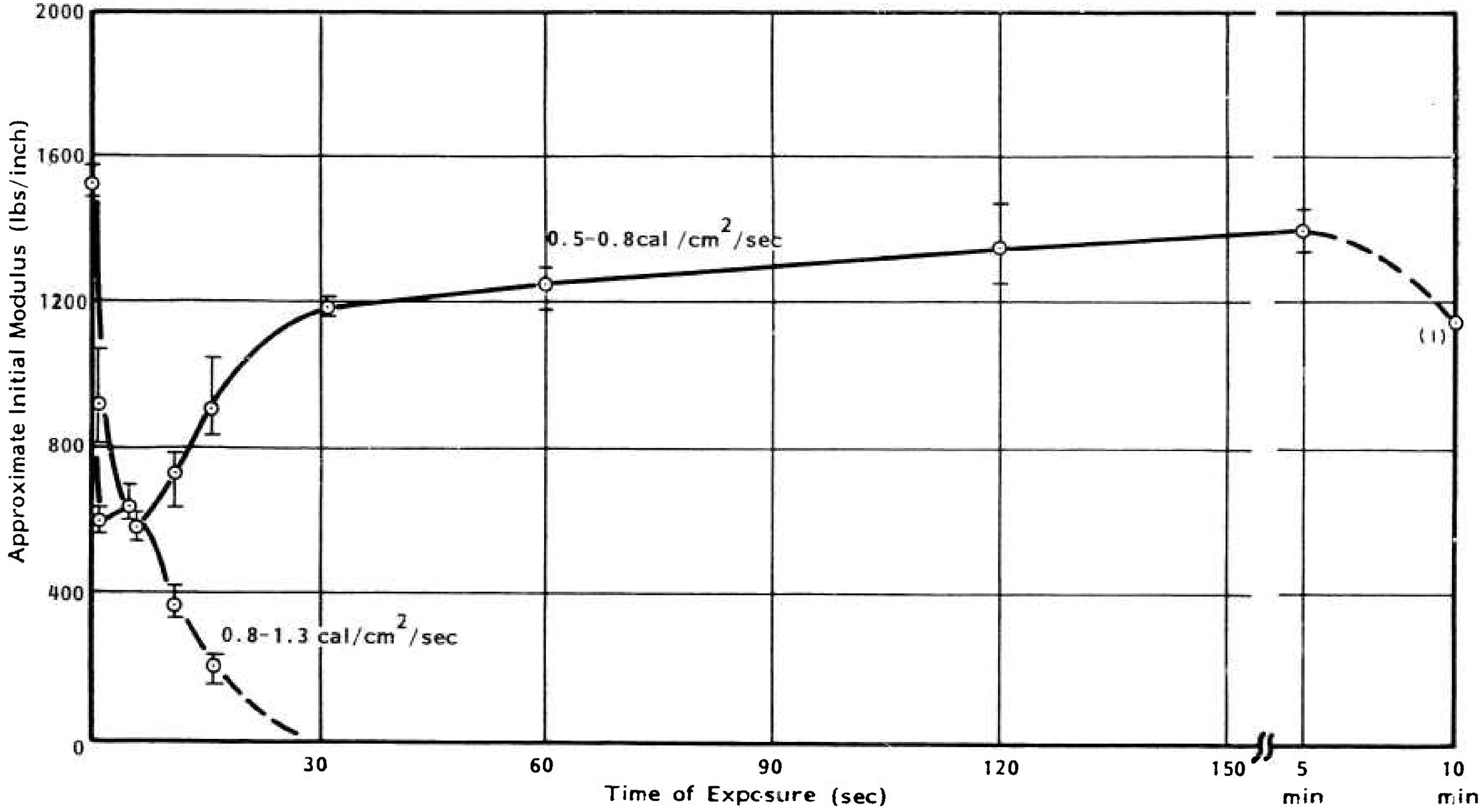

Figure 62. The Effect of Bilateral Radiant Heat Flux and Duration of Exposure on the Initial Modulus of HT-4 Fabric (4.7 oz/sq yd)

4. Future Plans

The foregoing work has established a technique for determining the tensile properties of fabrics exposed to varying levels of radiant heat flux for varying exposure times. Further, more precise measurement of the tensile response of irradiated fabrics will require infrared heaters capable of supplying a more spatially uniform heat flux. Such heaters are available on a custom basis from the manufacturers of those presently in use. If new heaters are acquired, both their thermal and optical properties should be well characterized.

All data obtained thus far has involved bilateral exposure of test fabrics, a situation in which the fabrics can be expected to reach the equilibrium temperature of the heaters almost immediately. The response of the fabrics when exposed to unilateral heat fluxes of the same magnitude is also of interest and will probably more closely relate to the requirements of protective clothing. With unilateral exposure, the rate of temperature rise within the fabric and the effect of heat flux on tensile properties would be slowed by the opportunity to lose heat more readily to the surroundings.

Another factor possibly affecting fabric tensile behavior in high radiant heat fluxes is the amount of air flow past the specimen during heating. It is hoped to carry out future testing in a completely sealed chamber to which a metered mixture of oxygen and nitrogen is supplied during exposure.

Other fabrics intended for inclusion in the test program, in addition to Durette and HT-4, include Nomex, Kynol, flame-retardant treated cotton, polyester and nylon - all in the approximate weight range of 4-6 oz/yd^2. Kevlar fabric may be added to the list as it becomes available.

It is hoped that this study can be refined and extended because of its value in predicting the utility of fabrics intended to provide thermal protection under various levels of heat flux and activity.

SECTION VII

KEVLAR 49 FIBER MORPHOLOGY

A preliminary microscopic study of the morphology of Kevlar 49 fiber has been undertaken using FRL's JEOL scanning electron microscope. The following photographs, Figures 63 through 69, depict the fiber's response to varying stress histories including cutting, rupture tension, twisting, bending, and lateral compression. Although the initial sampling of fibers in each case was necessarily small, the photographs presented have been selected primarily because they illustrate typical observed phenomena. This initial overview will serve to define those areas of fiber response of most interest for further study.

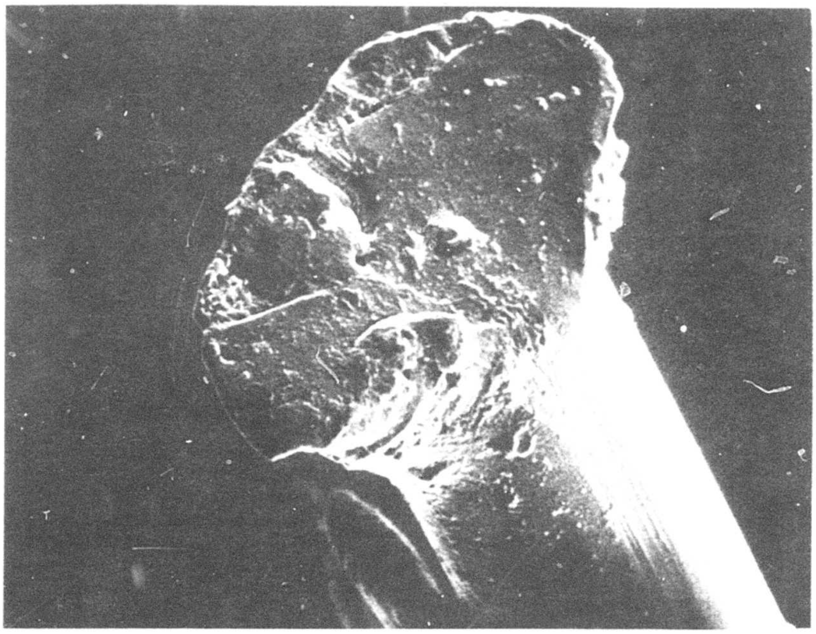

Figure 63. Fiber Cross-Sectioned with a Razor Blade (3000X)

The razor cut fiber end illustrates the smearing or material flow that has confounded all attempts to obtain useful cross-sections of Kevlar fiber.

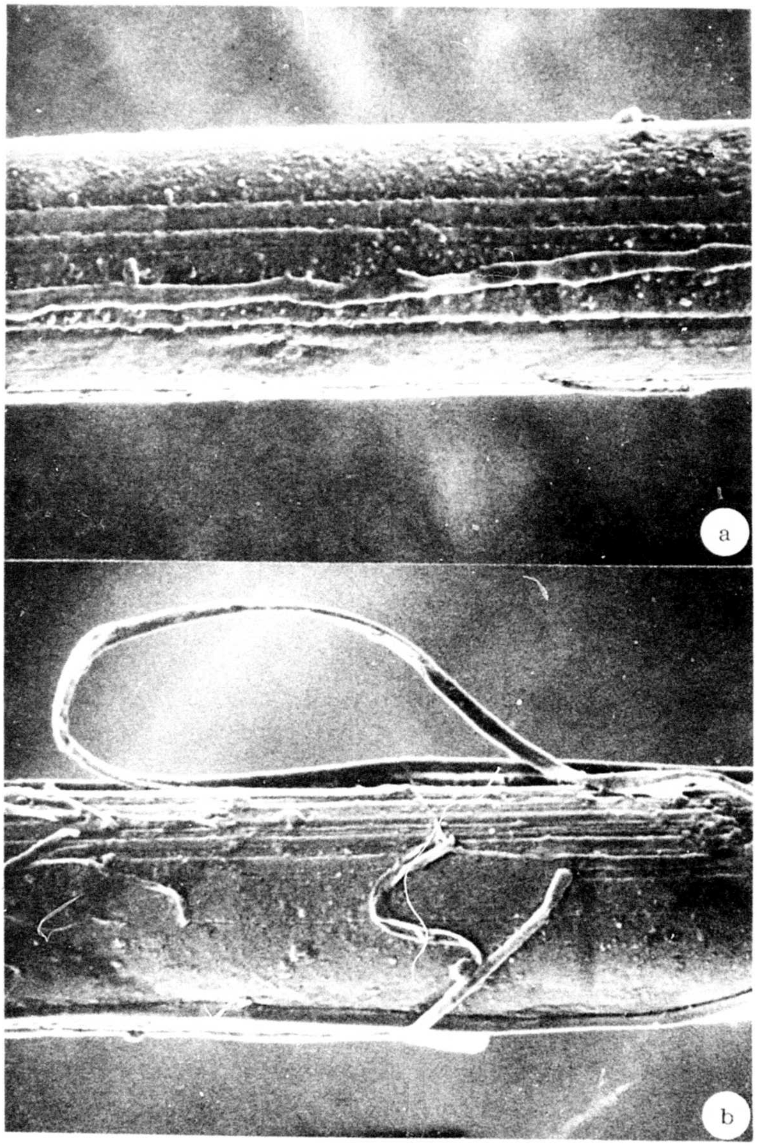

Figure 64. Longitudinal View of Virgin Fibers (3000X)

The surface of virgin Kevlar filaments contains many shallow longitudinal grooves of varying widths and globular material which appears to adhere to the surface. The wider grooves probably have resulted from the peeling off of strips of surface material as shown in (b). The globular material may be spin finish but could not be removed by extraction in perchloroethylene.

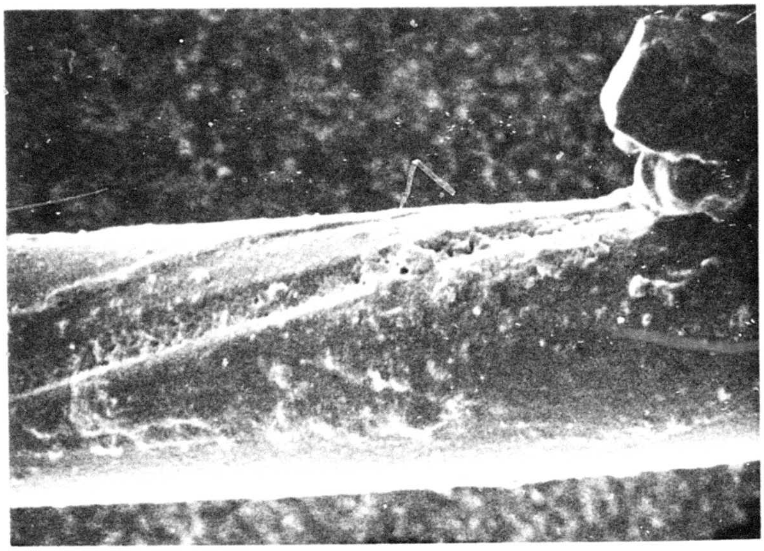

Figure 65. **Fiber Twisted 70 Turns/cm (3000X)**

The helical groove on the surface of this twisted specimen is similar to the longitudinal grooves observed on the virgin Kevlar fiber. Notice the granular appearance of the material within the groove.

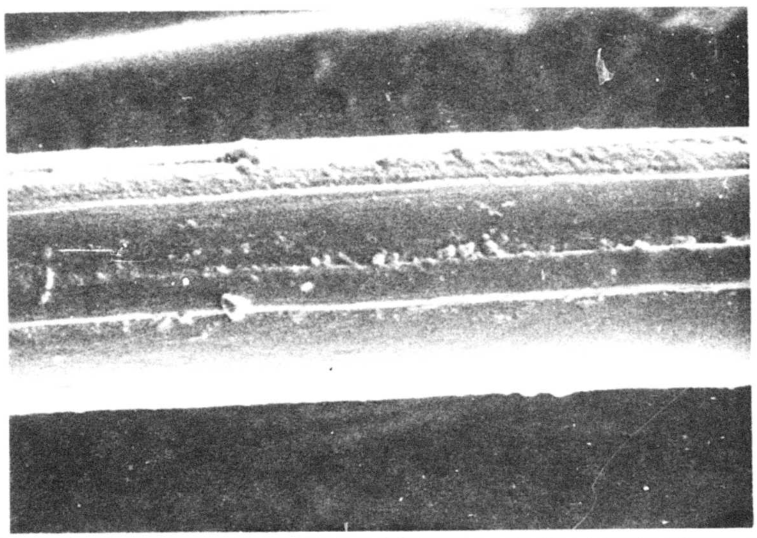

Figure 66. **Fiber Twisted 70 Turns/cm and Untwisted (3000X)**

Longitudinal grooves are again visible which presumably were similar in appearance, when twisted, to those seen in the previous photograph (Figure 65). The appearance is similar to that of the virgin fiber.

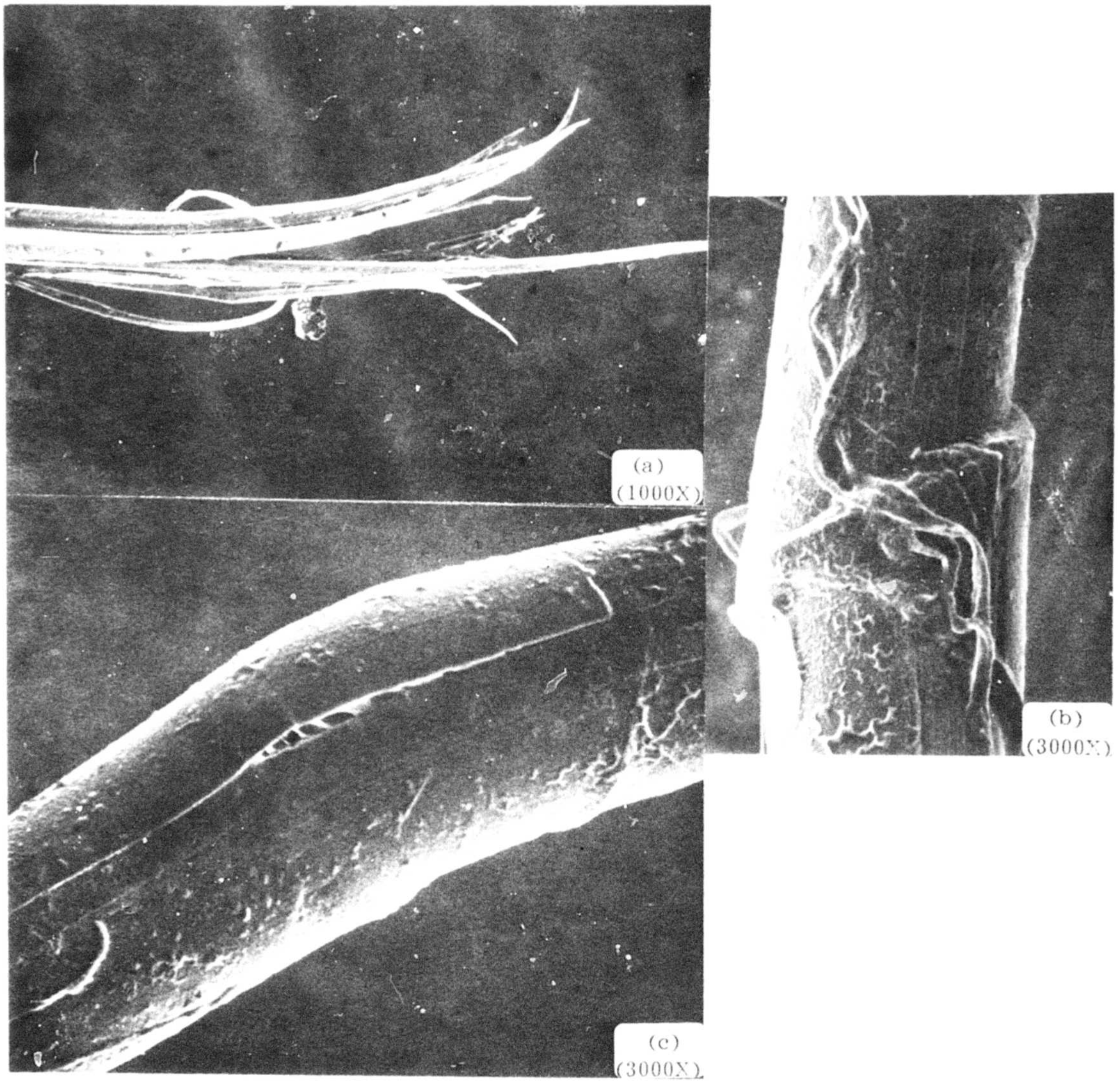

Figure 67. Fibers Broken in Tension

The majority of tensile fractures observed are characterized by lengthwise fragmentation and splintering as in (a). Buckling that accompanies snap-back after fracture can be observed in (b) and (c). In (b), the buckling manifests itself as a telescopic collapse, but (c) also shows some lengthwise delamination that is frequently observed a short distance away from fractured fiber ends. Notice the fibrillar bridgings connecting the partially detached surface material to the inner fiber structure.

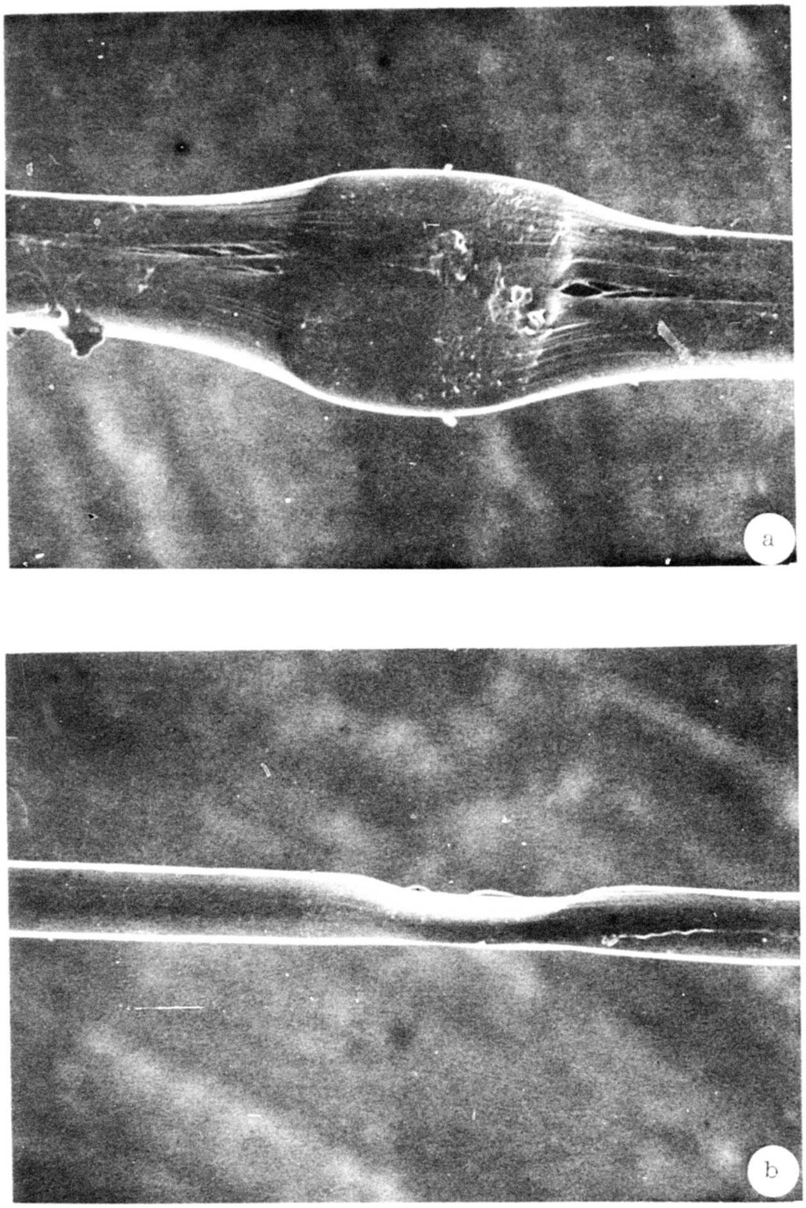

Figure 68. Laterally Compressed Fiber (1000X)

Crossed fibers were compressed laterally, separated and photographed from the top (a) and from the side (b). The resultant aspect ratio of the fiber cross-section is approximately 10 to 1. While the fiber remains essentially intact, some longitudinal splitting is visible at the boundary of the compressed region (a). A fine network of fibrillar branching can be seen within these splits.

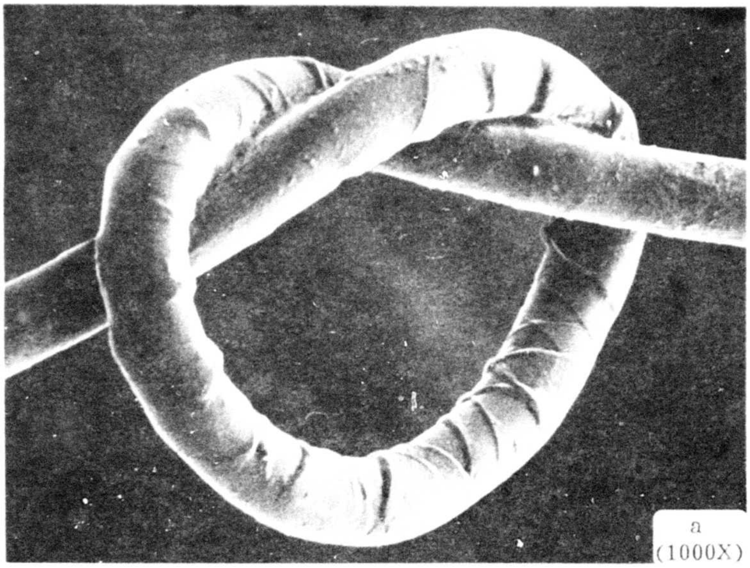

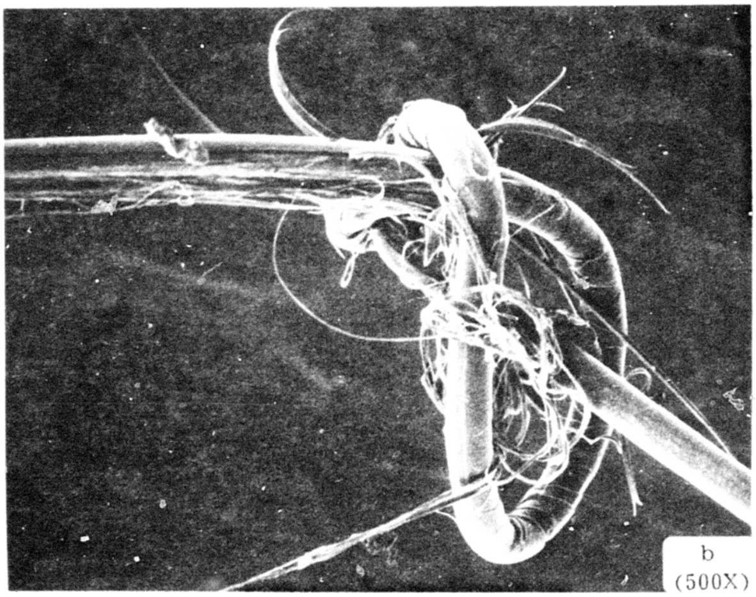

Figure 69. Overhand Knots in Single Fibers

In response to bending strains imposed by the knot, the fiber buckles severely in compression on the inside of the bend (a). Fracture does not occur even as the bending strain approaches 50%. Severe surface abrasion occurred as the knot in (b) was tightened.

SECTION VIII

CONCLUSIONS

The majority of this research has involved a detailed study of the mechanical properties of fibers and yarns made from Kevlar 29 and Kevlar 49. These are remarkable new fibers, having a combination of properties hitherto unobtainable in a textile fiber. Their extremely high tenacity offers the potential of designing fabrics having a uniquely high strength-to-weight ratio, an obvious advantage in many Air Force applications. Their relatively high modulus could provide a degree of dimensional stability unobtainable from commonly-used textile fibers. Their transverse and compressive properties provide a freedom from brittleness in twisting and bending unlike those of other high modulus fibers, and more like the common textile fibers. Their freedom from shrinkage when exposed to heat and relative nonflammability are additional important assets.

Undoubtedly, the Kevlar fibers are potentially important in applications of interest to the Air Force, and this study of mechanical properties has provided a background of invaluable information which will help to ensure that their characteristics can be utilized to best advantage.

REFERENCES

[1] Hearle, Grosberg and Backer, Structural Mechanics of Fibers, Yarns, and Fabrics, Vol. 1, J. Wiley & Sons. 1969.

[2] Schoppee, M.M. and Skelton J. "Bending Limits of Some High-Modulus Fibers," Textile Research Journal, 44, 968-975, 1974.

[3] Freeston, W.D., Jr. and Platt, M.M. "Mechanics of Elastic Performance of Textile Materials, Part XV: Filament Bending Recovery," Textile Research Journal, 34, 308-319, 1964.

[4] Abbott, N.J., Donovan, J.G. and Schoppee, M.M. "The Effect of Temperature and Strain Rate on the Tensile Properties of Kevlar and PBI Yarns," AFML-TR-74-65, Part II, May 1974.

☆ U. S. GOVERNMENT PRINTING OFFICE: 1975 — 657-630/74

SUPPLEMENTARY

INFORMATION

DEPARTMENT OF THE AIR FORCE

WRIGHT LABORATORY (AFMC)
WRIGHT-PATTERSON AIR FORCE BASE, OHIO

ERRATA

25 February 1994

FROM: ~~WL/DOA, Bldg 22~~
2690 C St Ste 4
Wright-Patterson AFB OH 45433-7411

SUBJ: Notice of Changes in Technical Report(s) AFML-TR-74-65

TO: Defense Technical Information Center
Attn: DTIC-OCC
Cameron Station
Alexandria VA 22304-6145

Please change subject report(s) as follows:

AFML-TR-74-65, Part I - AD ~~B000380~~
Part II - ~~AD B002047~~
Part III - AD B006949
Part IV - ~~AD B017280~~

All parts have been approved for public release; distribution is unlimited as of 23 Feb 1994.

ERRATA - AD-B006949

151.20/14
Public Release
A/O: 8 Mar 94

WM. F. WHALEN
Chief, Tech. Editing & STINFO Branch
Resource Management